Chromalveolate evolution:
chloroplast replacements in dinoflagellates
and the deep phylogeny of *Telonema*

Cand.scient thesis

By Marianne Aastebøl Minge

Cand.scient thesis

University of Oslo

The Faculty of Mathematics and Natural Sciences

Department of Molecular Biosciences

2005

CONTENTS

ACKNOWLEDGEMENTS

The laboratory and bioinformatical work was carried out at the at Centre for Ecological and Evolutionary Synthesis (CEES) at the University of Oslo, and at Tom Cavalier-Smith's lab at the Zoology building, University of Oxford in the period from November 2003-June 2005.

During the work on my thesis, I have enjoyed interaction with many inspiring and wonderful people. I want to thank Kjetill S. Jakobsen, who has been an enthusiastic and encouraging supervisor. Kamran Shalchian-Tabrizi has been a great support, and he deserves thanks for always being remarkably patient, extremely helpful and for teaching me so much about protist phylogeny. I also want to express my gratitude to both of them for giving me the opportunity to accompany Kamran's visit to Oxford University.

Dag Klaveness have taught me all I know about algal-culturing, and has always patiently answered all my questions. Emelita Nerli, Lise Broch and Sissel Brubak have been helping me at the DNA-lab and the algal culturing lab. I am also grateful to Nils-Christian Stenseth at CEES for financial support for my Oxford visit.

I also very much want to thank Tom Cavalier-Smith, Ema Chao, and the others at lab F7 at Oxford University. Tanja Auren, Trym and Folke also deserve big hugs for their friendliness and hospitality.

I also want to thank my parents and my sister, my grandparents and my friends for their support.

Finally, I want to thank Espen, for always being there for me.

Marianne Aastebøl Minge, June 2005

1. INTRODUCTION

1.1 THE EUKARYOTIC TREE OF LIFE AND ITS IMPLICATIONS FOR INTERPRETATIONS OF EVOLUTIONARY PROCESSES

The interpretation of the evolutionary history of eukaryotes and their internal phylogeny has changed dramatically the last few years due to extensive research applying molecular and morphological methods. The current understanding of eukaryote bio-diversity states that the eukaryotic tree of life can be divided into five hypothesized supergroups of related organisms (Cavalier-Smith 2004b; Harper et al. 2005; Keeling 2004b), as shown in figure 1.1. This interpretation is based on gene analyses of multiple and combined gene sequences, biochemical features, structural characters and rare genomic events such as insertions and gene replacements (Cavalier-Smith 2003b; Keeling 2004b). The supergroups are presently holding only informal names, as no universally accepted names yet have been determined, and a closer description of the supergroups is given in box 1.1. Animals, fungi (together: opisthokonts) and amoebozoa are found in one of these supergroups, the unikont group (Baldauf 1999; Baldauf et al. 2000; Stechmann and Cavalier-Smith 2002). The remaining four supergroups together constitute the bikonts (Cavalier-Smith 2003b), comprising the recently discovered rhizaria group, (Archibald et al. 2003; Cavalier-Smith 2003b; Keeling 2001; Nikolaev et al. 2004), the well-known plant group, (Baldauf et al. 2000; Moreira et al. 2000), the excavate group (Simpson 2003; Simpson and Patterson 2001) and finally, the chromalveolate supergroup, including the chromists and alveolates (Baldauf et al. 2000; Cavalier-Smith 1998; Fast et al. 2001; Harper and Keeling 2003; Harper et al. 2005; Yoon et al. 2002b), which will be the main subject matter in this study. The precise position of the last common ancestor of all extant eukaryotic lineages (i.e. the root) of the eukaryotic tree is unclear, however, the root have been postulated, based on two single amino-acid deletions in the enolase gene, to be among the excavate lineage (Keeling and Palmer 2000). This suggestion have later been contradicted in a paper by Stechmann and Cavalier-Smith (Stechmann and Cavalier-Smith 2002), demonstrating a derived gene-fusion shared by all bikonts, hence indicating a root near the bifurcation between the unikonts and the bikonts.

FIGURE 1.1

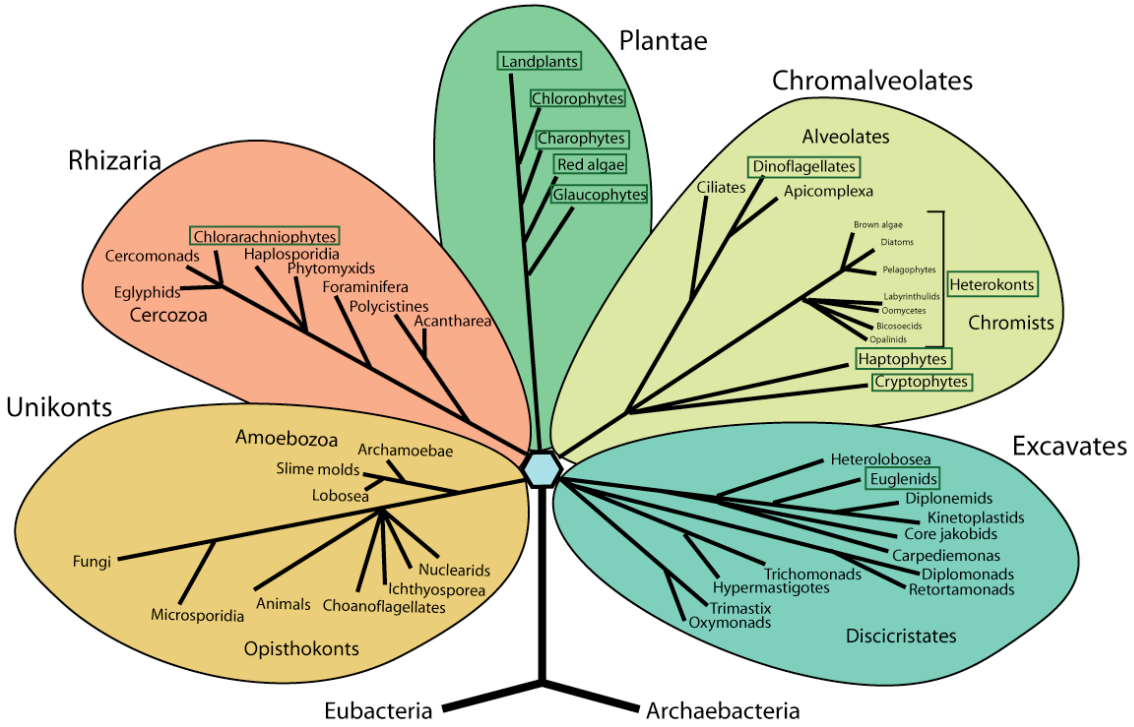

Figure 1.1: The hypothesized five divisions (supergroups) of eukaryotes representing the currently known eukaryotic diversity, consists of the unikonts, comprising the amoebozoa and the opisthokonta (fungi and animals). The remaining eukaryotic supergroups together comprise the bikonts: the recently recognized group rhizaria, including the chlorarachniophytes and the cercozoa; the well-known and well-supported plant-group comprising the red- and green algae, the glaucophytes and the land-plants; the chromalveolates consisting of dinoflagellates, apicomplexans, ciliates, cryptophytes, haptophytes and heterokonts; and the excavates, probably the loosest assembly of the supergroups, including the euglenoids and the diplomonads (Baldauf et al. 2000; Keeling 2004b). Lineages in which plastids are known are marked by green squares. Figure adapted from Keeling, 2004 (Keeling 2004b). A closer description of the supergroups is given in box 1.1.

Box 1.1

Unikonts: The unikonts, robustly united by numerous phylogenies, protein insertions and a gene fusion, comprise the opisthokonts (animals, fungi, choanoflagellates and a range of parasitic and free-living groups) and the amoebozoa (free-living heterotrophs feeding by use of a pseudopodia)(Simpson and Roger 2004). These organisms all originate from a putative heterotrophic uniciliate ancestor (Cavalier-Smith 2003b).

Bikonts: The bikonts comprise four supergroups of eukaryotes: rhizaria, plantae, excavates and chromalveolates, all descending from a common biciliate ancestor (Cavalier-Smith 2003b).
Rhizaria: This supergroup contains a broad range of free-living unicellular organisms (such as Foraminifera and Radiolara, as well as the specious phylum Cercozoa, which are abundant in environmental samples) and some animal parasites. The supergroup also contains a photosynthetic lineage, the chlorarachniophytes, a group of mixotrophic algae holding a secondary plastid of green algal origin. (Cavalier-Smith 2003b; Simpson and Roger 2004). The monophyly of this supergroup is supported in protein and rRNA-trees (Cavalier-Smith and Chao 2003; Keeling 2001; Nikolaev et al. 2004).

Plantae: The well-known plantae supergroup comprises land plants, green algae, red algae and glaucophytes. These lineages are phylogenetically connected by an evolutionary event, namely the primary endosymbiosis of a photosynthetic bacterium which most likely happened only once in their common ancestor (Simpson and Roger 2004). The monophyly of the group are supported by plastid gene phylogeny and gene organization (Simpson and Roger 2004).

Excavates: The members of the excavata are unicellular heterotrophic flagellates. Some of the excavates, such as trypanosomatids, *guillardia lamblia* and trichomonas, are notorious for causing disease, and are the agents of sleeping sickness, giardiasis and trichomoniasis respectively (Simpson and Roger 2004). Many excavate taxa possess modified mitochondria, and the supergroup also comprises a photosynthetic lineage (the euglenoids) which harbor a secondary derived green-algal plastid; (Simpson and Roger 2004).

Chromalveolates: The chromalveolates comprise a wide diversity of heterotrophic and phototrophic species. The group is divided in six distinct subgroups: dinoflagellates, apicomplexa and ciliates (together: the alveolates) and heterokonts, haptophytes and cryptophytes (together: the chromists), and is phylogenetically connected through a secondary endosymbiosis of a red-alga which putatively occurred in their common ancestor (Cavalier-Smith 2003b).

Chromists: The chromists comprise three subgroups; the cryptophytes, the haptophytes and the heterokonts (also called stramenopiles), apomorphically defined by the placement of their chlorophyll a + c containing plastid. The chromists have their plastid located within the lumen of the endoplasmatic reticulum, and share a homologous mechanism for plastid targeting of nuclear-coded plastid genes (Cavalier-Smith 2003b).

Alveolates: The biologically diverse assembly alveolates consist of ciliates, dinoflagellates, apicomplexans and some minor lineages (Fast et al. 2002). A few ultra structural features, such as cortical alveoli and micropores, are found in most alveolate members, but the six lineages are otherwise highly derived (Leander and Keeling 2004).

The ciliates are heterotrophic active predators defined by dimorphic nuclei and a distinctive cytoskeleton (Katz 2001; Leander and Keeling 2004).

The dinoflagellates express various modes of nutrition and strategies (phototrophy, heterotrophy, mixotrophy, parasitism), and defined by the specialized nucleus (dinokaryon) and a distinctive flagellar apparatus comprising two flagella (Hackett et al. 2004a). The phototrophic members of this group express an immense plastid diversity, and hold secondary and even tertiary derived plastids (i.e. derived from tertiary endosymbiosis, where an eukaryotic cell engulfs a eukaryote with a secondary plastid and retains it)(Tengs et al. 2000).

The apicomplexans are intracellular parasites of animals, apomorphically defined by a cell invasion apparatus called the apical complex. These parasites are well-known for comprising the agents causing human disease, including the severe tropical disease malaria and toxoplasmosis (Simpson and Roger 2004). Some of the apicomplexans contains an apicoplast (a vestigial chloroplast): a smoking gun of their ancestral state as phototrophs (Leander and Keeling 2004).

For a more detailed review of the eukaryotic supergroups (in Norwegian), see Klaus Høiland's paper from 2004 (Høiland 2004).

Deciding the position of the last common eukaryotic ancestor, however, has not been the only problem in the on-going process of revealing the eukaryote tree of life. The complete emergence of the eukaryotic tree have been challenged by difficulties associated with resolving the internal relationship between the eukaryotic supergroups and subgroups of organisms, caused by the lack of ultra structural characters suitable for phylogenetically relating the high-level taxonomic groups, especially among the unicellular organism (Keeling 2004b). Deciding whether similar structural features found in unicellular organisms indeed are homologous is associated with uncertainties and difficulties, as these characters could result from evolutionary convergence and parallel evolution rather than originating from a common ancestral structure. However, the introduction of molecular data to phylogenetic analyses provides additional data from which independent testing can be carried out to test the evolutionary hypotheses deduced from structural information. The supergroups have been established based on the combination of the conventional methods for phylogenetic interpretation and the phylogenetic information present in protein- or nucleotide sequences (Keeling 2004b; Simpson and Roger 2004), and may ultimately reveal the eukaryotic tree. Consequently, the current understanding of the supergroups implement all currently known methods for

phylogeny, interpreting the internal relationship based on ultra-structures, biochemistry and nuclear sequences.

Despite the extensive research resulting in the establishment of the supergroups, the evolutionary relationships between the groups remains unclear (Keeling 2004b). The deficient resolution of the eukaryotic phylogeny has implications for the current understanding of evolutionary processes, as a complete comprehension of evolutionary events requires knowledge about the phylogenetic relationships among the organisms in which the processes are found, making the task of unveiling the eukaryotic phylogeny the most important for correctly interpreting major evolutionary processes (Keeling 2004b). The introduction of molecular sequences to phylogenetic inference provided a new and promising method for taxonomical classification, and in the initial attempts of reconstructing the eukaryotic tree, a resolved phylogenetic tree was reconstructed based on the small ribosomal subunit (SSU) gene sequence (Sogin 1991). However, as more extensive analyses applying larger data-sets and several molecular markers were carried out, the rRNA phylogeny was shown to suffer from several limitations, mostly due to major systematic biases in the evolutionary mode of the SSU gene sequence that caused ambiguous placement of derived species with long branches (Cavalier-Smith 2004b). Long-branch attraction (LBA) artifacts are caused by variable evolution rate between species, as sequences with high evolution rate artificially attract to each other and to early diverging sequences (Dacks and Doolittle 2001). The practical problems associated with the erroneous LBA constructs are illustrated in the early rRNA phylogeny, where the mitochondrial-lacking lineages such as parabasalia, metamonads and Microsporidia were placed as early diverging lineages in the eukaryotic tree (Sogin and Silberman 1998). As the interpretation of the macroevolutionary eukaryotic history was based on this topology, the archezoa hypothesis was postulated, claiming an amitochondriate origin of eukaryotes (Cavalier-Smith 1998; Roger 1999). However, when long-branched outgroup taxa archaebacteria were removed from the analyses, the early divergence of these lineages was rejected, and the potentially deep-branching eukaryotic lineages were placed within the supergroup excavates and even among the opisthokonta, as the lineage Microsporidia was placed as close relative to fungi (Roger and Silberman 2002; Silberman et al. 2002). Despite the difficulties related to the phylogenetic use of the small ribosomal gene sequence, this is still used as an important marker for investigation of

eukaryotic phylogeny. However, as every gene sequence probably suffer from systematic biases and random errors (but most likely not the same biases and errors), analyses based on multiple gene sequences have been shown to provide increased support and phylogenetic resolution in several parts of the eukaryotic tree (Baldauf et al. 2000; Bapteste et al. 2002; Yoon et al. 2002b), and may contribute to a complete reconstruction of a global eukaryotic tree.

In addition to find molecular and structural markers appropriate for interpretation of the eukaryotic evolution, the incorporation of a broad taxon sample to the phylogenetic analyses is also of significant importance for resolving the eukaryotic tree of life, as a correct resolution probably requires members representing all extant major lineages to be included. One approach for screening for novel eukaryotic taxa, are by molecular surveys of environmental samples.

1.2 EXPLORING EUKARYOTIC BIO-DIVERSITY BY MOLECULAR APPROACHES

The phylogenetic placement of novel taxa is decided by combining information about gene sequences and investigation of ultra structural features. However, due to difficulties associated with laboratory culturing of protists, another method used for investigations of biodiversity is by screening for novel taxa by analyzing DNA from various environments. Hence, ensuing the introduction of molecular applications for phylogenetic inference, molecular surveys of various environments have been carried out using samples from extreme- and common-place environments from which total DNA are extracted and a phylogenetic marker, usually the small subunit ribosomal (SSU) gene, is amplified and subsequently used for construction of clone libraries (Richards and Bass 2005). The environmental sampling approach has revealed many eukaryotic lineages not previously described, some of which potentially belong to higher taxonomical levels, implying a substantial existence of unknown eukaryotic diversity (Lopez-Garcia et al. 2001; Richards and Bass 2005). Thus, the environmental sampling approach represents a powerful tool for unveiling this putative unknown reservoir of biodiversity.
Some of the novel sequences reported from two of these environmental surveys were initially reported to place outside all known eukaryotic supergroups, indicating that there

might be as much as eight new eukaryotic kingdoms (Dawson and Pace 2002; Stoeck et al. 2003), suggesting a massive amount of hidden eukaryotic high-level diversity. The number of suggested new kingdoms was astonishing, considering that only five supergroups of eukaryotes are currently known (Cavalier-Smith 2004b). However, more extensive analyses of these environmental sequences utilizing a dataset that included a wider range of eukaryotic taxa showed that all the novel sequences in fact could be placed among established phyla and classes (Berney et al. 2004; Cavalier-Smith 2004b), hence emphasizing the critical importance of a broad and representative taxon sampling for correct interpretation of phylogeny.

Even though these sequences did not represent novel eukaryotic kingdoms, they are examples of an immense undescribed diversity among eukaryotes also reported from several other environmental surveys. In an study including sampling of picoplankton from the Pacific ocean, a large diversity of sequences from unknown taxa was revealed, most of which could be assigned to known phyla including prasinophytes (green alga, viridiplantae), haptophytes (chromists), dinoflagellates (alveolates), heterokonts (chromists) and choanoflagellates (opisthokonts) (see figure 1.1 and box 1)(Moon-van der Staay et al. 2001). Additionally, in a similar survey utilizing samples from deep-seas a range of novel sequences was discovered, which were placed phylogenetically among the alveolates as sisters to dinoflagellates (Lopez-Garcia et al. 2001; Moon-van der Staay et al. 2001). These findings, as well as the results achieved by other environmental surveys, indicate that eukaryotic supergroups may already be discovered (Cavalier-Smith 2004b; Simpson and Roger 2004). However, a few sequences generated from environmental samples do not cluster within known eukaryotic phyla (Richards and Bass 2005), suggesting that there are higher-level eukaryotic lineages not yet discovered. Revealing these “missing links” in the eukaryote tree of life is probably necessary for resolving the global phylogeny, but will require efficient methods for environmental sampling and laboratory culturing.

1.3 ORGANELLE EVOLUTION: THE ENDOSYMBIOTIC ORIGIN OF THE PRIMARY PLASTID

One of the key evolutionary events in the history of eukaryotes is the incorporation of the chloroplast. The plastids are the organelles of plants and algae responsible for photosynthesis and various biochemical pathways in the cell, and it is now widely accepted that the first plastid arose from a merge between photosynthetic bacteria, possibly similar to modern cyanobacterium, and a non-photosynthetic host (Archibald and Keeling 2002; Howe et al. 2003; McFadden 2001). It remains unclear whether the primary uptake and integration of a photosynthetic bacterium happened only once or if this happened repeatedly. However, the currently favored scenario is a monophyletic model of primary plastid evolution, where the primary endosymbiotic event happened only once, although several uptakes from related cyanobacteria cannot be ruled out as multiple uptakes of closely related taxa probably are impossible to recognize in phylogenetic trees (Howe et al. 2003; McFadden 2001; Palmer 2003). As a consequence of the plastid incorporation, massive gene-transfer from the endosymbiont nucleus to the eukaryotic host occurs, only retaining a fraction of the endosymbiont genome in the plastid (Martin et al. 1998).

Three extant lineages harbor primary plastids from this first plastid endosymbiosis: the glaucophytes, the red algae and the green algae/land plants, found in the eukaryotic supergroup plantae (Palmer 2003). The great success of the plastid-bearing organisms is obvious when considering the eukaryotic tree of life, as plastid-bearing groups are scattered across four of the five major eukaryotic groups (viridiplantae, chromalveolates, excavates and rhizaria, see figure 1.1) (Keeling 2004b). However, only a fraction of these groups harbor plastids derived from the primary plastid uptake, as most photosynthetic eukaryotes, including the members of the chromalveolates, hold plastids of secondary endosymbiotic origin (Bhattacharya et al. 2004; Cavalier-Smith 2002; Delwiche 1999).

1.4 SECONDARY AND TERTIARY ENDOSYMBIOSIS: RECYCLING OF PLASTIDS

Secondary endosymbiosis is a phenomenon where a eukaryote engulfs a photosynthetic alga and permanently retains its originally primary plastid (see figure 1.2) (Cavalier-Smith 2002).

FIGURE 1.2

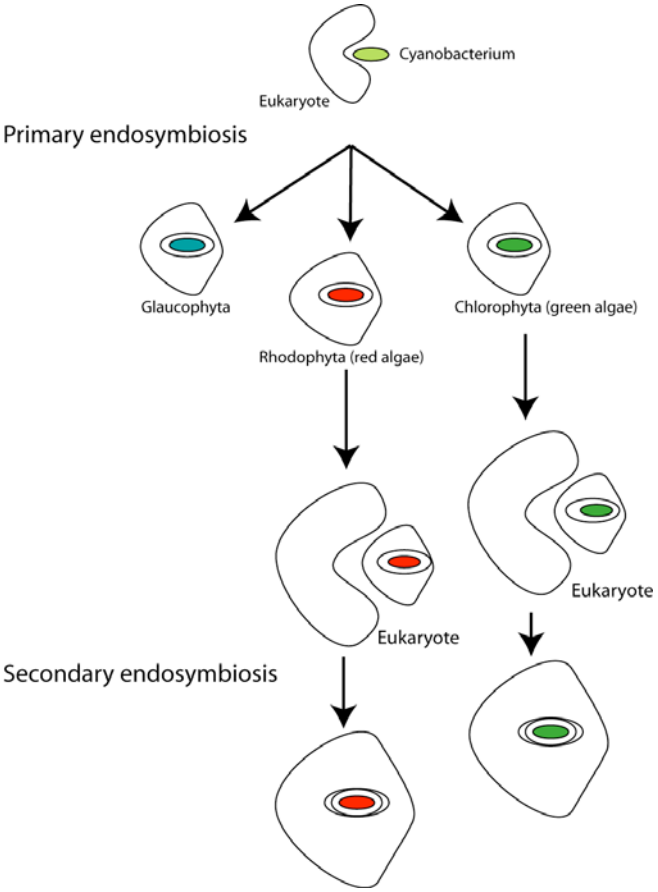

Figure 1.2: Primary and secondary endosymbiosis. In a primary endosymbiosis, a bacteria is taken up by a eukaryote. In a secondary endosymbiosis, a photosynthetic eukaryotic is engulfed by another eukaryote. No secondary endosymbiont of glaucophyte origin is found. The number of secondary endosymbiotic events involving red- and green algae is controversial, and the postulated number ranges from two to seven independent plastid uptakes.

Following the uptake of a secondary plastid is a massive gene transfer from endosymbiont to the host genome, as seen subsequent to a primary endosymbiosis (Cavalier-Smith 2002). The secondary plastids are characterized by the presence of three

or four bounding membranes, and two of the groups that harbor secondary plastids, the chlorarachniophytes and the cryptophytes, still retain a remnant nucleus of the algal symbiont (Bhattacharya et al. 2004). Both red and green plastids have been subject to secondary endosymbiosis, as plastids with a putative red algal origin is found in dinoflagellates, cryptophytes, haptophytes and stramenopiles (chromalveolates), and green-algal derived plastids are found in euglenoids (excavates) and chlorarachniophytes (rhizaria) (Falkowski et al. 2004; Keeling et al. 2004). In addition to these plastids, a vestigial plastid (i.e. an apicoplast) is found in the apicomplexans (Fast et al. 2001; Lang-Unnasch et al. 1998), putatively of red algal origin, even though indications of a green-algal origin also have been reported (Fast et al. 2001; Funes et al. 2002; Funes et al. 2004). There is an ongoing controversy associated with the number of secondary endosymbiosis that have occurred through the evolutionary history, and the postulated numbers of uptakes differ from two to seven (Cavalier-Smith 1999; Falkowski et al. 2004; Keeling 2004b). A common ancestry of the lineages holding green algal derived plastids have been postulated in the cabozoan hypothesis (Cavalier-Smith 1999; Cavalier-Smith 2000), however, current evidence indicates two independent secondary uptakes of a green plastid in the ancestral lineages of euglenoids and chlorarachniophytes, as a common ancestry of these lineages would imply a merge of the rhizaria and excavate supergroups not supported by molecular or structural data (Archibald and Keeling 2002; Baldauf et al. 2000). However, the main controversy is associated with the uptake of the red algal plastid in the chromists and alveolates, and two of the proposed models for plastid evolution in these lineages are shown in figure 1.3. Plastids of putative red algal origin are found in five of the chromist and alveolate lineages (dinoflagellates, apicomplexa, haptophytes, heterokonts and cryptophytes), and different evolutionary models have been postulated for explaining this diversity. Among these models are the chromalveolate hypothesis postulated by Tom Cavalier-Smith (Cavalier-Smith 1999), stating that despite the diversity of organisms carrying red algal derived plastids, all these plastids originated in a single endosymbiotic event that occurred in the common ancestor of all these lineages. Others claim that the numerous and diverse distribution of red plastids proves that secondary endosymbiosis has been a far more common event during the eukaryotic evolutionary history than implied in the chromalveolate theory, and

postulate an individual uptake in each of the lineages containing a plastid of red algal origin (Falkowski et al. 2004; Taylor 2004).

FIGURE 1.3

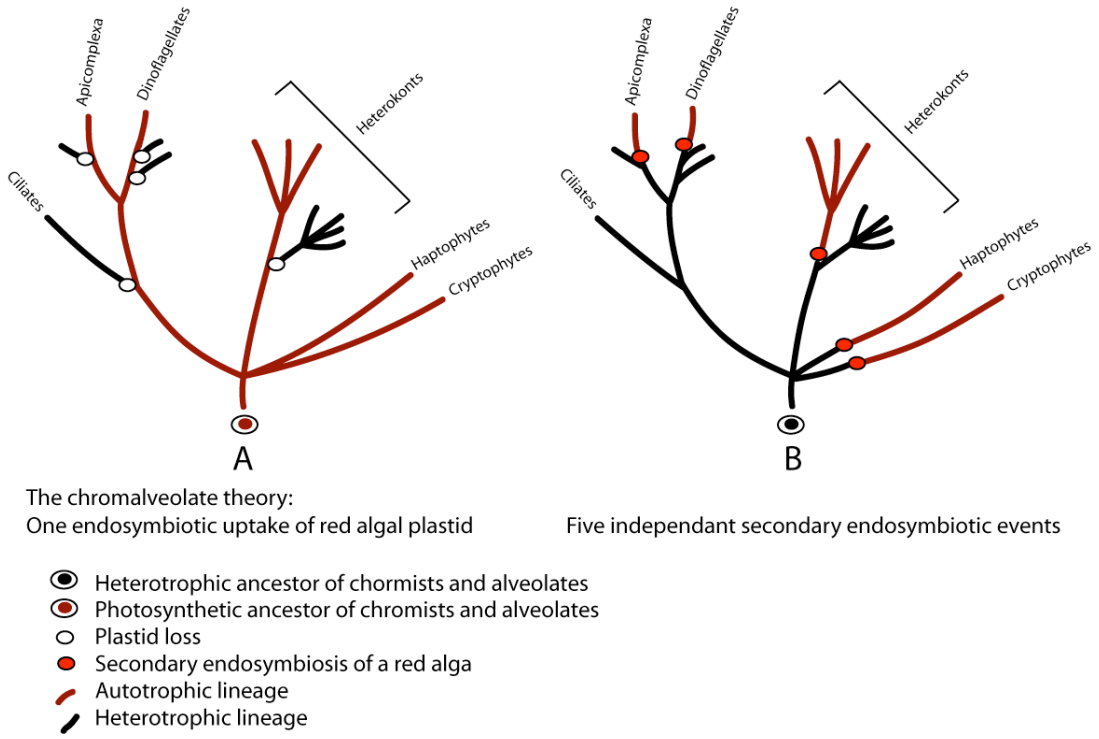

Figure 1.3. Two hypotheses of plastid evolution in chromists and alveolates, representing the "few" and the "many" controversy. A: The chromalveolate theory. The plastid harbored by chromists and alveolates was engulfed in one single endosymbiotic event. B: The red alga derived plastids found in chromists and alveolates were obtained by five separate secondary endosymbiotic events.

In the dinoflagellate group, even tertiary endosymbiosis have occurred (Tengs et al. 2000). In tertiary endosymbiosis, a photosynthetic eukaryote with a secondary plastid is engulfed by another eukaryote, a process that has only been shown to have happened among the dinoflagellate taxa *Karenia brevis*, *Karenia mikimotoi*, *Karlodinium micrum* and their close relatives (Tengs et al. 2000). The tertiary endosymbiont in these dinoflagellates have pigmentation and plastid ultra-structure that indicate that they are derived from a haptophyte, and this assumption have been supported in several molecular analyses (Takishita et al. 2004; Tengs et al. 2000).

1.5 DINOFLAGELLATES

Dinoflagellates (subphylum Dinoflagellata, phylum dinozoa) are a diverse group of organisms, constituting one of the tree major groups together forming the alveolates (see box 1.1). The dinoflagellates are ubiquitous in marine and fresh-water environments and flourish under favorable conditions, they are common as ecto-parasites, endo-parasites and symbionts, some of them are bioluminescent and many members are capable of producing toxins causing human illness, fish death and mortality of other marine fauna (Hackett et al. 2004a; Taylor 2004). The dinoflagellates are remarkable organisms in many aspects, as they express an immense diversity in form and nutrition that have stimulated a great deal of interest for this group. The dinoflagellates were once incorrectly thought to be so-called mesokaryotes constituting a separate intermediate kingdom between eukaryotes and prokaryotes, because of the amount of unique features present in the group, including a distinctive pattern of mitosis and nucleus, absence of histones and two unequal flagella (Hackett et al. 2004a). However, more extensive investigations of their phylogeny placed the dinoflagellates robustly among the eukaryotes (Hackett et al. 2004a). Two sets of characters have traditionally been used as taxonomical characters defining this group (Saldarriaga et al. 2004; Taylor 2004). One of these synapomorphic features is the dinokaryon, a uniquely designed nucleus containing permanently condensed chromosomes without histones, while the theca (the presence of cellulose or other polysaccharides in the vesicles found beneath the cell surface) is the other character used as a taxonomical fingerprint for this group, as different cell types can be recognized on the basis of presence or absence of theca tabulation (Taylor 2004). The thecal plates give the cells a distinct external pattern, and this pattern, as well as the number of theca, is used to distinguish between the different dinoflagellate orders. Dinoflagellates devoid of theca are said to be “naked” or unarmored (Saldarriaga et al. 2004). The dinoflagellate genome is organized in a high number of chromosomes, reflecting the exceptionally large amounts of DNA contained in each cell. A dinoflagellate cell can hold 3-250 pg DNA/cell, equivalent with a genome of around 3000-215000 MB, or 1-70 times the human genome (Hackett et al. 2004b).
Among the photosynthetic members of the dinoflagellates, constituting about one half of the dinoflagellate species, the vast majority hold a plastid containing chlorophyll a and c_2,

beta-carotene and peridinin (Hackett et al. 2004a). This synapomorphic dinoflagellate secondary plastid is surrounded by three membranes, is of putative red-algal origin and express an unique organization of the plastid genome, which is found on plastid minicircles each containing usually only one or two genes (Taylor 2004; Zhang et al. 2002). Many genes normally found in the plastid genome have in the peridinin-containing dinoflagellates been transferred to the nucleus, and only 16 protein genes are currently believed to have been retained in the chloroplast genome (Howe et al. 2003; Zhang et al. 2002).

In addition to the peridinin plastid, several other plastid types are also found among the dinoflagellates (Hackett et al. 2004a; Saldarriaga et al. 2004; Taylor 2004), illustrating the unique plastid diversity found in this group, a feature that makes the dinoflagellates ideal for investigations of the processes involved in plastid evolution. In this study, the dinoflagellates will be used for investigations of plastid evolution, an evolutionary event of particular interest and with large implications for the supergroup chromalveolates, as the putative common ancestry of this group is based on a very specific model of plastid evolution.

1.6 DINOFLAGELLATES AS A MODEL GROUP FOR INVESTIGATIONS OF PLASTID EVOLUTION

The extraordinary plastid diversity expressed in the dinoflagellates reflects evolutionary processes such as secondary and tertiary endosymbiosis, kleptoplastidy (i.e. temporarily uptake of plastids), plastid loss and plastid replacements (Hackett et al. 2004a), making the dinoflagellates an ideal group for investigation of plastid evolution.In addition to the predominating peridinin-plastid, the phototrophic dinoflagellates also harbor a variety of other plastids, as four additional plastids are known in this group. *Karenia brevis*, *Karenia mikimotoi*, *Karlodinium micrum* and their close relatives contain a chlorophyll a + c and 19'-hexanoyloxy-fucoxanthin containing plastid of putative haptophyte origin, bound by three membranes and most likely acquired by tertiary endosymbiosis (Takishita et al. 2004; Tengs et al. 2000). *Lepidodinium viride* and *Gymnodinium chlorophorum* are the only dinoflagellates that hold a plastid of putative green-algal origin, and their plastid of possible prasinophyte origin (a chlorophyte/green algae) contains chlorophyll a + b and the photopigment prasinoxanthin (Elbrächter and Schnepf 1996; Watanabe et al.

1990). The *Dinophysis* group have plastids with chlorophyll a + c and phycobilin of putative cryptophyte origin, surrounded by only two membranes (Schnepf and Elbrachter 1988). The plastid found in *Kryptoperidinium foliaceum* and *Peridinium balticum* is of plausible diatom origin, holding fucoxanthin as the main carotenoid (Chesnick et al. 1997; Chesnick et al. 1996).

Only the 19'-hexanoyloxy-fucoxanthin (hereafter 19') and chlorophyll a + b containing plastids are considered to be "true" plastids, i.e. fully established in the host (Cavalier-Smith 2003a). In the group holding a plastid of putative diatom-origin (including *Kryptoperidinium foliaceum* and *Peridinium balticum*), the endosymbiont still retains a nucleus, mitochondria and ribosomes, and no gene transfer appears to have occurred between the host and the endosymbiont even though the plastid seems to be permanent (McEwan and Keeling 2004). This clearly suggests that this plastid is not completely integrated in the cell, hence representing an intermediate stage of endosymbiosis (McEwan and Keeling 2004). An even earlier stage of endosymbiosis is demonstrated in the *Dinophysis* group, where the cryptophyte plastid probably is acquired by kleptoplastidy, a phenomenon whereby the host digests the algae while retaining the plastid structurally intact (Janson 2004; Takishita et al. 2002).

The origin of the peridinin plastid is a controversial issue of dinoflagellate evolution. Two of the postulated models for plastid evolution in dinoflagellates are shown in figure 1.4. Traditionally, the predominance of the peridinin-containing plastid have been considered as evidence for this plastid being the ancestral for dinoflagellates (Taylor 2004). If this is the case, the remaining plastid-types found in extant groups of dinoflagellates must have been obtained by replacement of the original peridinin-plastid or by uptake by a heterotrophic dinoflagellate belonging to a lineage that already had lost the peridinin-plastid (Saldarriaga et al. 2001). However, as the basal position of the peridinin-containing species are not robustly supported in phylogenetic analyses of ribosomal and protein genes (Saldarriaga et al. 2004; Saldarriaga et al. 2001; Zhang et al. 2005), the ancestral state of the peridinin plastid is not clearly demonstrated in molecular studies. Additionally, analyses of plastid genes done by Yoon et al. in 2002 indicated the

19'-plastid as the ancestral one in the dinoflagellate lineage, subsequently evolving into the peridinin plastid in all lineages except the *Karlodinium/Karenia* clade (Yoon et al. 2002a). Even though these analyses probably was mislead by codon use heterogeneity in plastid genes (Inagaki et al. 2004; Yoon et al. 2005), this enforces the uncertainty associated with the ancestral state of the dinoflagellate plastid. Due to these incongruent phylogenies, it is difficult to rule out any hypothesis of the origin of the peridinin-plastid.

FIGURE 1.4

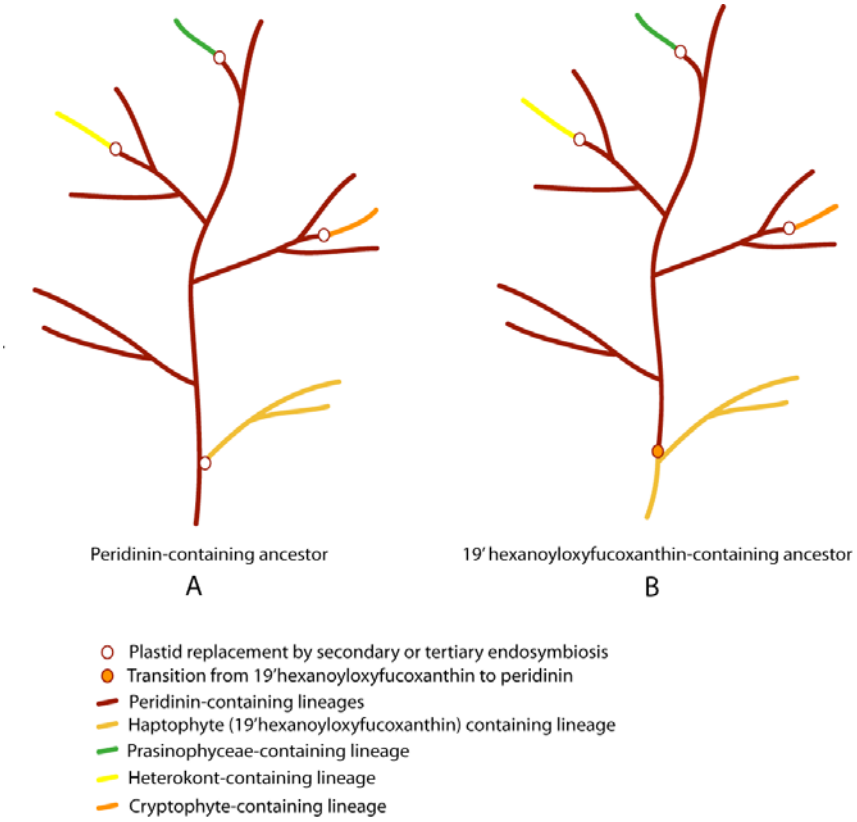

Figure 1.4. Two alternative hypotheses for plastid evolution in dinoflagellates. In tree A, peridinin is shown as the ancestral plastid. The remaining plastids are acquired by tertiary or secondary endosymbiosis by replacing the peridinin-plastid. In tree B, 19' is shown as the ancestral plastid, from which the peridinin plastid evolved. The prasinophyte-, cryptophyte- and heterokont-plastids were acquired by tertiary or secondary endosymbiosis, replacing the peridinin plastid. (Figure adapted from Kamran Shalchian-Tabrizi: "Studies on the Evolution of Chromists and Alveolates", dr.scient thesis, 2003 (Shalchian-Tabrizi 2003)).

1.7 THE CHROMALVEOLATES: A SUPERGROUP DEFINED BY A COMMON PLASTID ANCESTRY

A large fraction of known eukaryotic diversity is found within the supergroup chromalveolates, comprising the chromists (haptophytes, heterokonts and cryptophytes) and the alveolates (dinoflagellates, ciliates and apicomplexa) (see figure 1.1 and box 1.1). This group of organisms accounts for about half of the currently recognized species of protists and algae (Cavalier-Smith 2004a).

The photosynthetic members of the chromists (haptophytes, heterokonts and cryptophytes) share the pigment c_2 and have their plastid located within the endoplasmatic reticulum, and cluster as a monophyletic group in concatenated analyses of plastid-genes (Yoon et al. 2002b), indicating a common ancestry of this plastid.

The alveolates (dinoflagellates, apicomplexans and ciliates) all hold cortical alveoli or related structures beneath the plasma membrane, and have been shown to group as a monophyletic clade in several phylogenetic analyses of rRNA and protein-genes (Fast et al. 2002; Harper et al. 2005; Van de Peer and De Wachter 1997).

The members of the chromalveolate assembly share a few features supporting the postulated monophyly of this group; the photosynthetic members of chromists and the alveolates share a chlorophyll c containing plastid, as well as fundamentally similar mechanisms for plastid targeting of nuclear encoded proteins (Cavalier-Smith 2003a; Cavalier-Smith 2003b). The chromalveolates also share unique replacements of the plastid-targeted genes glyceraldehyde-3-phosphate dehydrogenase (GAPDH) and Fructose-1,6-bisphosphate (Fast et al. 2001; Harper and Keeling 2003; Patron et al. 2004), indicating that chromists and alveolates together constitute a monophyletic clade, the chromalveolates, with a common photosynthetic ancestor that engulfed a red alga in a secondary endosymbiotic event (Cavalier-Smith 1999). Despite these shared features and indications of a common ancestry, the chromalveolate supergroup has never been shown as a monophyletic clade in phylogenetic analyses of ribosomal- or protein coding genes (Harper et al. 2005). However, several molecular analyses suggest a close relationship between members of the chromists and the alveolates, as a relationship between the heterokonts and the alveolates have been indicated (Baldauf et al. 2000; Harper et al. 2005).

1.8 *TELONEMA:* A POSSIBLE EARLY CHROMALVEOLATE LINEAGE

As mentioned earlier, environmental surveys have revealed many sequences from unknown taxa indicating a massive amount of hidden eukaryote biodiversity, however, the number of undiscovered higher-level lineages remains unclear (Berney et al. 2004; Richards and Bass 2005). One potential high-level taxonomic lineage, of possible chromalveolate affiliation, was re-discovered in environmental sampling surveys of the pico-plankton diversity of the English Channel and Mediterranian Sea (Romari and Vaulot 2004; Shalchian-Tabrizi et al. 2005) Present in the clone libraries constructed from these surveys were sequences shown to belong to the unclassified organism *Telonema subtilis*, a heterotrophic taxon first described in 1913 by Griesmann from Roscoff and Naples (Shalchian-Tabrizi et al. 2005). Another possible member of the *Telonema* lineage with a SSU sequence similar to *Telonema subtilis*: *Telonema antarcticum*, was in parallel with the environmental sampling isolated from the Oslofjord and kept in culture for further molecular and morphological investigations (Klaveness et al. 2005; Shalchian-Tabrizi et al. 2005). The indications of the putative chromalveolate affiliation of the *Telonema* lineage are shown in phylognenetic SSU analyses (shown in figure 1.5). In this tree, *Telonema subtilis, Telonema antarcticum* and their related environmental sequences are placed as a distinct group outside all known clades, branching off at the base of a group consisting of stramenopiles, alveolates and cercozoans. This suggests that the *Telonema* lineage could comprise a new deep-branching phylum of possible chromalveolate origin.

FIGURE 1.5

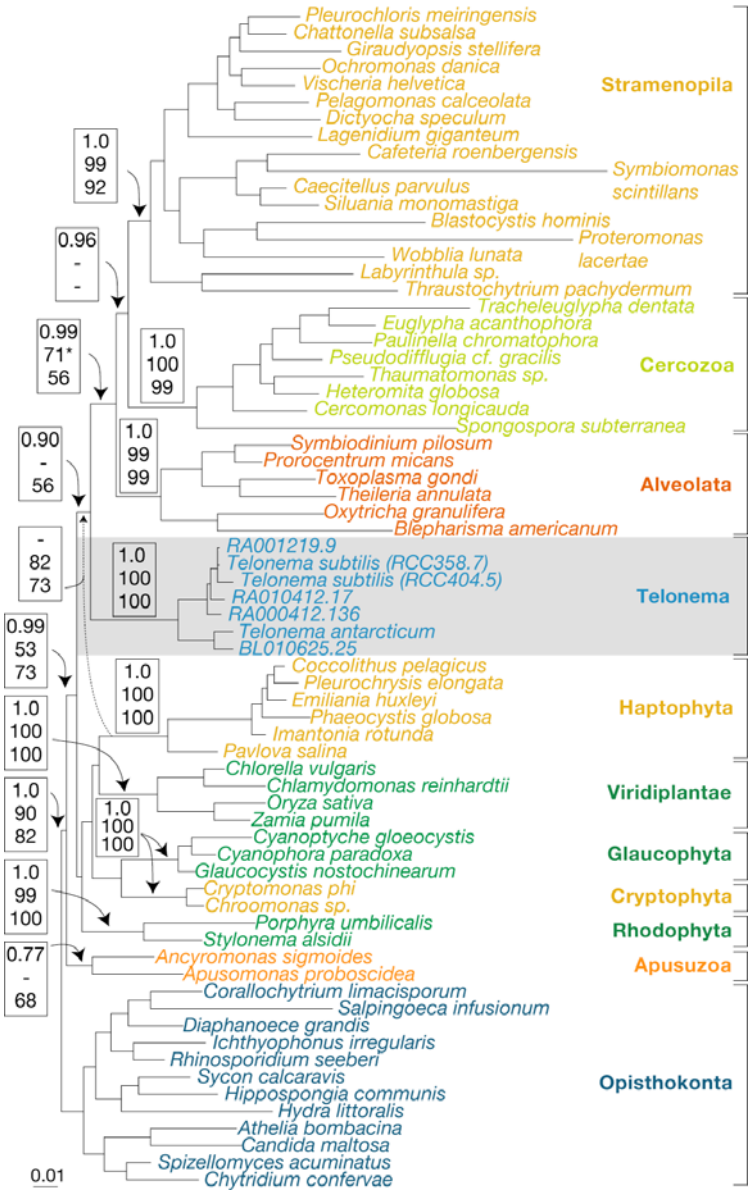

Figure 1.5: Phylogenetic analyses of SSU sequences. The numbers at the nodes represent from top to bottom posterior probability values >0.90, and bootstrap values >50% received from analyses with parsimony and distance (LogDet) methods, respectively. The asterisk indicates the bootstrap value for the clade except for the Cercozoa that clustered to the Haptophyta in the parsimony tree. The dotted line shows the placement of the haptophyte clade in ML, parsimony and distance analyses. (Figure and figure text from Shalchian-Tabrizi et al. 2005).

Unlike other environmental surveys, where the species from which the obtained sequences originate are unknown, the *Telonema* sequences could be identified to belong to a particular group of organisms, hence enabling morphological investigations necessary for a more accurate taxonomical placement. The morphological investigations showed that the two cultured *Telonema* species hold features also supporting the indicated relationship between *Telonema* and the chromalveolates (Shalchian-Tabrizi et al. 2005). Morphology and fine structure of *Telonema* are shown in figure 1.6. Traits supporting that *Telonema* is a close relative to the chromalveolates are the presence of mitochondria with tubular cristae and a complex cytoskeleton composed of layers of microtubuli and microfilaments (Shalchian-Tabrizi et al. 2005). Additionally, in *Telonema antarcticum*, tripartite tubular hairs and cortical alveoli are present (Klaveness et al. 2005), traits also found in different groups of chromalveolates (Andersen 2004; Taylor 2004).

However, as mentioned earlier, as phylogeny based only on SSU analyses have been shown to be unreliable for several species, additional analyses are necessary for deciding whether *Telonema* indeed comprise a separate phylum, possibly within or at the base of the chromalveolate supergroup. A discovery of a new deep-branching chromalveolate phylum will contribute significant information to the on-going controversy over the postulated chromalveolate monophyly, and will be of importance in the work searching to resolve the eukaryotic tree of life.

FIGURE 1.6

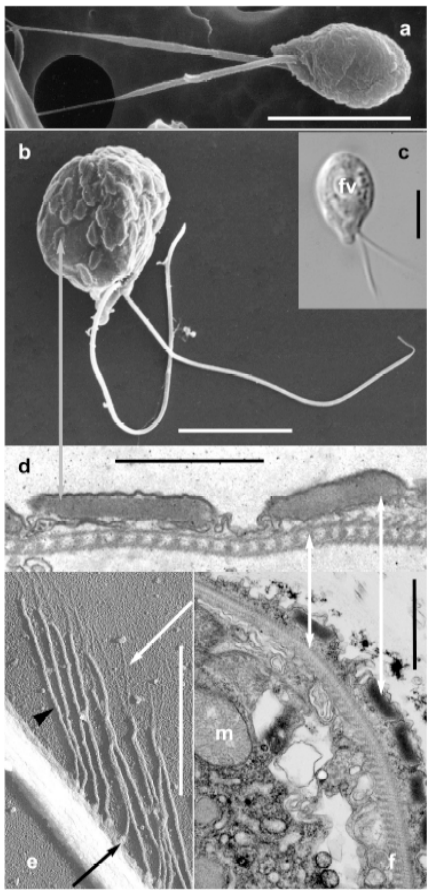

Figure 1.6: Morphology and fine structure of *Telonema*. Whole cell (a,b,c); a, *Telonema* subtilis scanning electron micrograph from natural sample (Guld or Naples). b, Cultured T.antarcticum from the Oslofjord, showing cortical alveoli (grey arrow); c, Light micrograph of cultures cell (RCC 404 from Roscoff) fv=food vacuole; Sub-cellular components (d,e,f); d, Section through cortical alveoli and cytoskeleton (white arrows); e, Detail of flagellum with tubular tripartite hairs as revealed by shadow cast whole-mount (see white arrow: distal filament; arrowhead: shaft; black arrow:base); f, Longitudinal section of embedded *T.antarcticum*, showing the cortical alveoli, complex cytoskeleton (white arrows), m=mitochondrium with tubular cristae. a, b, c – scale bar 5 μm; d, e, f – scale bar 1 μm. (Figure and figure text adapted from Shalchian-Tabrizi et al. 2005

1.9 AIMS AND RATIONALE FOR THE STUDY:

The overall objective of this thesis was to gain further understanding about the evolution, the diversity and the genomes of protists in general and the supergroup chromalveolates in particular.

The evolutionary history of chromalveolates will be addressed by two approaches, namely investigations of plastid evolution by investigating chloroplast replacement events in dinoflagellates, as well as analyzing the phylogeny of the potential deep-branching chromalveolate lineage *Telonema* for further understanding of the early evolution and putative monophyly of the group.

The following questions were formulated to address the main aim of the study:

- Is a magnetic bead based cell-surface binding DNA extraction kit suitable for use in molecular surveys of environmental samples and hitherto unknown species?
- Can phylogenetic inferences of multiple nuclear encoded genes be used to resolve dinoflagellate phylogeny, and thus the relationships between groups harboring different types of plastids?
- What is the ancestral plastid for dinoflagellates and how many times have anomaly pigmented plastids been acquired among this group?
- Can a revised dinoflagellate phylogeny and the discovery of novel groups, such as *Telonema,* give insight to processes in chromalveolate plastid evolution and provide information about the putative monophyletic origin of chromalveolates?

To investigate the aims, the following experimental approaches were utilized:

- Methods for investigation of protist bio-diversity will be addressed by testing a DNA kit with potential use for automated environmental sampling, putatively providing pure PCR-ready DNA of better quality than existing DNA-extraction kits, hence improving the efficiency of environmental sampling and DNA investigations of new species.

- cDNA libraries from two aberrantly pigmented dinoflagellates, *Gymnodinium chlorophorum* and *Karlodinium micrum* will be constructed to investigate the expressed genome of these species and generate genes of possible use in resolving the phylogeny of dinoflagellates.
- PCR-amplification and sequencing of nuclear encoded proteins that have shown to be useful for phylogenetic inference of eukaryotes will be carried out on the Telonemia phylum and a range of dinoflagellates.

2. MATERIALS AND METHODS

In this study, molecular approaches and bioinformatics tools have been used to address the aims described in the introduction.

- Two magnetic bead-based DNA extraction kits, using different protocols for DNA isolation, were tested qualitatively. To test the kit's possible usefulness in environmental sampling, DNA extraction and subsequent amplification of the small ribosomal subunit gene were carried out applying a range of laboratory cultures of protists. For one of the kits, the detection limit for algal cultures was tested.
- PCR amplification of the *hsp90* gene from a range of dinoflagellates as well as construction of cDNA libraries from two aberrantly pigmented dinoflagellate taxa were carried out for investigating genomic diversity and phylogenetic inference of dinoflagellates.
- PCR amplifications of the protein encoding genes *hsp90*, alpha-tubulin and beta-tubulin from *Telonema subtilis* and *Telonema antarcticum* were carried out.
- Phylogenies of dinoflagellates were inferred using Bayesian inference of phylogeny (described in 2.3), based on HSP90, small-ribosomal subunit (SSU), large ribosomal subunit (LSU), actin and GAPDH gene and amino acid sequences.
- Phylogenies of eukaryotes (including *Telonema*), based on the protein sequences generated in this study (HSP90, alpha-tubulin and beta-tubulin) were carried out by Kamran Shalchian-Tabrizi.

2.1 DNA ISOLATION ASSAYS AND PCR-BASED SEQUENCE ANALYSIS APPLYING SMALL-SCALE PROTIST CULTURES

2.1.1 Biological material and small-scale culture conditions

A variety of autotrophic and heterotrophic protist cultures were used in this study. Most of the cultures were provided from the culture collection at Program for Marine Biodiversity, Department of Biology, University of Oslo (UoO), except the

Chlamydomonas culture (kindly provided by Uwe Klein, Department of Molecular Sciences, University of Oslo). The small-scale cultures used are listed in table 2.1.

TABLE 2.1 Biological material used in this study

Species	Phylum
Gymnodinium chlorophorum	Dinophyceae
Karlodinium micrum	Dinophyceae
Alexandrium tamarense	Dinophyceae
Pyramimonas sp.	Prasinophyte
Isochrysis galbana	Haptophyta
Telonema subtilis	Telonemia
Rhinomonas sp.	Cryptophyta
Tetraselmis sp.	Cryptophyta
Ditylum brightwelli	Stramenopila
Chlamydomonas reinhardtii	Chlorophyceae

Table 2.1: Small-scale cultures used in DNA extraction experiments.

The majority of the cultures was grown in Erdschreiber seawater medium (Føyn 1934) at 15°C under illumination (12/12 h LD cycle), except for *Gymnodinium chlorophorum* and *Karlodinium micrum* which were grown in IMR/2 medium (Eppley et al. 1967), and *Chlamydomonas reinhardtii* which was grown in HS medium (see appendix 2). The heterotrophic protist *Telonema subtilis* was cultured with the haptophyte *Imatonia rotunda* as prey-organism.

The algal cultures used in the DNA-isolation experiments were enumerated by preserving an aliquot of the cultures in Lugol`s solution (0.6 M KI, 0.2 M I_2) before deciding the cell densities by counting individual cells in a Palmer-Malloney counting chamber using a light microscope.

The small-scale cultures were used directly for DNA extraction without centrifugation.

2.1.2 DNA-isolation assays

DNA was extracted from fresh cultures using two different magnetic-bead based systems; Dynabeads DNA DIRECT Universal from Dynal Biotech and ChlamCAP from Genpoint. All reagents used for DNA extraction, except ethanol and dsH_20, were supplied in the kits.

The DNA-isolation kit ChlamCAP (Genpoint AS, Norway) is a magnetic bead-based isolation kit that isolates the DNA in two steps by first associating the cells to the beads due to the bead's specially coated surface, followed by a subsequent washing step to eliminate PCR-inhibiting agents. After cell lysis, the DNA is captured to the same beads. The DNA was isolated according to the manufacturer's instructions. 700 μL of the cultures were used, and the DNA was eluted in 50 μL dH_2O.

The DNA DIRECT Universal kit (Dynal Biotech ASA, Norway) is also a magnetic bead-based isolation kit, developed for isolation of PCR-ready DNA from a variety of sample materials, e.g. cultured cells and tissues. With this system, the cells are lysed and the DNA subsequently captured to the surface of the Dynabeads and washed to eliminate PCR-inhibitors.

The DNA was extracted following the manufacturer's instructions. However, to be able to compare the results from this extraction to the ChlamCAP DNA isolation, the same amount of culture was used in this extraction as used in the ChlamCAP isolation, hence 700 μL of culture were used directly for extraction without prior centrifugation. The DNA/Dynabeads complex was then resuspended in 50 μL resuspension buffer, and the DNA was eluted off the Dynabeads by incubation at 65°C for 5 minutes.

As a high sensitivity of the DNA-isolation systems is required for efficient use in environmental sampling, the detection limit of the ChlamCAP kit was investigated. The algal cultures tested in this quantitative experiment were diluted 1:9 with BW-buffer (Genpoint AS, Norway) seven times before DNA-extraction was carried out on all dilutions to test the sensitivity of this kit.

All DNA samples were used directly for PCR or stored at -20°C.

2.1.3 DNA amplification

DNA from both isolation methods, as well as DNA from three additional species of dinoflagellates and *Telonema antarcticum* (some of the DNA isolations kindly provided from Emelita Nerli and Kamran Shalchian-Tabrizi) was amplified by use of Polymerase Chain Reaction (PCR). To measure a possible difference in the PCR-amplification yield between the Genpoint and the Dynal kit, as well as testing the sensitivity for the Genpoint kit, the small ribosomal subunit (SSU/18S) was generated from variety of laboratory algal cultures.

Several genes with possible use in phylogenetic inference of chromalveolates were amplified from the potential deep-branching lineage *Telonema* and several dinoflagellates. The 90-dDa heat shock protein (HSP90) gene sequence was amplified from *Telonema subtilis, Telonema antarcticum, Gymnodinium chlorophorum*, *Karlodinium micrum, Karenia brevis, Karenia mikimotoi* and *Alexandrium tamarense*, and alpha-tubulin and beta-tubulin were amplified from *Telonema subtilis* and *Telonema antarcticum*.

All together, 19 genes from a variety of species were amplified.

All PCRs included a negative control to check for contaminants in the reagents, and a positive control when possible. All PCR products were loaded and separated on a 1% agarose/0.5 TBE gel stained with ethidium bromide, visualized under UV-light and excised from the gel for cloning. All PCR-primers used in this study are shown in table 2.2.

The PCR-products were used directly in cloning, or they were stored at –20°C.

Small ribosomal subunit amplification:

The small ribosomal subunit (SSU) was amplified by PCR using eukaryote-specific primers. The SSU amplifications were performed on a Biometra T1 thermocycler in 25 or 50 μL volumes with following temperature cycles: 15 min at 95°C; 45 cycles of 15 s at 95°C, 30 s at 53°C and 1 min and 30 s at 72°C; and 10 min at 72°C. 1-10 μL of DNA template was used. The PCR-volumes contained 10 pmol of each primer, 200 μM dNTP, 1X HotStar Taq PCR buffer with MgCl and 1.5 U HotStar Taq DNA polymerase (Qiagen Sciences, USA).

Hsp90 amplification:

When amplifying the *hsp90* gene, degenerate primers were used in a semi-nested system. The PCRs were carried out in two rounds, where the primers HSP90-100F and HSP90-970R (Simpson et al. 2002) were used initially to make amplicons, invisible on the gel, that were reamplified using the same forward primer and reverse primer 8-HSP90-KeelinginnerR (Leander and Keeling 2004). The primer sequences are shown in table 2.2. The following temperature cycles were used in the reactions: 2-15 min at 95°C; 35-45 cycles of 15 s at 95°C, 20 s at 48-52°C and 1 min and 30 s at 72°C; and 10 min at 72°C. An annealing temperature of 48 °C was used in the initial round of PCR, and raised to 52 °C in the second round. All *hsp90* amplifications were carried out on a Perkin-Elmer thermocycler (GeneAmp PCR System 2400, Perkin-Elmer, USA) using 1 μL of template (of DNA-extraction or a 1:10 dilution of the initial PCR product), 40 pmol of each primer, 200 μM dNTP, 1x PCR buffer, 0.25 μg BSA and 1.5 U enzyme in a 25 μL PCR-volume. Different enzymes were used; HotStar Tag (Qiagen Sciences USA), HotMaster Taq (Eppendorf, Germany) and Taq DNA polymerase (Invitrogen, USA). In reactions where Taq DNA polymerase was used, 1.5 mM $MgCl_2$ was added, however in reactions using HotStar or HotMaster, $MgCl_2$ was supplied with the PCR-buffer. In reactions where HotMaster Taq polymerase was used, the elongation temperature was set to 68° instead of 72°.

Alpha- and beta-tubulin amplification:

Amplification of alpha-tubulin and beta-tubulin from *Telonema* was carried out using a Biometra T1 thermocycler, with following temperature cycles: 15 min at 95°C; 45 cycles of 15 s at 95°C, 30 s at 59-61°C and 1 min and 30 s at 72°C; and 10 min at 72°C. PCR volumes were 25 μL, and contained 40 pmol of each primer, 200 μM dNTP, 1X HotStar Taq PCR buffer with MgCl, 25 pmol BSA and 1.5 U HotStar Taq DNA polymerase (Qiagen, USA). The degenerate primers α-tubulin A, α-tubulin B, β-tubulin A and β-tubulin B were used (Edgcomb et al. 2001).

TABLE 2.2 Primers used for PCR

Target	Forward primer	Reverse primer
SSU	1F*: AACCTGGTTGATCCTGCCAGT	1528R*: TGATCCTTCTGCAGGTTCACCTAC
Hsp90	100F: CAGCTGATGTCCCTGATCATYAAYACNTTYTA	970R: TCGAGGGAGAGRCCNARCTTRATCAT
Hsp90	100F: CAGCTGATGTCCCTGATCATYAAYACNTTYTA	8KEELINGINNER: CGCCTTCATDATNCKYTCCATTRTTNGC
α-TUB	A: RTGNGGNAAYGCNTGYTG	B: CCATNCCYTCNCCNACRTACCA
β-TUB	A: GCAGGNCARTGYGGNAAYCA	B: AGTRAAYTCCATYTCRTCCAT

*1F and 1528R are universal eukaryotic 18s primers

Table 2.2: The primers used for targeted PCR amplification of rRNA and protein encoding genes

2.1.4 TOPO-TA cloning

Before carrying out the cloning reaction, PCR products of the protein genes *hsp90*, alpha- and beta-tubulin from the *Telonema* species and the dinoflagellate species were gel-purified using the Wizard SV Gel and PCR clean-up system (Promega, USA). All reagents and tubes used were supplied in the kit.

The band of predicted length was excised of the gel using a clean razor blade, and the PCR-products were extracted from the gel following the manufacturer's instructions.

The purified PCR product was loaded on a 1% agarose/0.5 M TBE-buffer gel stained with ethidium bromide and visualized in ultraviolet light for deciding the yield.

The purified PCR-products were ligated into the pCR-2.1 TOPO vector using the TOPO-TA cloning kit (Invitrogen, USA). A further description of the TOPO-cloning method is found in box 2.1.

The cloning reactions were set up according to table 2.3. The quantity of PCR-products used was adjusted according to the yield from the gel purification process.

Box 2.1

TOPO-TA cloning

The TOPO cloning reaction is a one-step cloning strategy for PCR products amplified by *Taq*-polymerase. The *Taq* polymerase adds a single a to the 3' ends of the amplicons that enable the PCR-products to be ligated into the plasmid vector due to the single 3`-thymidin overhangs in the supplied linearized plasmid (the TOPO-vector). The plasmid also have a covalently bound Topoisomerase I that binds specifically to duplex DNA, cleaves the phosphodiester backbone and conserves the energy by formation of a covalent bond between the 3`-phosphate on the cleaved strand and a tyrosyl residue of Topoisomerase I. The phospho-tyrosyl bond is then attacked by the 5`hydroxyl and the Topoisomerase subsequently released. (Reference: www.invitrogen.com).

TABLE 2.3 TOPO cloning reaction

Reagent	Quantity
PCR-product	1-3 μL
Salt solution	1 μL
Sterile water	1-3 μL
TOPO vector	1 μL
Total quantity	6 μL

Table 2.3: The set-up of the TOPO-TA cloning reactions

The reaction mix was mixed gently and incubated for 30 minutes at room temperature. The longest possible incubation time recommended in the instructions following the kit was chosen to ensure maximum yield of colonies. Competent TOP10F *E.coli*-cells were thawed on ice, and 2 μL of TOPO cloning reaction were added to a vial of the cells for transformation. The transformation mix was incubated on ice for 5 minutes, before the cells were heat-shocked for 30 seconds at 42 °C without shaking.

250 μL of room temperature S.O.C medium were added to the cells, the tubes were capped and shaked horizontally for 1 hour at 37°C before 50-70 μL of the transformations were spread on prewarmed LB plates containing 40 μL of 20 mg/ml X-gal (Invitrogen, USA) and 100 mg/ml ampicillin. Two volumes of transformation reaction were plated to ensure that at least one plate would have evenly spaced colonies. The plates were incubated overnight at 37°C.

2.1.5 Analyzing positive clones

The TOPO-TA pCR-2.1 kit utilize blue-white selection to screen for transformed colonies, hence light blue and white colonies were picked and analyzed for insert by PCR with the primers HR/HU and M13F/M13R, flanking the insert site. A standard PCR protocol was used, and colonies with correct insertion were used to make bacterial overnight cultures that were incubated overnight at 37°C in LB-medium with ampicillin.

2.1.6 Plasmid isolation

The plasmids from the overnight cultures of transformed bacteria were purified using the BIO-RAD Quantum Prep Plasmid Miniprep Kit (BIO-RAD, USA). The BIO-RAD kit uses the traditional alkaline lysis technology for plasmid DNA isolation, and utilizes the silicon dioxide exoskeleton of diatoms as the DNA binding matrix.
Overnight cultures of 2 ml transformed cells in LB-medium were used. The isolation was done according to the manufacturer's instructions.

2.1.7 DNA sequencing

Sequencing was carried out using plasmids with PCR-insert rather that directly sequencing of PCR-products. As initial sequencing tests where PCR-products were used directly proved not to be successful, cloning was carried out before all the following sequencing reactions (see box 2.2).

Box 2.2

Sequencing of plasmids versus direct sequencing of PCR-products

Sequencing of plasmids with inserted PCR-products has the benefit that it produces high quality sequence reads, and the problem with mixed peaks on the sequencing chromatogram due to non-pure PCR-products is avoided. On the other hand, this method increases the effect of additional errors that incorporates during plasmid copying in the bacteria, since all plastids may contain the same error.

Some of the plasmids were sent to MWG Biotech AG, Germany, for sequencing while others were sequenced at the MegaBACE lab at University of Oslo, or at the sequencing facility at department of Zoology, University of Oxford. Samples for MWG Biotech and MegaBACE lab were delivered the sequencing labs as isolated plasmids, however, the

sequencing reactions analyzed at the sequencing lab at Oxford University were carried out on the lab before delivering the reaction to the sequencing lab for gel analysis. The sequencing reaction utilized ABI BIGDYE^{TM} Terminator Cycle Sequencing Ready Reaction Kit (Applied Biosystems, USA), and was set up as shown in table 2.4.

TABLE 2.4 Sequencing reaction set-up

Reagent	**Quantity**
Template	2-6 μL
Primer	3 pmol
Sequencing buffer	5X
Sterile water	-

Table 2.4: The set-up of the sequencing reactions carried out at the sequencing facility at the University of Oxford. The sequencing buffer contains BIGDYE dye terminator cycle sequencing pre-mix contains labeled A-dye terminator, C-dye terminator, G-dye terminator and T-dye terminator, dNTP, AmpliTaq DNA polymerase, $MgCl_2$ and Tris-HCl buffer, pH 9.0.

The cycling conditions for the sequencing reactions were: 25 cycles of 10 s at 96°C, 5 s at 50°C and 4 minutes at 60°C.

The reactions were cleaned by adding 25 μL 95% ethanol and 1 μL NaOAc to each sample, leaving the samples in room temperature for 15 minutes and then centrifuged at 3000 rpm for 30 minutes before discarding the supernatant.

Sequence analyzes were carried out on sequencing machines ABI3700/ABI3730 (Applied Biosystems, USA).

Different primers were used for sequencing. Initial sequences were obtained by using M13R and M13F sequencing primers, and additional internal sequencing primers were designed for those sequences that were needed to be full-length. The primer sequences are shown in table 2.5.

TABLE 2.5 Sequencing primers

Target	Sequence	Tm °C
K.brevis hsp90	L482: GGAACAAAAGTGATCTGCTA	52.98
	U717: AAGCACCTCTTCACAAGATT	54.04
G.chlorophorum hsp90	L481: TTTCACTGTCCAGAAAGACA	54.20
	U729: CATTTCTTCACGAGGTTTTT	54.53
A.tamarense hsp90	L512: ATGGCGGAAGTACTACAGTT	54.00
	U682: TGACCAAGTTCTTCTTGATG	53.69
G.mikimotoi hsp90	L651: CGAGAAATCCAAAGAGAAAG	54.33
	U851: AGGTCTTCAGAATCGACAAC	54.26
K.micrum hsp90	KMIL: GAAATGGTTCATGGTGAGGT	57.26
	KMIR: GCAGGATCTTGTTCTGCTG	57.01
T.subtilis/T.antarcticum hsp90	490F: ACGACGACGAGCAGTACATC	58.91
	1026R: ATGTTCAGGGGAAGGTCCTC	60.31
***T.subtilis* β-tubulin**	BtubL935Tsub: AGCTCACATCATGTTCTTGG	56.21
TOPO-TA vector insert	M13F(-20): GTAAAACGACGGCCAG	53.20
	M13R: -CAGGAAACAGCTATGAC	46.11

Table 2.5: Primers used for sequencing of genes from several dinoflagellates, *Telonema subtilis* and *Telonema antarcticum.* The custom made sequencing primers were all ordered and synthesized at MWG-Biotech, Germany.

2.2 cDNA LIBRARY CONSTRUCTIONS FROM LARGE-SCALE CULTURES OF DINOFLAGELLATES

2.2.1 Biological material and large-scale culturing

To generate sufficient amounts of cells from which enough mRNA/DNA to make cDNA-libraries could be extracted, large-scale culturing of *Karlodinium micrum* and *Gymnodinium chlorophorum* was carried out. Cultures of the dinoflagellate species *Gymnodinium chlorophorum* and *Karlodinium micrum* were grown in a modified IMR/2 medium (Eppley et al. 1967) in several 10 liter polycarbonate- or glass bottles. To ensure a rapid growth, the algal cultures were grown under 24 h illumination, however, approximately a week before harvesting the cultures, the illumination was set to a10/14 h LD cycle to avoid possible down-regulation of chloroplast genomes.

A total of approximately 70 liters of *Karlodinium micrum* culture and approximately 100 liters of the less dense *Gymnodinium chlorophorum* culture were grown and subsequently

harvested in log-face and centrifuged in a continuous-flow centrifuge by adding small amounts of algal culture through a pasteur pipette. After centrifugation, the supernatant was discarded and the algal samples were immediately frozen in liquid nitrogen and subsequently preserved at -80° or freeze dried.

2.2.2 Construction of cDNA libraries

Cells from 40 liters of *K.micrum* and 40 liters of *G.chlorophorum* were sent to GENterprise GENOMICS in Germany for construction of cDNA-libraries.

The cDNA library from *Karlodinium micrum* was constructed applying an oligo (dT) primer with an internal NotI site. The ligation of the Sal I adapters and the subsequent restriction using NotI allowed directional cloning into the vector pSport1 x SalI x NotI as shown in figure 2.1. This vector contains the lacZ gene, hence enabling blue-white screening of clones with insert.

FIGURE 2.1

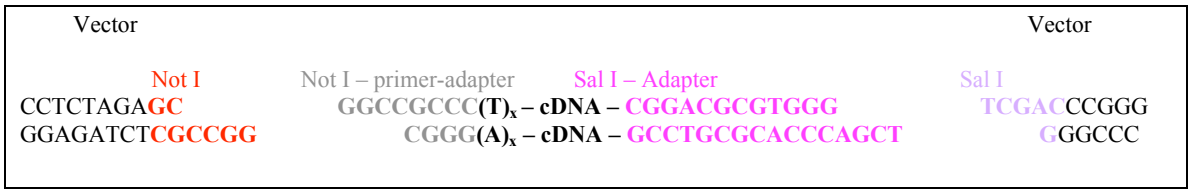

Figure 2.1: The restriction sites and primer adapters used for construction of *Karlodinium micrum* library

The constructed *K.micrum* cDNA library was returned to us for sequencing. Approximately 200 clones from the *K.micrum* cDNA-library were grown in 2 ml LB-medium, and the plasmids were isolated with Eppendorf FastPlasmid isolation kit (Eppendorf, Germany). This kit lyses and resuspends bacterial cells in one step, and the released plasmid DNA is captured directly from the lysate on a filter device during centrifugation. As over 200 clones were to be sequenced, the rapid and simple protocol of FastPlasmid was preferred for extracting plasmids from the cDNA-library clones instead of the BIO-RAD kit described in chapter 2.1.7. 5'-end sequencing of the cDNA was done at the sequencing facility at University of Oxford, as described in chapter 2.4.5.

The cDNA-library from *Gymnodinium chlorophorum* was constructed using the SMART technology, selectively priming the mRNA by their poly-A tail using an oligo(dT) primer containing a built-in sequence for restriction and PCR-amplification. Full-length sequences were generated using primer extension. By this method, synthetic adapter sequences incorporates at both ends of the cDNA: by the oligo(dT) primer at the 5'-end, and by a specialized SMART oligo that hybridizes to the cytosines added by the reverse transcriptase at the 3'-end. The fragments were then cut using restriction enzymes and cloned into the vector psport1.

2.3 BIOINFORMATIC TOOLS AND PHYLOGENETIC ANALYSES

2.3.1 Single-gene and concatenated alignments

Protein- and nucleotide sequences of HSP90 from a wide range of organisms, and actin- and GAPDH sequences of different alveolates were obtained from GenBank (http://www.ncbi.nlm.nih.gov/). The sequences were edited and assembled using BBEdit 6.1 for OS X, aligned in ClustalX and manually inspected and adjusted in MacClade version 4.0 PPC.

Initial alignments for alpha-, beta-tubulin, SSU and LSU were provided by Kamran Shalchian-Tabrizi, and were further enlarged by adding additional sequences from GenBank.

The new sequences generated in this study were checked for identity using NCBI BLAST (http://www.ncbi.nlm.nih.gov/BLAST/) and added to the nucleotide alignments using MacClade, before they were translated into protein sequences (in MacClade) and added to the protein alignments for phylogenetic analysis.

Ambiguously aligned areas were excluded from the alignments before the phylogenetic analysis.

The HSP90, alpha- and beta-tubulin alignments that were used in the phylogenetic analyses of *Telonema* contained sequences from a wide range of eukaryotes, representing all main eukaryotic groups from which these sequences were available. The HSP90 alignments used for investigating dinoflagellate phylogeny were constrained to contain

only dinoflagellate species, *Oxyrrhis marina*, *Perkinsus marinus* and 3 apicomplexan and ciliate outgroup taxa. The alignment dimensions are shown in table 2.6. Individual SSU and LSU alignments were also constructed, containing sequences from the same species represented in the HSP90 alignment.

Concatenated alignments combining different gene alignments were made using BBEdit 6.1 for OS X. The large HSP90 alignment, including representatives from all major eukaryotic supergroups and *Telonema*, was combined with small ribosomal subunit (SSU), alpha- and beta-tubulin alignments. The dinoflagellate HSP90 alignment was combined with SSU and large ribosomal subunit LSU. The species missing available LSU sequence were filled with question marks.

The alignment dimensions are shown in table 2.6.

TABLE 2.6 Alignment dimensions

Alignment	Number of taxa	Number of characters
HSP90 (dinoflagellate)	17	523
HSP90+SSU+LSU	15	2398
SSU	17	1448
LSU	12	400
Actin	19	250
GAPDH	26	235
Alpha-tubulin	40	355
Beta-tubulin	39	383
HSP90 (*Telonema*)	33	465
HSP90+alpha-tubulin+beta-tubulin	30	1203
HSP90+SSU (*Telonema*)	33	1813

Table 2.6: Alignment dimensions of single-gene and concatenated alignments.

2.3.2 Primer design

The custom made sequencing primers were designed using Primer3 Input (primer3_www.cgi v 0.2) (http://frodo.wi.mit.edu/cgi-bin/primer3/primer3_www.cgi)

2.3.3 Intron folding

The secondary structure of the insertion found in *Alexandrium tamarense* was estimated using the web interface of the Vienna RNA Secondary Structure Prediction (http://rna.tbi.univie.ac.at/cgi-bin/RNAfold.cgi).

2.3.4 Selecting protein substitution models for phylogenetic analyses

The dinoflagellate protein gene alignments were tested in Prottest (http://darwin.uvigo.es/software/prottest.html). This is a program for finding the most appropriate protein evolution model for a given alignment. As different models can be applied for estimating the relative rates of amino acid substitution, this program estimates the best fitting candidate models for the datasets based on two different criterions based on two different criteria: the Akaike Information Criterion (AIC) and the Bayesian Information Criterion (BIC).

The general time reversible (GTR) model of nucleotide substitution was used in the single-gene SSU and LSU analyses, as well as in the SSU and LSU partition of the combined HSP90 + SSU + LSU dataset

The WAG amino acid substitution model was used in the *Telonema* analyses.

2.3.5 Phylogenetic analyses

PAUP*v4.0b10 for Macintosh was used to construct neighbor-joining trees used to ensure that the DNA-sequences obtained from the *Telonema/Imantonia* culture belonged to *Telonema subtilis*, and not the haptophyte prey-organism, before doing more accurate and extensive analyses.

The large HSP90 alignment including *Telonema*, as well as the concatenated alignments containing this protein gene sequences, was analyzed by parsimony, distance, maximum likelihood and Bayesian methods. (Analyses done by Kamran Shalchian-Tabrizi.)

The alignments with alveolate amono acid sequences from actin, GAPDH, HSP90 and the concatenated alignments were analyzed in a Bayesian framework. For more information about Bayesian inference, see Box 2.3.

Box 2.3

BAYESIAN INFERENCE OF PHYLOGENY

Bayesian inference of phylogeny is based on the posterior probability distribution of trees. The posterior probability is approximated using a simulation technique called Markov chain Monte Carlo (MCMC), takes account of the prior probability, the model and the data. The prior distributions of the parameters are formulated before the analyses, and shows beliefs about the parameters before any data has been sampled. The posterior probability of a tree shows the probability of the tree according to the phylogenetic observations, and is proportional to the likelihood times the prior probability of that tree. When the prior probability distribution is flat, i.e. if all parameters have the same prior probability, the posterior distribution is proportional to the likelihood distribution. The prior distribution can be decided using earlier analysis results, i.e. by using the posterior probability of one analysis as the prior probability in the following analysis (Felsenstein 2003).

The stochastic simulation used by MCMC samples topologies from the posterior distribution of trees, and inferences are calculated using the Bayesian formula. The posterior probability distribution of trees can contain multiple peaks, and because of this, the MCMC can become trapped in a local optima separated by deep valleys from other, possible higher peaks. A heated chain sees the tree landscape as flattened relative to the cold chain, and by applying multiple heated chains to the analyses, the deep valleys can be more readily crossed. This is called Metropolis-coupled MCMC $(MC)^3$, and allows multiple peaks in the tree landscape be explored more extensively (Nylander et al. 2004).

Bayesian analyses were carried out using MrBayes*v3.0b4 on the Bioportal (http://www.bioportal.uio.no/). Different among-site rate variation models were tested in the phylogenetic inferences: gamma distributed rates across sites (Γ), a combination of gamma-distributed rates across sites with a covarion substitution model (Γ + COV), a proportion of the sites invariable and the remaining sites of gamma-distributed rates (Γ + I) or a combination of these settings (Γ +I + COV). The covarion-like model of substitution allows the rate at a site to change over its evolutionary history, allowing the sites to be either on or off. Three heated and one cold chain was used in the Metropolis coupled Markov chain Monte Carlo (MCMC), and 1,000,000-2,000,000 generations was carried out. Randomly generated trees were used as starting point for the MCMC chains, and burn-in trees was set to 3,000-5,000 trees based on assessment of the likelihood plots. Sampling of trees was done every 100 generations, and the consensus of the sampled trees was used to calculate the posterior probability for the tree topology. In the analyses of the concatenated alignments one char set per gene was defined, and these char sets

were defined as the partition and used in the analyses. Different model parameters were unlinked across the partitions of the data to allow parameters to be different across partitions. The parameters unlinked in the HSP90+SSU+LSU concatenated alignments were the parameters for gamma shape, branch lengths, switching rate for the covarion model, substitution rates of the GTR model and the character state frequencies.

2.3.6 Analyzing the cDNA-library sequences

The sequenced cDNAs were analyzed using the Salmon Gene Project (SGP) pipeline (Analyses done by Torgeir Ruden Andersen) for automatic quality check, vector-trimming and GO-annotation. The sequences were aligned with public database sequences applying the SGP standalone version of NCBI BLAST. Each query sequence was run against different databases: Blastx (translated query vs protein database) was run against the pdb, swissprot and nr protein databases, and blastn (nucleotide query vs nucleotide database) was run against the nr polynucleotide sequence database. Automatic annotation of the gene products was carried out, based on Gene Ontology (GO) terms from the Gene Ontology Consortium (http://www.geneontology.org/). Sequences with BLAST hit E-values lower than $1.0e^{-10}$ against the pdb database (blastx) or lower than $1.0e^{-15}$ against the swp (blastx) and nr (blastx and blastn) database were annotated by applying the GO assignments for the UniProt database produced by the GOA-project (http://www.ebi.ac.uk/GOA/) of the European Bioinformatics Institute.
The cDNA-sequences also were aligned against the NCBI EST-database (http://www.ncbi.nlm.nih.gov/dbEST/).

3. RESULTS

The results of this study comprise several parts, somewhat independent, but also connected as incorporated building blocks together contributing to decipher the overall aim addressed in the introduction of this thesis. A novel DNA isolation method will be tested, cDNA sequences from cDNA libraries will be analyzed and phylogenetic analyses will be carried out using different molecular markers. The investigated protist groups are the dinoflagellates, addressing plastid evolution, and a deep-branching organism, *Telonema*, whose ancestor possibly diverged from its relatives early in the evolution of the chromalveolate lineage.

3.1 TESTING MAGNETIC BEAD-BASED DNA-ISOLATION SYSTEMS FOR POTENTIAL USE IN ENVIRONMENTAL SAMPLING

Efficient DNA isolation and PCR-amplification of molecular markers are required for preventing random errors and systematic biases in molecular surveys of environmental samples. Magnetic bead-based extraction methods provides a faster, more efficient and less hazardous protocol for isolation of PCR-ready DNA compared to the traditional DNA-isolating methods involving organic solvents, and the method is also well suited for automation, a feature of use in surveys of biodiversity and surveillance of harmful algal blooms. In this study, initial testing of two different magnetic bead-based DNA-isolation systems (ChlamCAP, Genpoint AS, Norway and DNA Direct, Dynal Biotech AS, Norway) of potential use in environmental sampling was carried out.

As the Genpoint kit not previously had been applied to eukaryotes, and the Dynal kit only had been tested on a few protist taxa, the kits were tested qualitatively by extracting PCR-ready DNA from a broad range of laboratory cultures of autotrophic and heterotrophic eukaryotes. Both kits tested utilize magnetic beads for DNA extraction. However, as the protocols and the rationale behind the procedures are quite different (see introduction), there could possibly be differences between the two kits considering DNA-yield and DNA purity, features affecting the PCR-amplification efficiency and thereby the utility of the kits in environmental sampling.

For the kits to be useful in molecular surveys of environmental samples, high sensitivity is required. As the detection limit of the ChlamCAP kit not earlier had been tested on algal-cultures, quantitative experiments were carried out in this study applying several species representing major algal groups.

3.1.1 Qualitative results using the kits ChlamCAP and DNA Direct

DNA was isolated and PCR-amplification was carried out on the species listed in table 3.1 (*Chlamydomonas reinhardtii, Karlodinium micrum, Gymnodinium chlorophorum, Alexandrium tamarense, Isochrysis galbana, Rhinomonas sp., Tetraselmis sp., Pyramimonas sp., Telonema subtilis* and *Ditylum brightwellii*), representing a wide selection of algal and protist groups. Agarose gels with the SSU PCR-amplification products from the some of the DNA-extraction experiments are shown in figure 3.1. Both kits gave sufficient DNA yield for PCR amplification of the small ribosomal subunit (SSU) in all the species tested.

FIGURE 3.1: Qualitative results

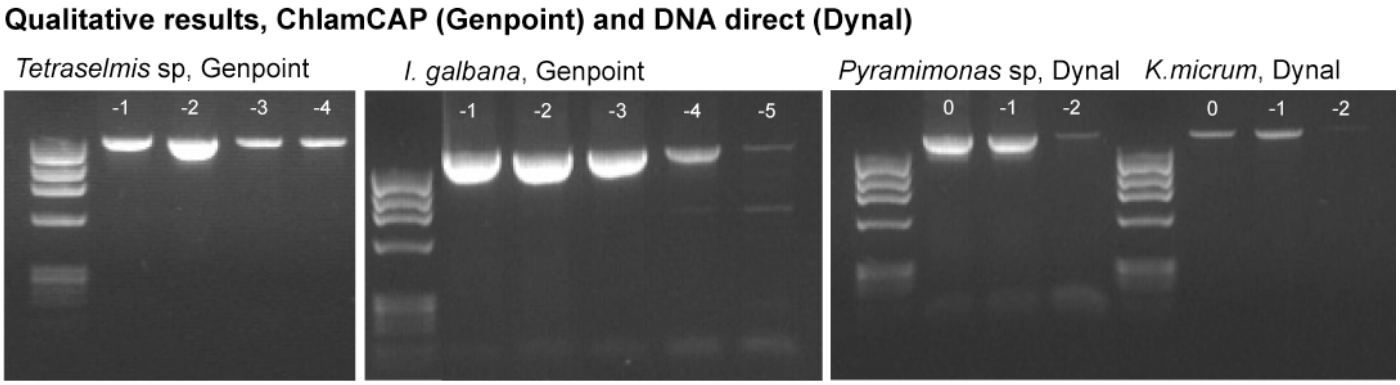

Figure 3.1: The agarose gel pictures show the PCR-amplifications of the small ribosomal subunit (SSU) using ChlamCAP and Dynal DNA-extraction kits. DNA marker used is HaeIIIphi174. Dilutions of the DNA-extraction used in the PCR-reaction range from 10^0 (0) to 10^{-5} (-5).

3.1.2 Detection limit of the ChlamCAP kit

The sensitivity of the ChlamCAP kit was tested using a total of five species from four different phyla (*Chlamydomonas reinhardtii, Karlodinium micrum, Isochrysis galbana, Tetraselmis sp. and Pyramimonas sp*.). The quantitative results are listed in table 3.1, and agarose gels with PCR-amplification products from some of the quantitative experiments are shown in figure 3.2. The detection limit of four of the species tested (*C.reinhardtii, K.micrum, Tetraselmis* sp. and *Pyramimonas* sp.) was measured to be between 1.5 x 10^3 and 2.8 x 10^3 cells/ml. For one of the species, the sensitivity was measured to be 1.6x10^5 cells/ml (*I.galbana*) – an unexpected low sensitivity.

TABLE 3.1 Species from which PCR amplifiable DNA was extracted

Species	Group	Amplicon	Sensitivity*
Chlamydomonas reinhardthii	Chlorophyceae	18S rDNA	1.5x10^3 cells/ml
Karlodinium micrum	Dinophyceae	18S rDNA	2.0x10^3 cells/ml
Gymnodinium chlorophorum	Dinophyceae	18s rDNA	N/A**
Alexandrium tamarense	Dinophyceae	18s rDNA	N/A**
Isochrysis galbana	Haptophyta	18S rDNA	1.6x10^5 cells/ml
Rhinomonas sp.	Cryptophytes	18s rDNA	N/A**
Tetraselmis sp.	Prasinophyta	18S rDNA	2.1x10^3cells/ml
Pyramimonas sp.	Prasinophyta	18S rDNA	2.8x10^3 cells/ml
Telonema subtilis	Telonemia	18s rDNA	N/A**
Ditylum brightwellii	Stramenopile	18s rDNA	N/A**

*: Measured using ChlamCAP
**: Not measured in this study
Table 3.1: Table showing species from which PCR amplifiable DNA was extracted using ChlamCAP (Genpoint AS) and DNA direct (Dynal Biotech AS).

FIGURE 3.2 Quantitative results

Sensitivity testing, ChlamCAP (Genpoint)

K.micrum *C.reinhardtii*

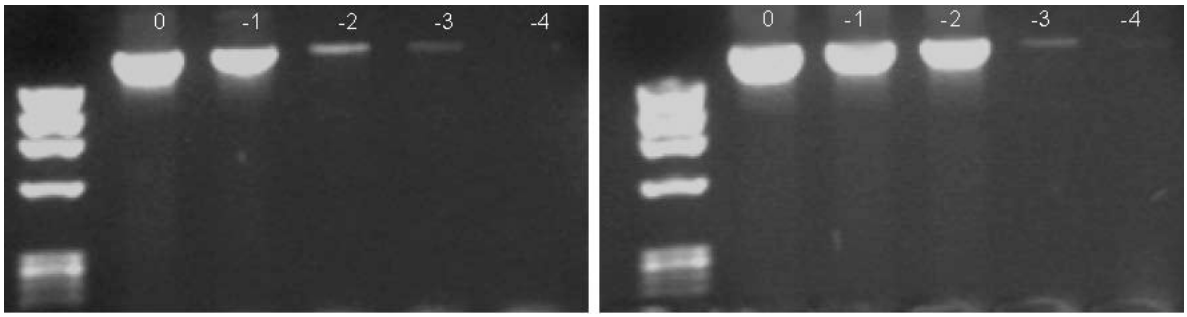

Figure 3.2: Agarose gel pictures depicting PCR-amplicons of SSU from the sensitivity testing of the ChlamCAP kit. Dilutions of algal-cultures range from 10^0 (0) to 10^{-4} (-4). DNA marker used is HaeIIIphi174.

3.2 GENOMIC DIVERSITY OF DINOFLAGELLATES: cDNA LIBRARIES FROM TWO ABERRANTLY PIGMENTED TAXA

cDNA-libraries from *Karlodinium micrum* and *Gymnodinium chlorophorum*, two dinoflagellate species of particular interest for evolutionary studies of chromalveolates (see introduction), were constructed to generate sequences for investigation of their genomic diversity and evolutionary history.

3.2.1 *Karlodinium micrum* cDNA library

Two hundred and twenty seven 5'-end sequenced cDNAs were analyzed using the Salmon Genome Project (SGP) pipeline as described in chapter 2.5.3. When processing the 227 sequences, 42 of the sequences failed due to bad sequence quality. 27 of the 42 failed sequences had poly-A tails early in the sequences, which probably caused the failed sequencing. The remaining 185 sequences were checked manually, and 14 of these were excluded from further analyses due to extensive poly-A tails.

The remaining 171 sequences of good quality were used for further analyses. The distribution of the trimmed sequence lengths without poly-A tail is shown in figure 3.3. The average length of the sequences was approximately 480 base pairs (bp).

FIGURE 3.3 Distribution of trimmed cDNA lengths

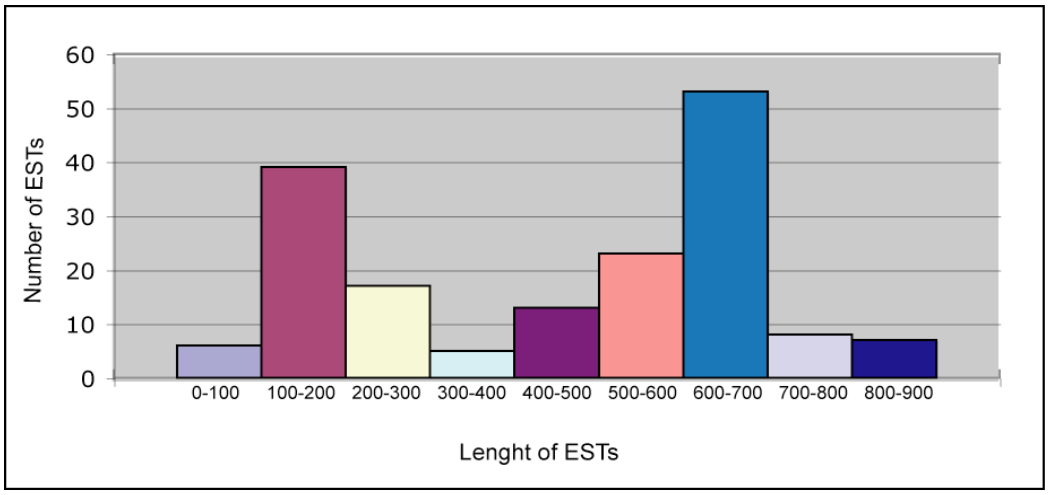

Fig,3.3: Distribution of readable sequence length for cDNAs from *Karlodinium micrum*. The total number of analyzed good-quality sequences was 171, and the average sequence length was approximately 480 base pairs.

BLAST searches were carried out using the quality-checked cDNA sequences, and sequences were identified by BLASTx and BLASTn searches against different databases (swissprot, pdb and nr). Table 3.2 lists the tentatively identified clones according to the BLAST searches sorted in functional categories, based on the modified EGAD-categories as presented in Kuo et al 2004 (Kuo et al. 2004). The average length of the annotated sequences was longer than the average sequence length, 615 bp.

TABLE 3.3: List of tentatively identified clones

Functional category	Clone no.	Putative product
Cell structure/motility	38	Actin
	97	Dynein light chain
RNA synthesis/transcription factors	85	DEAD BOX RNA helicase
	199	Ribonucleoprotein
	1-39	Major basic nuclear protein,Hcc
Protein synthesis/turnover	106	Ubiquitin
	4	Heat shock protein 70
	1-54	Polyubiquitin
	118	Elongation factor 3
	143	60S ribosomal protein L34-a
	1-29	Proteasome subunit

Metabolism	138	Qin-induced kinase
	35	Flavin-binding family monooxygenase
	139	Phosphoglycerate mutase 1
	44	Triose Phosphate Isomerase
	173	Fumarate reductase, NADH
	68	Pyridine nucleotide transhydrogenase
	95	Vacuolar ATP synthetase
	16	S-adenosyl-L-homocystein hydrolase
	168	Nucleoside phosphorylase* (pdb)
	20	GTP-binding protein era* (pdb)
	1-41	Oxidoreductase
	1-52	Glyceraldehydes-3-phosphate dehydrogenase
	1-31	Protease
Unclassified	24	Unnamed protein product
	80	Putative protein Arabidopsis thaliana
	9	16S small subunit ribosomal RNA gene* (nt)
	97	Hypothetical protein str0548

*: no significant hit in nr database, based hit in other database

Table 3.3: The table shows the annotated cDNAs in functional categories. The annotation is based on the hit in the nr database. 3 of the sequences did not have significant hits in the nr database (marked with asterisks), and these are annotated based on another database. The average length of the annotated sequences was 615 base pairs.

Figure 3.4 shows the distribution of cDNAs sorted in functional categories. 143 (83.6%) of the sequences had no BLAST hits lower than the threshold value ($1.0e^{-10}$ for blastx/pdb and $1.0e^{-15}$ for blastx/swissprot, blastx/nr and blastn/nr), 2 (1.2%) was involved in cell structure and motility, 3 (1.8%) in RNA synthesis, 6 (3.5%) in protein synthesis, 13 (7.6%) in metabolism and 4 sequences (2.3%) were unclassified. The annotation output, including best BLAST hits for all sequences in nr, nt, pdb and swissprot databases are found at the following webpages:
http://www.salmongenome.no/htdocs/km_res/blast_all_trimmed/blastSum_km_all_trimmed.html
http://www.salmongenome.no/htdocs/km_res/new/blast_new/blastSum_km_new.html

FIGURE 3.4 Distribution of cDNAs in different functional categories

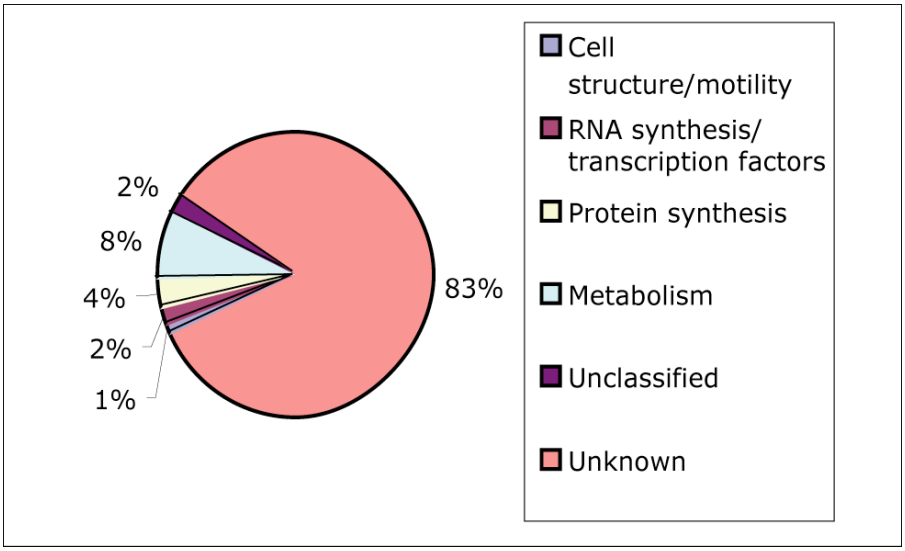

Figure 3.4: The chart shows the distribution of cDNAs in functional categories calculated from the total number of good-quality sequences.

The sequences were also manually blasted against the NCBI EST-database. In this blast search, 8 of annotated sequences (actin, DEAD box helicase, ubiquitin, elongation factor 3, phosphoglycerat mutase, fumarat reductase, ATP synthase and S-adenosyl-L-homocystein hydrolase) and 5 of the unidentified sequences had significant hits against ESTs generated from the dinoflagellate libraries of *Karenia brevis*, *Alexandrium tamarense*, *Amphidinium carterae* and *Lingulodinium polyedra*, while one of the sequences had hits against an EST-library from apricot fruit, a viridiplantae.
Two of the generated sequences were used for phylogenetic analyses of dinoflagellate phylogeny (actin and GAPDH).

3.2.2 *Gymnodinium chlorophorum* cDNA-library

The SMART protocol (see materials and methods) was applied to construct a cDNA library from *Gymnodinium chlorophorum.* However, this construction was not very successful as a large fraction of the clones generated contained only very short inserts. A few of the inserts were of proper length, and four of these were sequenced at Genterprise AG. Three of these sequences were approximately 1000 bp, and one was approximately 800 bp.

When aligned using BLAST, three of the sequences did not have hits with E-value lower than the threshold value ($1.0e^{-10}$). One sequence was identified as actin, a cytoskeletal protein involved in filament formation, also found in the *K.micrum* library. This sequence was used in phylogenetic inference.

3.3 SPECIFIC PCR-AMPLIFICATION OF MOLECULAR MARKERS AND PHYLOGENETIC INFERENCE OF DINOFLAGELLATE SEQUENCES

For interpretation of the complex plastid-evolution in dinoflagellates, a phylogeny resolving the relationship between the heterotrophic-, the peridinin-containing and the aberrantly pigmented species are necessary. The nuclear protein HSP90 has recently been shown to be useful for phylogenetic inference of protists in general as well as for alveolates (Leander and Keeling 2004; Stechmann and Cavalier-Smith 2003). In this study, new sequences from the *hsp90* gene were generated from both peridinin-containing and anomaly pigmented dinoflagellate species, and used in single-gene and concatenated analyses with SSU and LSU from public databases for inference of dinoflagellate phylogeny.

Dinoflagellate phylogeny was also inferred based on actin and GAPDH sequences generated from the cDNA-libraries.

3.3.1 Dinoflagellate sequences of possible use in phylogenetic analyses generated in this study

As the public databases at this date (June 2005) only contain five *hsp90*-sequences from dinoflagellates, five new dinoflagellate *hsp90*-sequences were generated in this study (listed in table 3.1), and an additional unpublished dinoflagellate *hsp90* sequence (*Amphidinium carterae*) was kindly provided by T.Bachvaroff and used in the analyses.

Three sequences of potential use for phylogenetic inference were generated from the cDNA libraries (actin from *Gymnodinium chlorophorum* and *Karlodinium micrum*, and GAPDH from *Karlodinium micrum*).

TABLE 3.4: Sequences generated by PCR or cDNA libraries used in dinoflagellate phylogeny

Taxa	Sequences generated by PCR or cDNA libraries	
	PCR	**cDNA**
Gymnodinium chlorophorum	*Hsp90*	Actin
Karlodinium micrum	*Hsp90*	Actin, GAPDH-C2
Karenia brevis	*Hsp90*	
Karenia mikimotoi	*Hsp90*	
Alexandrium tamarense	*Hsp90*	

Table 3.4: A summary of the new sequences generated in this study used for phylogenetic analyses of dinoflagellates

3.3.2 A large insertion was found in the *Alexandrium tamarense hsp90* gene

A large insertion, possibly an intron, was found in one of the *hsp90* sequences, as the *Alexandrium tamarense hsp90* sequence was interrupted by a 358 bp sequence flanked by canonical GT-AG sequences. The nucleotide distribution of the putative intron was slightly different than the rest of the gene, as G and C comprise 45.2% of the insertion and 50.8% in the remaining gene sequence. Folding of the intron was carried out the web interface Vienna RNA Secondary Structure Prediction (http://rna.tbi.univie.ac.at/cgi-bin/RNAfold.cgi). The predicted secondary structure of the whole intron (A, 358 bp) and the 5'-end of the intron only (B, approximately 180 bp) are shown in figure 3.5, illustrating that the whole insertion, as well as the first part of the insertion have strong palindromic properties. The palindromic structure of the may suggest that the insertion can comprise a hierarchy of palindromic sequences. Hence, the secondary structure of the 5' end (approximately 90 bp) of the putatively duplicated sequence (i.e. 5' end of the whole insertion, approximately 180 bp) of the intron sequence was also predicted (see figure 3.5 C), and showed that this sequence also contains palindromic sequences. The putative branching site of the entire intron is found 31 bp upstream of the 3' intron boundary with sequence GACTAAT, a sequence similar to the branching points of *Saccharomyces cerevisiae* (TACTAAC) and *G.lamblia*/*T.vaginalis* (AACTAAC) (Nixon et al. 2002; Vanacova et al. 2005). The insertion contains an open reading frame (ORF) in-frame with the *hsp90* gene with a putative start codon 7 bp downstream the 5' boundary and a stop codon positioned 25 bp upstream the 3' intron boundary. BLAST searches of the putative ORF were carried out without significant hits.

FIGURE 3.5

Figure 3.5: A: Predicted secondary structure of the 358 bp insertion found in *Alexandrium tamarense*. **B:** Predicted secondary structure of the 5'-end of the 358 bp insertion. **C:** Predicted secondary structure of the 5'-end (90 bp) of B.
Canonical AG-GT splicing sequences marked in red, putative branching site marked in green and start/stop codon of putative ORF marked in blue.

3.3.3 Finding the best model for phylogenetic inference of dinoflagellate phylogeny

Phylogenetic inference of the alignments was done in a Bayesian framework (See box 2.3). The SSU and LSU phylogenies were inferred using a dataset comprising the same taxon-sampling as the HSP90 dataset, using sequences available in public gene banks. Covarion structure (where homological sites evolve with different rate in different sequences) have recently been suggested to be a substitution pattern in gene sequences (Huelsenbeck et al. 2002; Lopez et al. 1999). Hence, for each dataset, the estimated model fit were estimated with and without applied covarion parameters and compared by

calculating the Bayes factor (defined as 2 times the marginal log likelihood (i.e. the mean harmonic value) values obtained from stationary MCMC runs (Kass and Raftery 1995; Newton et al. 1994)).
The harmonic marginal likelihood scores for each of the single-gene tree analyses (SSU, LSU, HSP90, GAPDH and actin) are shown in table 3.4. The covarion distribution parameter was applied when the marginal likelihood value between the analyses with and without applied covarion parameters varied significantly with a mean harmonic value of 5, i.e. a Bayes factor of 10.

Generally, the differences in marginal likelihood value between the distribution models Γ (gamma distributed rates across sites) and the Γ + I (a proportion of the sites invariable, while the rate for the remaining sites are drawn from a gamma distribution) were small, with a difference in marginal likelihood value of about 1.5, or a Bayes factor of 3. Hence, the gamma distribution was chosen for all datasets to prevent over-parameterization of the analyses.

Consistent with previous analyses of SSU sequences (Lopez et al. 1999), the marginal likelihood increased significantly with a Bayes factor of nearly 14 when applying the covarion distribution to the SSU analyses, hence this parameter was applied in combination with the GTR substitution model (allowing all nucleotide substitution rates to be different) and the gamma distribution. There was no significant increase in marginal likelihood when applying the covarion parameter to the LSU dataset, hence the GTR substitution model in combination with gamma distribution were chosen.

For the protein datasets, the more appropriate amino acid substitution model for each dataset was estimated using the Prottest program. This program estimates the likelihood of candidate models by two different criterions, the Akaike Information Criterion (AIC) and the Bayesian Information Criterion (BIC), which are two different criteria used to decide to best fitted model a the given dataset.
For the HSP90 dataset, the Prottest program found the amino acid substitution model RtREV + Γ to be the best fitted model using both criteria.

When testing the actin data set, the AIC and the BIC favored different substitution models, RtREV + Γ + I and WAG + Γ respectively. As the latter model has fewer parameters than the first, this was applied in the analyses.
For the GAPDH dataset, the AIC favored the model WAG+Γ+I, while the BIC found the model WAG+Γ to be the best fitting model. According to the principle of choosing the model with the fewest parameters, WAG+Γ was used in the analyses.

In table 3.4, the applied model used for phylogenetic inference is shown in italics.
In the combined SSU+LSU+HSP90 analyses, the parameter-combination estimated to be best fitted for the datasets was applied to each partition.

TABLE 3.5 Values of harmonic mean of the marginal likelihood

Sequence data	**Harmonic mean of the marginal likelihood**				**Bayes factor**
	Γ	**Γ+I**	**Γ+cov**	**Γ+I+cov**	
HSP90	***-4438.42***	-4439.28	-4433.95	**-4435.63**	8.94
SSU	-7760.78	-7757.94	*-7751.45*	**-7750.99**	13.9
LSU	*-2991.40*	-2994.56	-2992.83	**-2991.34**	0.12
actin	*-1566.80*	-1566.00	**-1566.59**	-1566.59	0
GAPDH-C2	***-4584.45***	-4586.28	N/A*	N/A*	NA*

Table 3.5: Harmonic mean of the marginal likelihood for evolutionary models estimated in Bayesian MCMC and Bayes factors between the best model with or without the COV parameters (best fitting model in bold and applied model in italics**).** The applied amino acid substitution models were RtREV (HSP90) and WAG (actin and GAPDH). The applied nucleotide substitution model was general time reversible model (GTR) (SSU and LSU).

3.3.4 Phylogenetic inference of dinoflagellates using HSP90, SSU, LSU, actin and GAPDH sequences

Dinoflagellate phylogeny was inferred in a Bayesian framework using HSP90, SSU, LSU, actin and GAPDH sequences.

SSU:

The reconstructed tree based on SSU sequences is shown in figure 3.6. The taxon sample and accession numbers are listed in appendix 1, table 1.

In this phylogeny, the ciliate and apicomplexan species branches off as basal species excluding the remaining protalveolate and dinoflagellate species with posterior probability (hereafter pp) 0.66. *Perkinsus marinus* branches off as a sister to *Oxyrrhis marina* and the dinoflagellates *sensu stricto* with pp=0.80, and *Oxyrrhis marina* branches off as a sister to the dinoflagellates with pp= 0.65. The monophyly of dinoflagellates are supported by pp=0.51. The haptophyte-plastid containing species cluster together as a monophyletic clade with pp=0.84, while the prasinophyte-plastid harboring species *Gymnodinium chlorophorum* and *Lepidodinium viride* form a monophyletic clade with pp=1.0. The remaining nodes in the tree are poorly supported with low posterior probability values. The species belonging to the Gonyaulacales cluster together in a group with pp=0.28 consisting of, in addition to the gonyaulacalean-species, the diatom-plastid containing *Kryptoperidinium foliaceum* and the peridinin-plastid harboring *Amphidinium carterae*, belonging to the Peridiniales and the Gymnodiniales, respectively. *Prorocentrum micans*, taxonomically placed among the Prorocentrales, branches off as a sister to the haptophyte-containing species with pp=0.59. The remaining peridinialean-species, *Heterocapsa triquetra* and the heterotrophic *Lessardia elongata,* branches off as a sistergroup to the prasinophyte-plastid containing clade with pp=0.52.

FIGURE 3.6 SSU

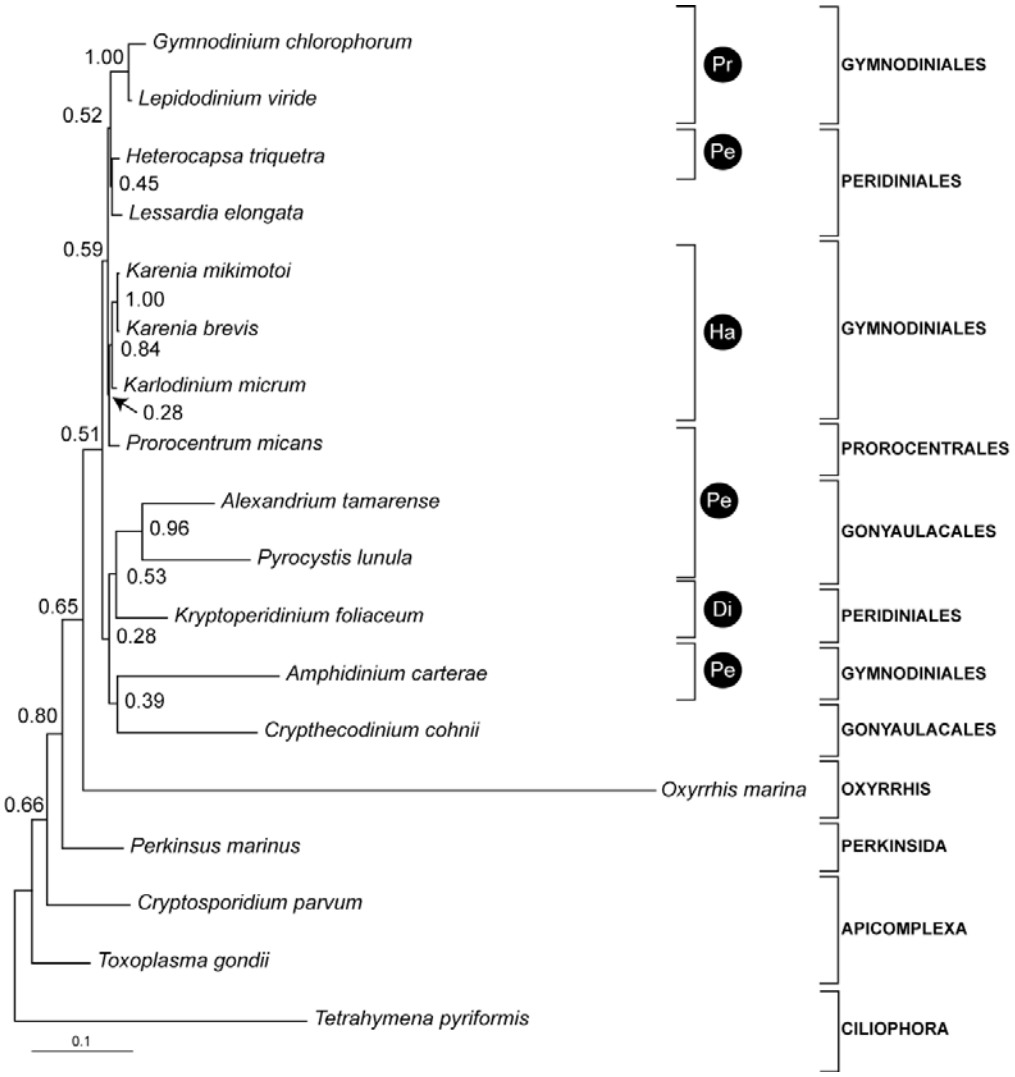

Figure 3.6: Phylogenetic tree of dinoflagellates based on SSU rRNA sequences (1448 nucleotides) from 17 species of alveolates constructed in a Bayesian framework (GTR+Γ+COV model). Dinoflagellates plastid types are indicated with a black circle. **Di**: Putative diatom-derived plastid **Pe**: Peridinin containing plastid **Pr**: Putative prasinophyte derived plastid **Ha**: Putative haptophyte derived plastid

LSU:

The reconstructed phylogenetic tree based on LSU sequences is shown in figure 3.7. The taxon sample and accession numbers are listed in appendix 1, table 1.

In this tree, only a few branches are supported with values exceeding pp=0.50. The apicomplexan and ciliate species are excluded from the dinoflagellates *sensu stricto* (pp=0.87), and two of the haptophyte-plastid containing species (*Karenia brevis* and

Karenia mikimotoi) group together with pp=0.88. The rest of the tree was unresolved, with posterior probability values on some nodes as low as 0.07.

FIGURE 3.7 LSU

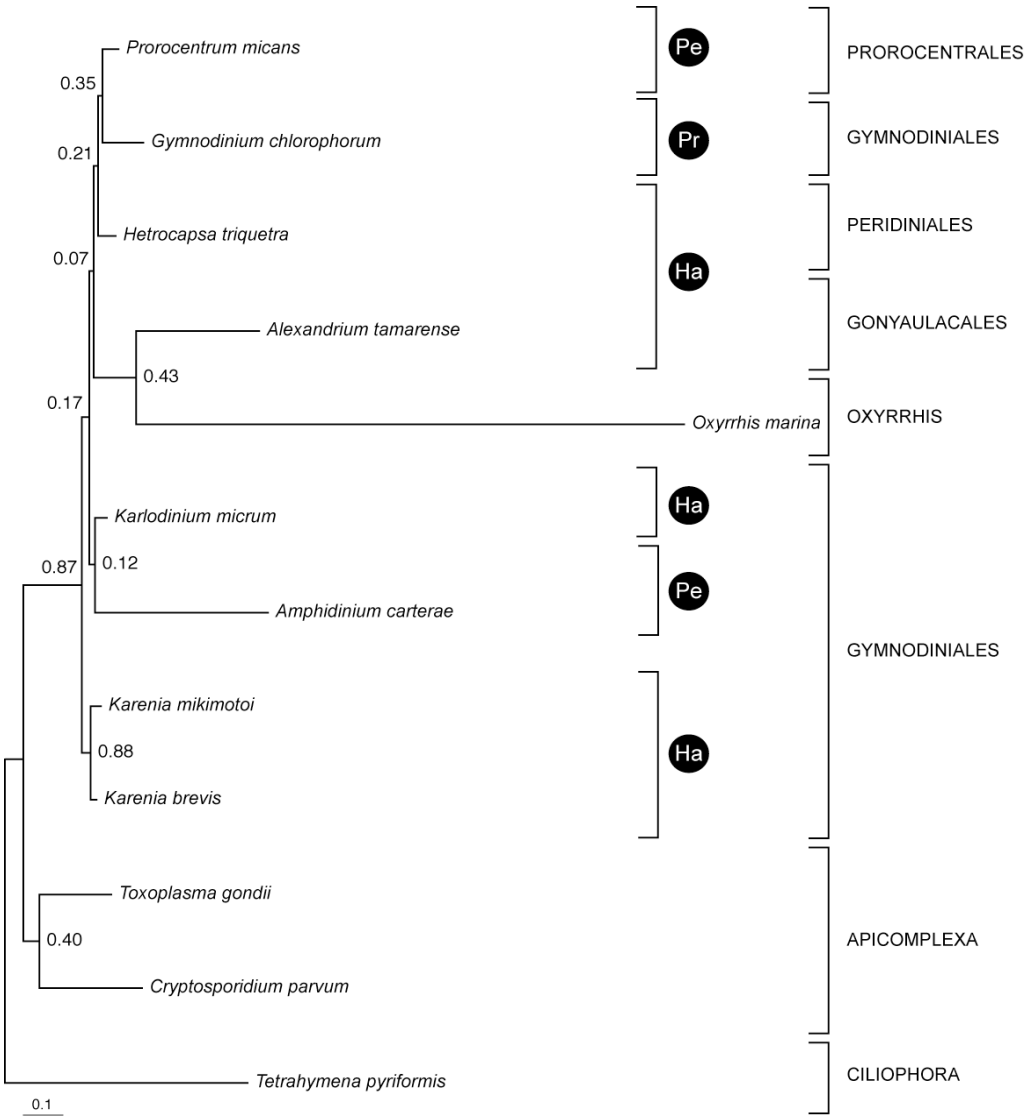

Figure 3.7: Phylogenetic tree of dinoflagellates based on LSU rRNA sequences (400 nucleotides) from 17 species of alveolates constructed in a Bayesian framework applying the GTR+Γ model. Dinoflagellates plastid types are indicated with a black circle. **Di**: Putative diatom-derived plastid **Pe**: Peridinin containing plastid **Pr**: Putative prasinophyte derived plastid **Ha**: Putative haptophyte derived plastid

HSP90:

The reconstructed dinoflagellate phylogeny inferred based on HSP90 protein sequences, is shown in figure 3.8. The taxon sample and accession numbers are listed in appendix 1, table 1.

In this phylogeny, the protalveolates and dinoflagellates *sensu stricto* clustered together excluding the ciliate and apicomplexan species with posterior probability value 1.0. The protalveolate species *Perkinsus marinus* and *Oxyrrhis marina* branch off as basal lineages with high support (pp=1.0). The Gymnodiniales forms the basal group, and the peridinin-plastid containing taxa *Amphidinium carterae* branches off as the most basal of the dinoflagellates with posterior probability 1.0. The species holding a plastid of haptophyte origin (*K.brevis, K.mikimotoi* and *K.micrum*) (Tengs et al. 2000) form a monophyletic clade with high support (pp=1.0) and branches off within the peridinin-plastid containing Gymnodiniales with posterior probability 0.97. The green dinoflagellate *Gymnodinium chlorophorum*, containing a plastid of possible prasinophyte origin (Watanabe et al. 1987) also branches off within the peridinin-containing species with support 0.97, while *Prorocentrum micans* branches off as a sister to the clade consisting of gonyaulacalean- and peridinialean-species with pp=0.99. *Lessardia elongata* branches off as the most basal of the polyphyletic Gonyaulacales/Peridiniales group. The Peridiniales and the Gonyaulacales form a polyphyletic clade excluding the Gymnidiniales and Prorocentrales with pp=0.95. The heterotrophic dinoflagellates represented in the data set, *Crypthecodinium cohnii* and *Lessardia elongata* do not form a monophyletic clade, as *Crypthecodinium cohnii* groups with the dinoflagellate *Kryptoperidinium foliaceum*, harboring a plastid of diatom-origin, with pp=0.98. Together, these two taxa constitute a sister clade to *Heterocapsa triquetra* with pp=0.96.

FIGURE 3.8 HSP90

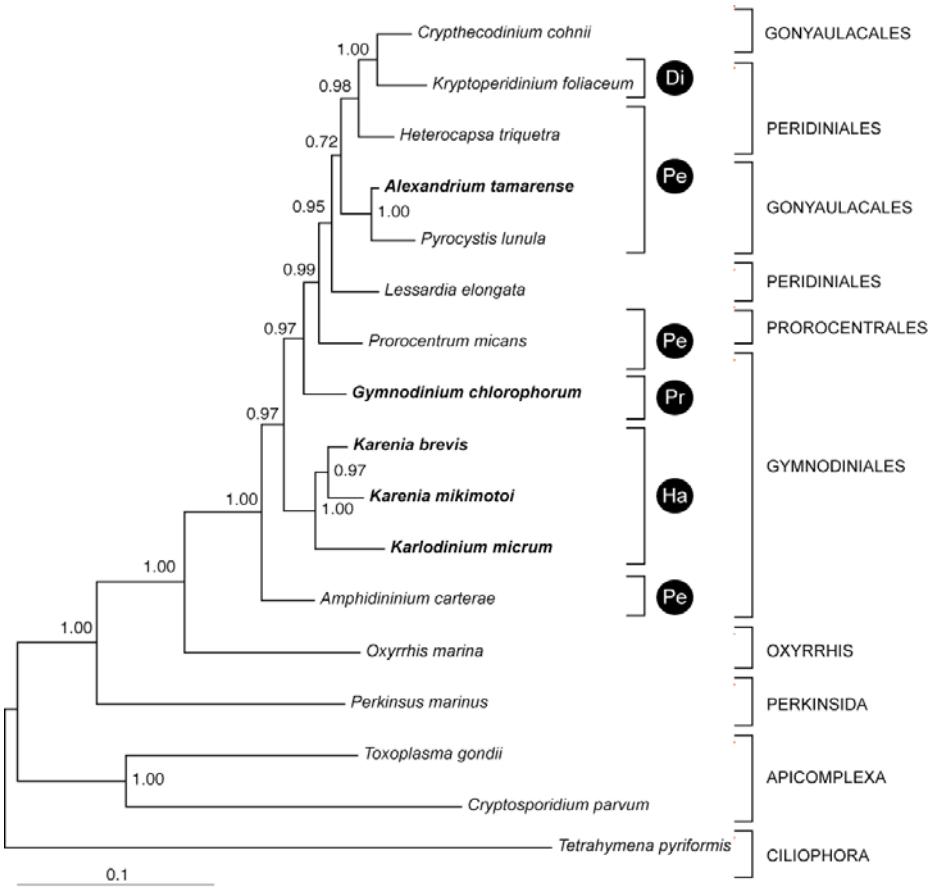

Figure 3.8: The evolutionary relationships of dinoflagellates based on HSP90 amino acid sequences j(17 taxa, 523 amino acids), applying the rtRev+Γ model in a Bayesian framework. Sequences generated in this study marked in bold. Dinoflagellates plastid types are indicated with a black circle. **Di**: Putative diatom-derived plastid **Pe**: Peridinin containing plastid **Pr**: Putative prasinophyte derived plastid **Ha**: Putative haptophyte derived plastid

HSP90+SSU+LSU

The taxon-sampling is listed in table 1, appendix 1, and the reconstructed phylogeny is shown in figure 3.9. The topology and node-support of the concatenated phylogeny combining SSU, LSU and HSP90 is congruent to the HSP90 single-gene tree. The only topological difference is the placement of *Lessardia elongata*, which is placed together with the Gonyaulacales in the concatenated tree.

FIGURE 3.9 HSP90+SSU+LSU

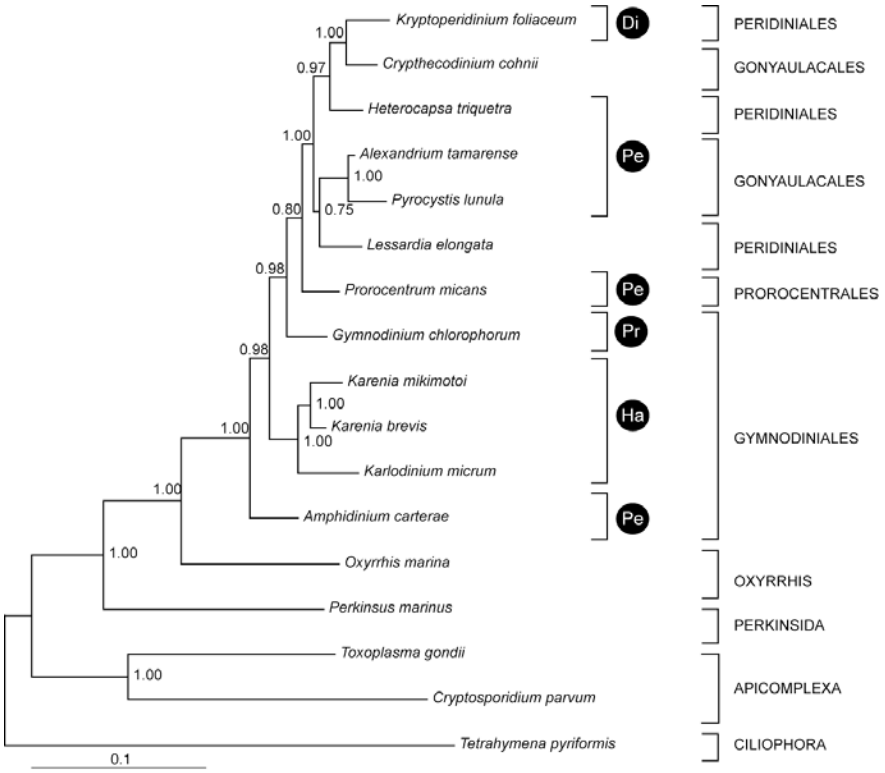

Figure 3.9: Phylogenetic tree of dinoflagellates constructed in a Bayesian framework based on combined SSU+LSU+HSP90 sequences (1848 nucleotides+523 aminoacids) from 17 species of alveolates. Dinoflagellates plastid types are indicated with a black circle. **Di**: Putative diatom-derived plastid **Pe**: Peridinin containing plastid **Pr**: Putative prasinophyte derived plastid **Ha**: Putative haptophyte derived plastid

Actin:

The dataset used in this inference is different than the SSU, LSU and HSP90 datasets, and includes a heterokont (here called stramenopile) outgroup in addition to the alveolates (the taxa used are listed in table 2 in appendix 1). The reconstructed phylogenetical tree is shown in figure 3.9. As with the SSU and LSU trees, many nodes in the actin tree have low support. In this phylogeny, *Perkinsus marinus*, *Oxyrrhis marinus* and the dinoflagellates *sensu stricto* excludes the apicomplexan and ciliate outgroups with pp=0.98, with *Perkinsus marinus* and *Oxyrrhis marinus* branching off as the basal lineages in the protalveolate/dinoflagellate lineage. *Gymnodinium chlorophorum* branches off as the most basal off the dinoflagellates excluding the other dinoflagellates with pp=0.99. *Karlodinium micrum* cluster with *Karena brevis* with

pp=0.94, this haptophyte-plastid containing clade constituting a sister clade to all remaining dinoflagellates. The peridinin containing *Lingulodinium polyedra* and the heterotrophic *Cryphecodinium cohnii*, both belonging to the Gonyaulacales, cluster together with pp=0.89.

FIGURE 3.10 Actin

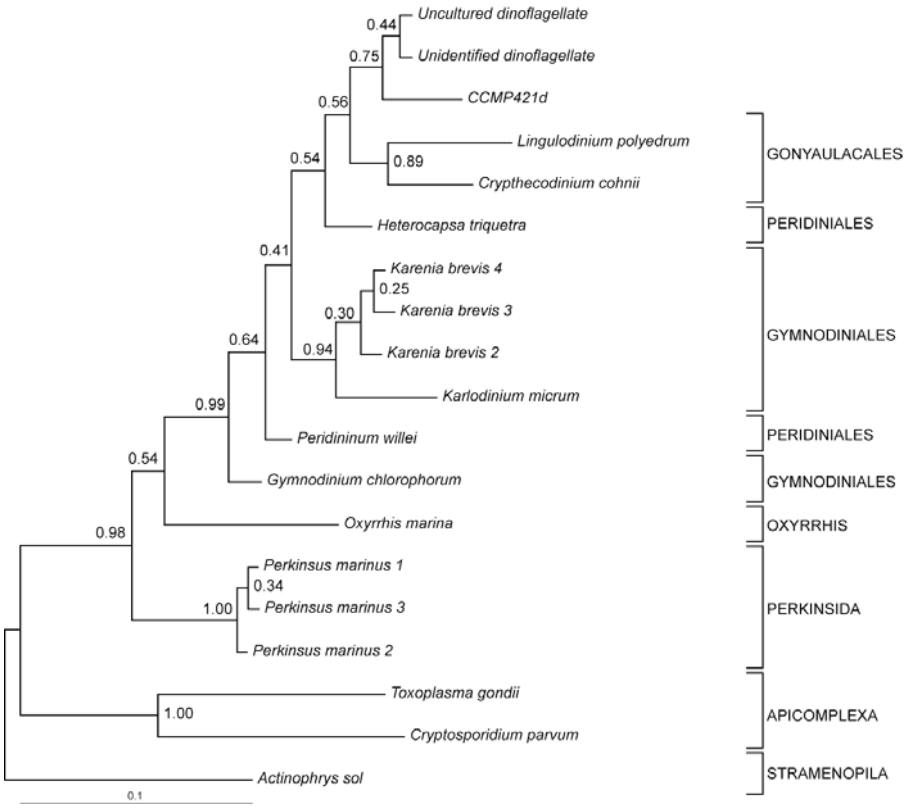

Figure 3.10: Phylogenetic tree inferred in a Bayesian framework based on 19 actin sequences (250 aminoacids) from alveolates and chromists. Three of the taxa belong to unidentified dinoflagellate species ("uncultured dinoflagellate", "unidentified dinoflagellate" and CCMP42fd).

GAPDH:

The GAPDH dataset comprises a different taxon-sampling than the other phylogenetic trees in this study, including the available cytosolic isoforms of GAPDH from dinoflagellates and a few ciliate and apicomplexan outgroups (see table 3 in appendix 1). The phylogenetic tree inferred based on cytosolic GAPDH sequences (shown in figure 3.11) reflects the presence of multiple versions of this gene (4 cytosolic isoforms in *Karenia brevis*), as it splits into two distinct clades comprising the C1 and C2 isoforms of

the gene commonly found among phototrophic dinoflagellates (Takishita et al. 2003). The *Karlodinium micrum* sequence from the cDNA library robustly clusters (pp=1.0) with *Karenia brevis* in the grouping comprising the C2-versions of GAPDH. The apicomplexan taxa branches off as the basal group in the C2 clade with pp=0.80, before a clade comprising two symbiodinium taxa and *Gymnodinium simplex* (Gymnodiniales) branches off with pp=1.0. *Gonyaulax polyedra* (Gonyaulacales), *Heterocapsa triquetra* (Peridiniales), *Scrippsiella* (Peridiniales) and *Akashiwo sanguinea* groups with pp= 0.50, and *Polarella glacialis* (Suessiales) branches off before the gymnodinialean species (*Karenia brevis, Karlodinium micrum* and *Amphidinum operculatum*), which group together with pp=0.69.

FIGURE 3.11 GAPDH

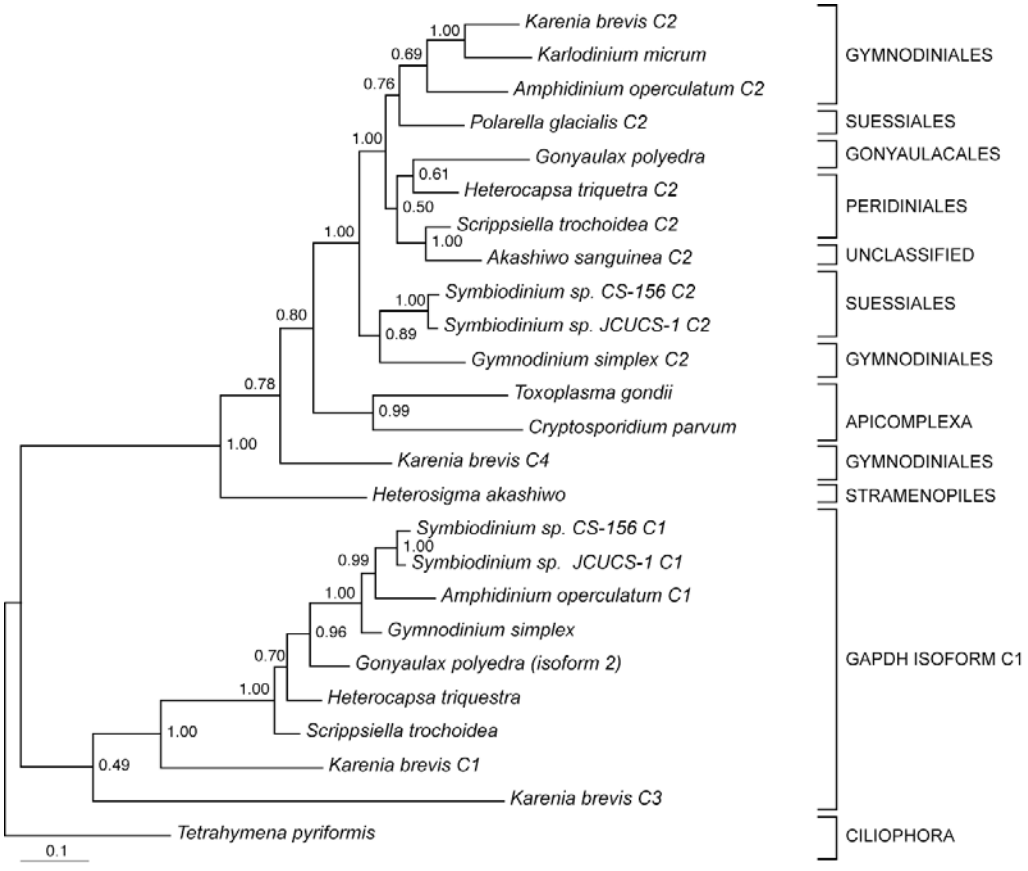

Figure 3.11: Phylogenetic tree of dinoflagellates reconstructed by Bayesian inference of phylogeny (Γ + WAG model), using 26 cytosolic GAPDH sequences (235 aminoacids).

3.4 PHYLOGENETIC ANALYSES OF *TELONEMA*

Telonema was recently identified in molecular surveys of the pico-plankton diversity of the English Channel and Mediterranian Sea (Romari and Vaulot 2004; Shalchian-Tabrizi et al. 2005), isolated and kept in laboratory culture for further molecular and morphological investigations. The initial analyses of the lineage, based on SSU rRNA gene sequence, indicate that the *Telonema* lineage is a deep-branching eukaryote related to the chromalveolates (Shalchian-Tabrizi et al, 2005). However, as phylogenies based on SSU sequences have been shown to give ambiguous and potentially misleading trees, additional molecular investigations are required for firmly placing the *Telonema* lineage in the eukaryotic tree of life.

3.4.1 Phylogenetic markers generated from *Telonema* in this study

In this study, the protein gene markers *hsp90*, alpha-tubulin and beta-tubulin were generated from *Telonema subtilis* and *Telonema antarcticum* and used in phylogenetic analyses. The taxon-samples in these analyses included a range of taxa representing all major eukaryotic supergroups (described in box 1). The taxon sampling is listed in table 4 in appendix 1.

3.4.2 Phylogenetic inference using HSP90, alpha- and beta-tubulin

The analyses of the eukaryotic phylogenies including the *Telonema* sequences were carried out by Kamran Shalchian-Tabrizi.

For all new sequences generated, initial trees were reconstructed to ensure that the sequence did not originate from contaminating DNA from the prey organism in the *Telonema* cultures (*Imantonia rotunda* (haptophyte) and *Rhodomonas* (cryptophyte)). The *Telonema* sequences clustered together with pp= 1.00 in all single gene trees as well as the tree constructed using the concatenated alignments.

Model testing was carried out in a Bayesian framework, comparing the likelihood for models allowing for variable substitution rates across sites (Γ + I) and variable substitution rates across sites and across sequences (Γ + I + COV) by calculating the Bayes factor, which is defined as 2 times the difference of the harmonic mean of

marginal log likelihood scored of competing evolution models. For alpha- and beta-tubulin, the datasets applying the covarion parameter were favored over the dataset without this parameter, hence this was applied in these analyses. Consistent with the analyses carried out in chapter 3.4.2, the dataset comprising the HSP90 amino acid sequences was not sensitive to model choice.

TABLE 3.6 Values of harmonic mean of the marginal likelihood

Sequence data	Harmonic mean of the marginal likelihood			Bayes factor
	Γ+I	**Γ+cov**	**Γ+I+cov**	
HSP90	**--10979.60**	-10982.57	**-10983.41**	5.94
Alpha-tubulin	**-**5474.19	**5449.08**	-5478.75	50.22
Beta-tubulin	-5178.84	**-5158.56**	-5158.97	40.56
HSP90+alpha-tubulin+beta-tubulin	-17140.44	**-17091.61**	N/U*	97.66

*: Not used model

Table 3.6: Harmonic mean of the marginal likelihood for evolutionary models estimated in Bayesian MCMC. The Bayes factor (2 times the difference of the harmonic mean of the marginal log likelihood scores) between the competing model with or without the COV parameters are calculated.

Alpha- and beta-tubulin:

The trees constructed based on alpha- and beta-tubulin gene sequences are depicted in figure 3.12. The taxon sampling is listed in table 4 in appendix 1.The excavates, including kinetoplastids, euglenoids and jakobidae, are scattered around both trees. In the alpha-tubulin tree, the alveolates have split into to groups where the ciliates groups with the excavates and *Telonema*, while the apicomplexan and dinoflagellates form a monophyletic group with cryptophytes, and the Cercozoa are not monophyletic. In the beta-tubulin tree, the alveolates are monophyletic with pp=0.92, and the Cercozoan species are grouped together with the haptophytes. *Telonema* is placed together as a group in both trees, however, their placement are different in the two trees, as the *Telonema* group is placed in a group consisting of euglenids/kinotoplastids/*Jakoba libera* (excavates) and ciliophora, while in the beta-tubulin tree, the *Telonema* group is placed in a clade together with plants, cryptomonads and euglenoids/kinetoplastids (excavates).

FIGURE 3.12 Alpha- and beta-tubulin

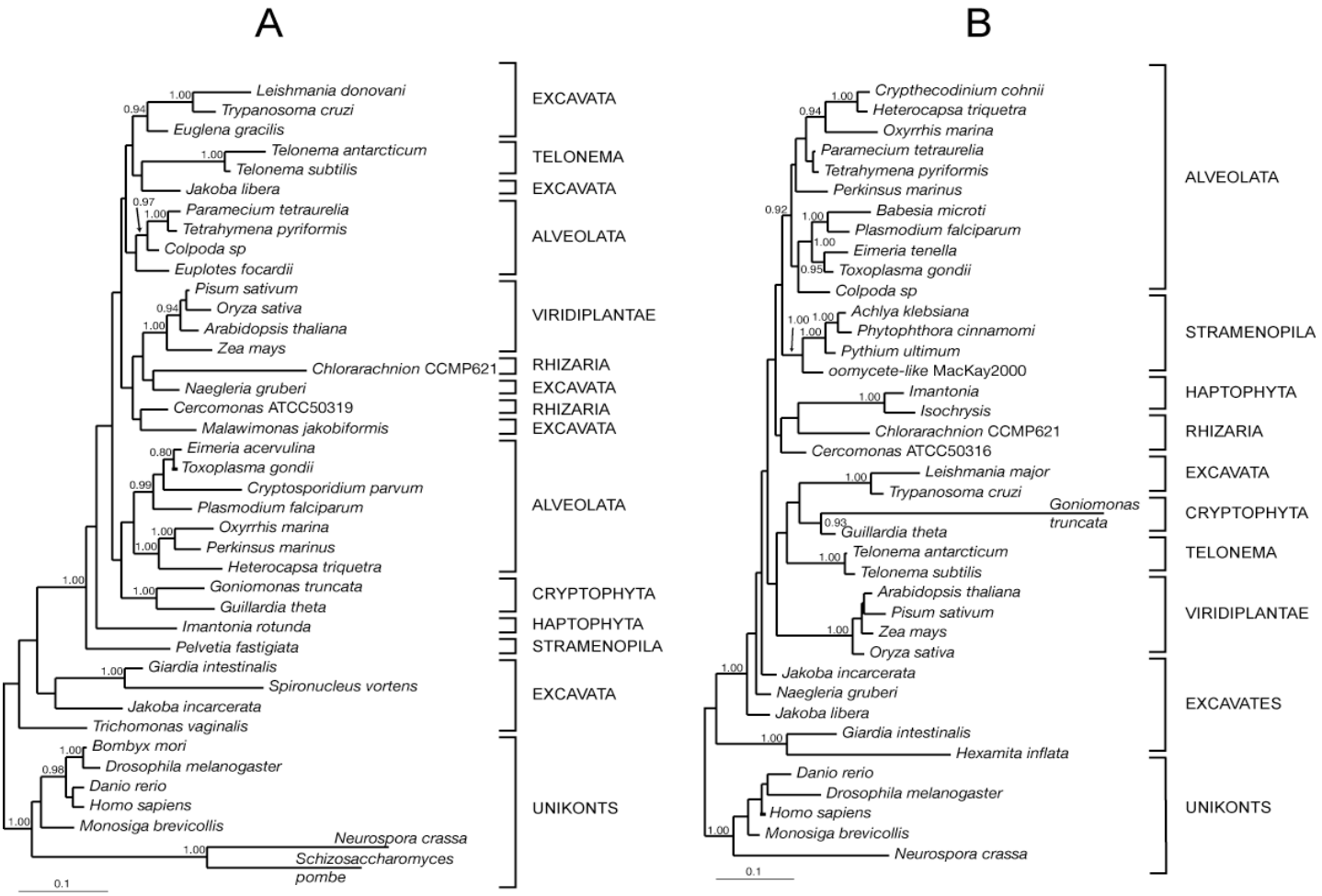

Figure 3.12: Phylogenetic trees reconstructed using Bayesian inference of phylogeny (Γ + WAG model). Tree A is based on alpha-tubulin sequences from 40 eukaryotic taxa (355 amino acids). Tree B is based on beta-tubulin sequences from 39 eukaryotic taxa (383 amino acids).

HSP90 and concatenated trees:

The taxa included in the analyses are listed in table 4 in appendix 1. The concatenated trees and the HSP90 single-gene tree showed congruent topology, and resulted in different tree topology compared to the tubulin trees. The inferred phylogeny hold the features found in most eukaryotic phylogenetic trees, including the monophyly of alveolates, excavates, plants and opisthoconta. The concatenated trees are shown in figure 3.13 (HSP90+alpha+beta-tubulin) and 3.14 (HSP90+SSU). The chromalveolates do not form a monophyletic clade as *Thaumatomonas* sp. (Cercozoa) branches off as sisters to

the alveolates, and the chromists splits in two subgroups in which cryptophytes and haptophytes group as sister groups, and the stramenopiles is placed closer to alveolates and Cercozoa.

The *Telonema* clade does not cluster within any of the known groups in the HSP90 and HSP90 + SSU concatenated phylogeny, but branches off within the bikont part of the eukaryotic tree forming a clade together with plants, cryptophytes and haptophytes. In the HSP90+alpha+beta-tubulin concatenated tree, the *Telonema* clade branches off within the same clade as in the HSP90 + SSU tree, but as a sistergroup to the cryptophytes after the divergence of the haptophyte clade instead of a basal branch.

FIGURE 3.13 HSP90 + alpha- + beta-tubulin

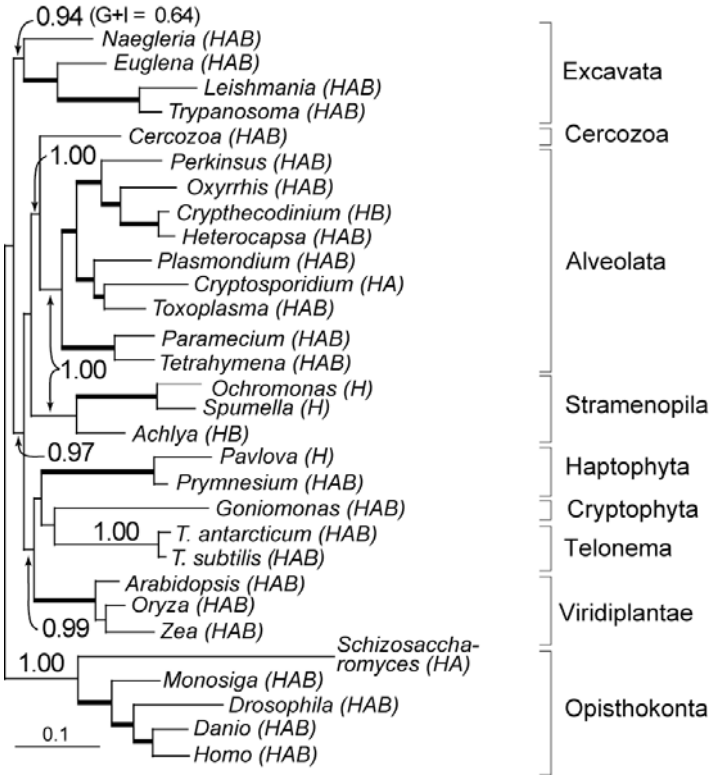

Figure 3.13: Phylogeny of *Telonema* from concatenated HSP90+alpha+beta-tubulin sequences from 30 taxa (1203 aminoacids) reconstructed using Bayesian inference (Γ + COV). Posterior probability values >0.9 are depicted as numbers of thick branches. Some of the taxa are chimeric and assembled from different species (see table 4 in appendix 1). The sequences used in concatenated analyses are written in parentheses: H=HSP90, A=alpha-tubulin, B=beta-tubulin.

FIGURE 3.14 HSP90+SSU

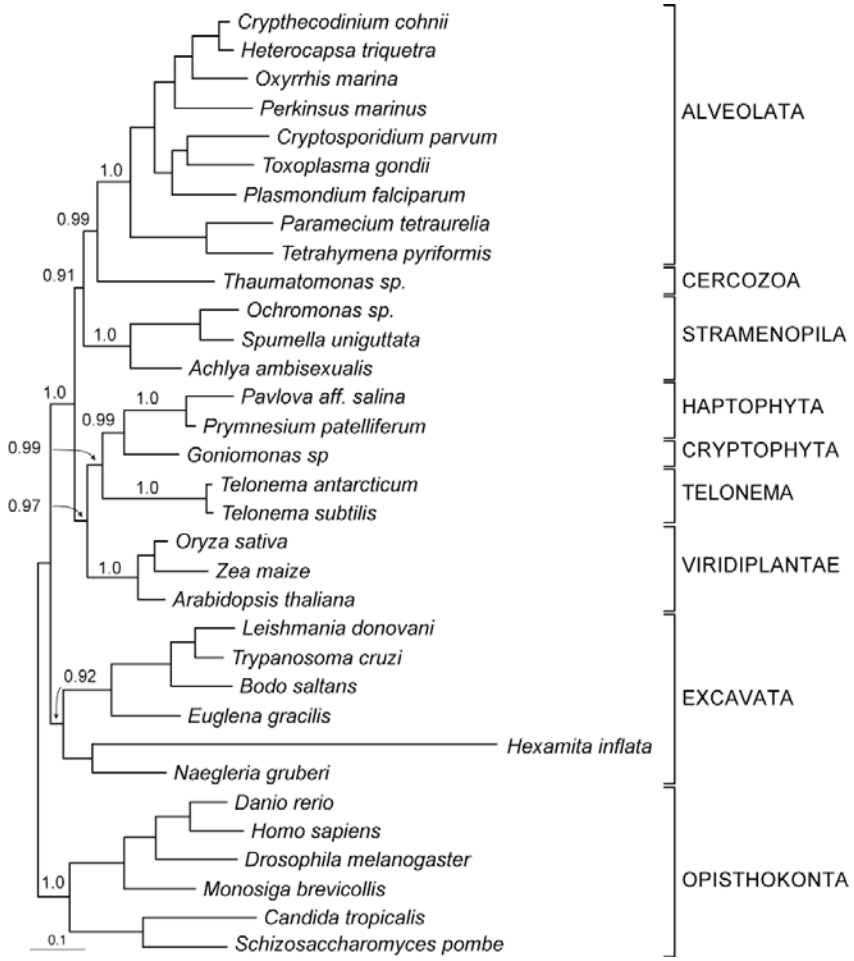

Figure 3.14: Concatenated HSP90+SSU trees from 33 taxa (1813 characters**)** using Γ+I model for the HSP90 partition and Γ+I+COV for the SSU partition of the alignment.

4. DISCUSSION

4.1 MOLECULAR SURVEYS OF ENVIRONMENTAL SAMPLES PROVIDES INCREASED KNOWLEDGE ABOUT EUKARYOTIC DIVERSITY

4.1.1 Environmental sequences can reveal unknown eukaryotic diversity

Amplification of molecular markers, such as the SSU gene, from DNA sampled from extreme and common-place eukaryotic communities has revealed a larger eukaryotic diversity than previously known (Lopez-Garcia et al. 2001; Moon-van der Staay et al. 2001; Richards and Bass 2005). Some of these sequences represent deep-branching lineages or sister-groups of known eukaryotic clades (Richards and Bass 2005), such as the potentially deep-branching chromalveolate lineage *Telonema* (discussed later in this study) and the putatively early diverging dinoflagellate lineages revealed by environmental surveys of coastal- and deep-sea communities (Lopez-Garcia et al. 2001; Romari and Vaulot 2004; Shalchian-Tabrizi et al. 2005). Applying sequences obtained from the environment has also contributed to the global phylogeny of eukaryotes since the hidden microbiological diversity may include high-level taxon groups required for recovering the eukaryotic tree of life (Lopez-Garcia et al. 2002).

However, a major problem in obtaining sequences directly from the environment is the huge biases in the PCR towards amplification of certain groups, and virtually lack of amplification of abundant but diverged groups (Richards and Bass 2005). Some of the problems can be caused by mismatch of the applied primers and use of non-optimal PCR and cloning strategies (Richards and Bass 2005). Another crucial point is to use proper DNA extraction protocol, as high quality of the isolated DNA is required for an efficient PCR amplification of the majority of the present DNA diversity. Thus, improvement of the DNA isolation method for extracting sufficiently pure PCR-ready DNA from environmental samples could provide a valuable contribution in the work to expand the current knowledge about eukaryotic diversity.

4.1.2 Testing of the kit ChlamCAP (Genpoint) for potential use in environmental surveys

The magnetic-bead based DNA-extraction kit ChlamCAP is designed to isolate pure PCR-ready DNA. The protocol of the kit is rapid and no centrifugation is needed. In contrast to other available commercial kits, the magnetic beads in the ChlamCAP kit binds the outer surface of bacterial cells and allows an additional washing step prior to cell lysis. Since samples taken from the environment could contain PCR inhibiting particles, the washing step in ChlamCAP should in principle improve the quality of the extracted DNA. However, as the kit has only been optimized for bacterial cells, the kit needs to be tested on eukaryotes. As the protocol used in this kit involves capturing of the cells by a mutual attraction between molecules on surface of the cells and beads, the DNA yield could differ among protist species due to variable affinity between the cells surface and beads. Thus, the sensitivity of the kit could vary between different types of species.

To test whether this kit could be applied to eukaryotes, DNA extractions with subsequent PCR-amplifications of the eukaryotic small ribosomal subunit (SSU) were carried out applying a wide range of different autotrophic and heterotrophic protist phyla from laboratory cultures. DNA was successfully isolated and SSU amplified from all the cultures tested without changing the manufacturer's general instructions for bacterial DNA-extraction, suggesting that the specially coated surface on the ChlamCAP magnetic beads are able to attract and capture cells from a wide range of eukaryotic phyla.

To investigate the sensitivity of the ChlamCAP kit, DNA was extracted from diluted cultures of five different marine- and fresh-water species. Four of the species (*Karlodinium micrum, Tetraselmis* sp., *Pyramimonas* sp. and *Chlamydomonas reinhardtii*) showed a sensitivity ranging from 1.5×10^3 cells/ml and 2.8×10^3 cells/ml, indicating a sufficient sensitivity of the kit for use of PCR on environmental samples. One of the species (*Isochrysis galbana*) had sensitivity significantly lower than this: 1.6×10^5 cells/ml. The lower sensitivity for this species could be due to either inefficient attraction between the magnetic beads and the surface of *Isochysis galbana* or sub-

optimal PCR conditions for this particular alga. Further optimization of the DNA extraction and PCR protocols may reduce the sensitivity differences between the species.

As these results show, the ChlamCAP kit designed for extraction of PCR-ready DNA from bacteria can also be applied to a broad range of micro-eukaryotic lineages. The sensitivity of the kit is shown to be as low 1500 cells/ml, which makes the kit suitable for PCR amplification of environmental sequences, thus providing possibilities for a simplified protocol for clone library construction.

4.1.3 Measuring differences in PCR-yield between two magnetic bead-based kits

In parallel with testing of the ChlamCAP kit, DNA was extracted using another magnetic-bead based DNA isolation kit: Dynabeads DNA direct from Dynal. The Dynal kit has previously been shown to extract DNA efficiently from some algal groups (dinophyceae, chlorophyceae, phaeo-phyceae (stramenopiles), crysophyceae (stramenopiles) and rhodophyceae (red algae) (Rudi et al. 1997), but have never been systematically tested for application of other types of organisms. Hence, the range of groups was in this study extended to include dinophyceae, chlorophyceae (green algae), stramenopiles, cryptophytes, haptophytes, prasinophytes and a heterotrophic eukaryote (*Telonema*).

The Genpoint kit is expected to produce lower yield than the Dynal kit, because it uses an additional cleaning-step prior to lysis that may cause substantial loss of cells. On the other hand, the Genpoint kit should in principle give purer DNA that is easier to amplify in a subsequent PCR-reaction. However, both kits gave successfully amplified PCR-products from all species tested, and none of the kits could be concluded to provide DNA more suitable for PCR than the other when considering the amount of PCR-products obtained.

Further experiments are required to conclude whether the ChlamCAP kit or the Dynal kit is the most appropriate for use in molecular surveys of environmental samples. The results shown in this study have demonstrated that both kits apply to eukaryotes of interest for environmental sampling, and that the high sensitivity requirement is

submitted by the Genpoint kit. DNA extractions from mixed cultures and real environmental samples are needed for concluding whether protocol the Genpoint kit is appropriate and better compared to other protocols for DNA extraction from environmental samples, and the kit is currently being tested in environmental surveys of fresh-water lakes in a project searching for additional taxa. with affiliation to the *Telonema* clade.

4.2 INSIGHT TO THE GENOMICS OF THE DINOFLAGELLATES APPLYING SEQUENCES FROM cDNA LIBRARIES AND TARGETED PCR

Only a few sequences were available from aberrantly pigmented dinoflagellates when this study was initiated, hence targeted PCR and construction of cDNA libraries were carried out to investigate the expressed genomic diversity among this group.
Due to the exceptionally high DNA content of dinoflagellates (Hackett et al. 2004a), whole genome projects are difficult to carry out for this group cDNA and Expressed sequence tag (EST), however, have earlier been constructed from other species of dinoflagellates, including the peridinin-containing species *Gonyaulax polyedra*, *Amphidinium carterae* and *Alexandrium tamarense* and the 19'-containing *Karenia brevis* (Bachvaroff et al. 2004; Hackett et al. 2004b; Takishita et al. 2004; Yoon et al. 2005).

4.2.1 cDNA libraries from two dinoflagellates with aberrant plastids.

In this study, cDNA libraries from the aberrantly pigmented dinoflagellates *Karlodinium micrum* and *Gymnodinium chlorophorum* were constructed. During the work on these libraries, we got to know that another research-group already had constructed a *Karlodinium micrum* library and generated more than 10,000 sequences that would be public available in short time. Knowing this, we decided not to do as extensive research on our *Karlodinium micrum* library as originally planned. The first attempts of constructing a library from the *Gymnodinium chlorophorum* was not successful, and only four sequences have currently been generated from this library.
231 sequences were generated from the cDNA libraries. 56 were discarded from the gene-annotation pipeline due to low sequence quality. Most of the discarded sequences

were useless due to polymerase slippage in long stretches of poly-A tails in the clones. As the sequences were read from the 5' end, poly-A tails early in the sequence would be due to either very short inserts or unsuccessful directional cloning.

All the good-quality sequences were singletons, and approximately 16% of these were annotated using the BLAST algorithm (at National Center for Biotechnology Information, NCBI) and the Salmon Gene Project (SGP) pipeline. This is slightly lower than the percentage identified in the *Alexandrium tamarense* library where 20% of the sequences were annotated (Hackett et al. 2005), however, it is difficult to conclude about the sequence quality of our library based on this difference, as dissimilar threshold values for significant hits may have been utilized in the annotation pipelines.

Most of the annotated sequences were identified as proteins involved in cell metabolism (7%), including several proteins involved in transferase (kinase, phosphorylase) and energy production (triose-phosphate isomerase). This is inconsistent with the results of other EST libraries from dinoflagellates, where the most abundant sequences are associated with protein synthesis, histone-like proteins or luciferin-like genes (Hackett et al. 2005; Hackett et al. 2004b) However, consistent with the high abundance of histone-like proteins in dinoflagellates indicated in the *Alexandrium tamarense* EST-library , one histone-like protein was also identified in out dataset. Additionally, three sequences involved in RNA synthesis and transcription regulation were identified, including a putative DEAD box helicase, which is a protein associated with preRNA splicing and other RNA associated processes.

Nearly 84% of the sequences were not identified using BLAST against the swissprot, pdb and nr databases, and only a few of these had hits against other dinoflagellate sequences when blasting against the NCBI EST-database. The low hit percentage against other generated EST-libraries was unexpected, as the sequences were predicted to hit against sequences of previously constructed dinoflagellate cDNA libraries, especially from *Karenia brevis*, a close relative to *Karlodinium micrum* from which over 6000 ESTs have been sequenced (Yoon et al. 2005). The low frequency of hits against the EST-database may indicate that there are sequences obtained in our cDNA library not earlier found in dinoflagellate cDNA libraries. However, this could also be due to non-overlapping sequences: that different parts of the genes have been sequenced in the different EST

projects, as the *Alexandrium tamarense* library (Hackett et al. 2005), with 11,000 published sequences (Hackett et al. 2005), was sequenced from the 3' end and may have contributed to the unexpected low hit percentage against this library.
The papers published based on other EST-surveys of dinoflagellates have foremost concentrated on plastid-targeted genes (Hackett et al. 2004b), which were also our major interest, however, no plastid-targeted genes were identified among the 175 good-quality sequences generated (171 from *Karlodinium micrum* and 4 from *Gymnodinium chlorophorum*).
Three of the genes present in the EST libraries are genes previously used for phylogenetic analyses (GAPDH, actin and HSP70) (Harper and Keeling 2003; Harper et al. 2005). Two of these (GAPDH and actin) were used for phylogenetic inference of dinoflagellates in this study. HSP70 has earlier been shown to be useful for phylogenetic analyses (Harper et al. 2005), but the number of public dinoflagellate sequences from this gene is low and therefore not suitable for phylogenetic studies.

4.2.2 Dinoflagellate introns have various branching sequences

When sequencing the *Alexandrium tamarense hsp90* gene, a 358 bp insertion was found. The other dinoflagellate *hsp90* sequences did not contain this insertion. The insertion is most likely a spliceosomal intron, as the insertion was bordered with the canonical GT-AG dinucleotides, as well as containing a stop-codon.
The putative branchpoint sequence was found 30 bp upstream of the 3'end of the insertion. The branchpoint sequence (GACTAAT) is similar to the conserved branch-point sequence required for splicing in yeast (TACTAAC) and in the deep branching parabasilid and diplomonad (excavates) lineages *Giardia lamblia* and *Trichomonas vaginalis* (AACTAAC; (Johnson 2002; Nixon et al. 2002; Vanacova et al. 2005), and have not earlier been reported from dinoflagellate introns. The finding of the canonical 3' and 5' splicing-site sequences as well as the conserved branching-point sequence are untypical for the hitherto described dinoflagellate introns, as these often lack conserved sequences (Okamoto et al. 2001; Schott et al. 2003), suggesting that different recognition mechanisms for introns are present in the spliceosomal apparatus in dinoflagellates.

The putative intron also expresses another feature not earlier reported from dinoflagellate introns, as the intron seems to consist of a palindromic sequence, where one part of the intron is an inverted duplication of the other part. The folding of the 3'-part and the 5' part of the insertion separately shows that these parts also possess palindromic properties (data shown only for the 5'-end (180 bp) of the intron), and when the 5'-end (90 bp) of one of these 180 bp sequences are folded, even more complementary sequences are seen, indicating that the intron may comprise a hierarchy of repeated palindrome sequences. The insertion contains an open reading-frame, putatively encoding a protein consisting of 108 aminoacids. However, when this possible ORF was blasted against public databases, no homologues were found. This could possibly be due to few available genomic sequences from dinoflagellates in public databases.

4.3 INVESTIGATIONS OF CHROMALVEOLATE EVOLUTION

Investigations of the evolution in the eukaryotic supergroup chromalveolates were carried out by different approaches. The phylogeny and plastid evolution of dinoflagellates were investigated using nuclear protein-encoding genes alone and multi-gene alignments combined with ribosomal DNA sequences, and large-scale eukaryotic phylogeny was inferred including the putative deep-branching *Telonema* lineage.

4.3.1 Dinoflagellate phylogeny inferred by nuclear encoded protein genes

The dinoflagellates are famous for their remarkable plastid diversity, resulting from evolutionary events such as secondary and even tertiary endosymbioses, plastid losses and chloroplast replacements (Hackett et al. 2004a). The peridinin plastid is postulated to be the ancestral plastid type in the group (Takishita et al. 2004; Taylor 2004) and according to the chromalveolate hypothesis, this originates from the ancestral chromalveolate plastid engulfed in the common ancestor of dinoflagellates, apicomplexa, ciliates, haptophytes, cryptophytes and heterokonts. As described in the introduction, the unveiling of the complex plastid evolution history in the dinoflagellates requires a resolution of the dinoflagellate phylogeny.

The SSU and LSU sequences are common markers for inferring eukaryote phylogeny, but these rRNA markers seem to contain deficient phylogenetic information for complete resolution of the dinoflagellate phylogeny (Saldarriaga et al. 2004; Saldarriaga et al. 2001), probably due to the rapid and early divergence of this group. Additionally, the asymmetry of the evolutionary rates and the potential covarion substitution pattern found in various rRNA gene sequences may contribute to the resolution problems associated with these markers (Galtier 2001; Lopez et al. 1999). Consistent with this, the Bayesian tree based on dinoflagellate SSU sequences in this study applying the covarion parameter were a Bayes factor of 14 better than the best model without applied covarion model, which is substantially higher than 10 usually regarded as good evidence for the model (Kass and Raftery 1995; Newton et al. 1994). However, despite the improved likelihood obtained when applying the covarion parameter, the dinoflagellate SSU tree was poorly resolved. Thus, due to the limitations of the rRNA gene markers, other phylogenetic markers are needed for a complete resolution of dinoflagellate phylogeny. In this study, the dinoflagellate phylogeny has been inferred using the nuclear encoded protein genes *hsp90*, actin and GAPDH. The 90 kDA cytosolic heat shock protein HSP90, a highly conserved molecular chaperone (Stechmann and Cavalier-Smith 2004), is useful for phylogenetic inference because of the uniform evolution and length of the protein, making the protein especially interesting for analyses including species with rapidly evolving rRNA (e.g.*Oxyrrhis marina*), and deep-branching alveolates, such as *Perkinsus marinus* (Leander and Keeling 2004; Stechmann and Cavalier-Smith 2003). Hence, this gene was amplified from several dinoflagellates and subsequently sequences from three species holding a 19'-hexanoyloxy-fucoxanthin plastid (*Karenia brevis, Karlodinium micrum* and *Karenia mikimotoi*), the chlorophyll a+b containing *Gymnodinium chlorophorum* and a peridinin-holding dinoflagellate (*Alexandrium tamarense*). The phylogenetic inference of the dinoflagellates based on the HSP90 protein sequences resulted in resolved phylogenetic trees with higher posterior probability than the rRNA gene trees on almost all internal nodes and basal branches. The support of the nodes in the trees constructed on basis of HSP90 sequences, and grouping of species in agreement with morphology-based classification of dinoflagellates suggest that this gene is a good marker for inferring dinoflagellate phylogeny, and that this protein gene can be used as a

useful addition to rRNA and cytochrom b sequences for inferring dinoflagellate phylogeny (Zhang et al. 2005). However, since the taxon sampling is relatively poor in the HSP90-tree, further sequencing of a wider taxon sampling is needed before it can be concluded that this gene resolves the dinoflagellate phylogeny better than the rRNA genes.

The two other genes applied for dinoflagellate phylogeny, the actin and GAPDH, were obtained from the cDNA-libraries constructed from *Karlodinium micrum* and *Gymnodinium chlorophorum*. Actin was generated from both libraries, while GAPDH was generated from *Karlodinium micrum* only. Phylogenetic analyses based on actin gave an unresolved tree with only a few supported nodes. This low support indicates that this gene may not be suitable for inferring dinoflagellate phylogeny . The tree reconstructed based on GAPDH sequences had some nodes with relatively strong support, but the many gene duplication events of the gene may obstruct extensive use of this marker for phylogenetic inference (Fast et al. 2001; Takishita et al. 2003; Takishita et al. 2004). Hence, of the three genes tested for use in dinoflagellate phylogeny, HSP90 seems to be the most appropriate.

4.3.2 Dinoflagellate haptophyte- and prasinophyte-derived plastids were each acquired only once, replacing the ancestral peridinin-plastid

The phylogenetic trees constructed from SSU, HSP90 and concatenated HSP90+SSU+LSU gene sequences contained five species of dinoflagellates with true aberrantly pigmented plastids; *Gymnodinium chlorophorum* holding a putative prasinophyte-plastid, and *Karlodinium micrum*, *Karenia brevis* and *Karenia mikimotoi*, holding a haptophyte derived plastid (Chesnick et al. 1997; Chesnick et al. 1996; Elbrächter and Schnepf 1996; Tengs et al. 2000). Additionally, *Lepidodinium viride*, harboring a plastid of putative green-algal origin (Watanabe et al. 1990), were included in the SSU analysis. The SSU tree, although poorly resolved in many nodes, grouped the green colored species *Gymnodinium chlorophorum* and *Lepidodinium viride* with high support (pp=1.0), strongly implying a monophyletic origin ofboth the species and their plastid.

The HSP90 single gene tree and the concatenated HSP90+SSU+LSU tree showed congruent topology with slightly different node support. The haptophyte-containing species clustered together as a monophyletic clade with high support, establishing the prediction of a common ancestry for these species belonging to the order Gymnodiniales, which earlier have been supported by variable degrees of bootstrap support (de Salas et al. 2003; Takishita et al. 2004; Tengs et al. 2000; Zhang et al. 2005).

The clustering of the two groups of dinoflagellates holding 19' hexanoyloxy-fucoxanthin and the chlorophyll a + b respectively in two separate monophyletic groups indicates that the true aberrant plastids (i.e. fully integrated plastids) most likely were acquired in two endosymbiotic events, where a haptophyte was engulfed and established as a tertiary plastid in the ancestor of *Karlodinium* and *Karenia*, and a putative prasinophyte-like algae was incorporated in the ancestor of the green-colored species in a serial secondary endosymbiosis (i.e. replacement of a secondary plastid by another secondary plastid (Keeling 2004b)). The phylogenetic trees indicate that these endosymbioses occurred relatively early in the dinoflagellate evolution in approximately the same time period after the divergence of the earliest peridinin-containing species. The peridinin-containing taxon *Amphidinium carterae* branches off as the most basal of the dinoflagellates *sensu stricto* (i.e. dinoflagellates with dinokaryon). The divergence of the haptophyte and prasinophyte plastid-containing clades within the peridinin-containing species indicates a peridinin-containing ancestor of the dinoflagellates, which in some lineages substituted the original plastid with a new plastid in a replacement event. These results are consistent with the previous indications supporting that the last common ancestor of all dinoflagellates harbored a peridinin-plastid (Ishida and Green 2002; Saldarriaga et al. 2001; Takishita et al. 2004; Tengs et al. 2000; Yoon et al. 2005; Zhang et al. 2005), and are thereby contradictory with the hypothesis postulated by Yoon et al in 2002, suggesting that the haptophyte-plastid was the ancestral plastid in dinoflagellates (Yoon et al. 2002a). The trees also indicate an early divergence of the unarmored taxa in the order Gymnodiniales, suggesting an evolution of the dinoflagellates from naked into armored lineages (Prorocentrales, Gonuaylacales and Peridiniales). This is contradictory to the interpretations deduced from previous phylogenetic inference of SSU, where the naked Gymnodiniales is suggested to be derived from thecate orders (i.e. armored),

presumably by plate loss during the dinoflagellate radiation (Saldarriaga et al. 2004; Saldarriaga et al. 2001; Taylor 2004).

In addition to the photosynthetic groups holding 19' or chlorophyll a+b plastids, there are also other groups of phototrophic dinoflagellates harboring other plastids than the ancestral peridinin-plastid. One of these was represented in the analyses carried out in this study: *Kryptoperidinium foliaceum,* which harbors a plastid of putative diatom origin. This plastid is not considered to be completely integrated in the host, since it retains several traits usually lost during integration in the host cell, such as the nucleus and mitochondria. In addition, no genes have been shown to have been transferred from the symbiont to the host, and several genes (e.g. HSP90, tubulin and actin) that have been lost in the true secondary plastids still retains in the nucleus of this plastid (Chesnick et al. 1997; Chesnick et al. 1996; McEwan and Keeling 2004). In the HSP90 and concatenated analyses, *Kryptoperidinium foliaceum* does not group with the haptophyte or the prasinophyte plastid-containing clades, but clusters with *Crypthecodinium cohnii*, a heterotrophic dinoflagellate which earlier have proven to be difficult to place in phylogenetic trees (Saldarriaga et al. 2001; Zhang et al. 2005).

Other dinoflagellates holding anomaly pigmented plastids not represented in these analyses includes *Dinophysis* and *Noctiluca* (Saldarriaga et al. 2004). These species have in earlier analyses shown to group in separate clades (Edvardsen et al. 2003; Saldarriaga et al. 2004; Saldarriaga et al. 2001), suggesting that separate plastid replacements have occurred in these lineages, indicating that plastid replacements are a widely distributed process among dinoflagellates

Perkinsus marinus and *Oxyrrhis marina* branches off as basal lineages prior to the dinoflagellates *sensu stricto* in the HSP90 and concatenated HSP90+SSU+LSU trees, robustly placing *Oxyrrhis* as a sister group to the remaining dinoflagellates. Due to a very divergent SSU sequence, *Oxyrrhis* has proven difficult to place in large-scale rRNA analyses, where it tends to strongly affiliate with the Gonyaulacales (Saldarriaga et al. 2004). However, the phylogenetic placement shown in our analyses, where *Oxyrrhis* branches off as a basally diverging protalveolate, is consistent with morphological investigations and several other phylogenetic analyses of protein genes (Leander and Keeling 2004; Saldarriaga et al. 2003).

4.3.3 Phylogenetic inference of the recently re-discovered *Telonema* clade

Phylogenetic analyses of the small ribosomal subunit as well as morphological investigations of the *Telonema* clade suggest that this lineage is a deep branching eukaryotic lineage related to the supergroup chromalveolates. This indication was further established in the analyses carried out in this study, where single-gene and concatenated protein alignments were subject for phylogenetic inferences.

The phylogenetic analyses of the protein gene sequences HSP90, alpha-tubulin and beta-tubulin placed *Telonema* as a single, distinct group with no clear relationship to any other group. However, the alpha- and beta-tubulin trees were incongruent and did not group alveolates, cercozoa and excavate species as monophyletic clades, characteristics often seen in other phylogenetic eukaryote trees (Baldauf et al. 2000; Harper et al. 2005). These topological discrepancies could result from these genes having an evolutionary history that violate the assumptions in the underlying model used in the phylogenetic inferences. In general, if sequences have evolved differently in separate phyla, large-scale phylogenies would be difficult to deduce (Lopez et al. 1999). Applying the covarion model on the concatenated HSP90+alpha-tubulin+beta-tubulin sequences, the excavates were grouped together with considerable increased support values, supporting a heterogeneous evolution of sequences in some of the groups. This is also consistent with the emerging consensus that the tubulin genes are not suitable for large-scale eukaryotic phylogenies. (Tom Cavalier-Smith and Andrew Roger, personal communication). However, the trees based on the HSP90 single-gene alignment and the alignments combining HSP90 with SSU hold the features often robustly supported in eukaryotic trees, such as the monophyly of alveolates, opisthokonts, excavates, heterokonts and plants (Baldauf et al. 2000). Due to this, the HSP90 single-gene tree and the HSP90 + SSU concatenated tree were used for interpretation of the phylogenetic placement of the *Telonema* lineage in the eukaryotic tree.

4.3.4 Establishing *Telonema* as a deep, diverging eukaryotic lineage by combining phylogenetic inference of gene sequences and morphological traits

The *Telonema* lineage groups on its own in both the HSP90 and the concatenated HSP90+alpha tubulin+beta tubulin phylogenies, hence confirming the phylogeny seen in the SSU trees. All the trees are also consistent in placing *Telonema* together with one or several chromalveolates. However, since *Telonema* was placed either close to the haptophytes and cryptophytes in the HSP90 trees (both single-gene and concatenated trees) and the close to the alveolates and stramenopiles[1] in the SSU tree, the exact origin of the group remains unclear.

Consistent with the phylogenetic inference, the morphological investigations of the *Telonema* species indicate a relation to members of the chromalveolates. Structural features supporting the evolutionary affinity to chromalveolates are mitochondria with tubular cristae (also found in also called stramenopiles, haptophytes and the alveolates), a complex cytoskeleton (also found in alveolates, but not in chromists), tripartite hairs; a trait regarded as a synapomorphic trait for stramenopiles, as well as characteristic alveoli; a trait also seen in the alveolate, stramenopiles and glaucophytes (Andersen 2004; Shalchian-Tabrizi et al. 2005). Of these features, the tripartite tubular hairs on the long flagellum probably constitute the strongest link to the chromalveolates, since this trait is regarded as the only synapomorphic character defining the stramenopiles (Andersen 2004). The stramenopile tripartite hairs are tubular, composed of a hollow base and tubular shaft as well as none-tubular distal fibers (see figure 1.6d), and the synthesis of this structure involves complex processes including synthesis, assembly and transport (Andersen 2004). The structure of these hairs causes a swimming behavior in stramenopiles that is different from many other protist group, as it involves the forward directed flagellum pulling the cell by means of the tripartite tubular hairs that is attached to it (Andersen 2004), a swimming behavior also seen in *Telonema*. The complex biosynthetic pathway such as the one required to construct tripartite hairs is unlikely to have evolved several times, and together with the shared mechanism for movement, this indicates that *Telonema* belongs to the stramenopile clade. Although the tubular shape of

[1] In this part of the discussion, the term stramenopiles is used to describe the heterokonts, mainly because the term heterokont often refers to photosynthetic species, while the term stramenopiles often refers to both phototrophic and heterotrophic species.

the hairs in *Telonema* has never been confirmed, the partition of the hairs, and the peculiar movement, suggests a close relationship between the *Telonema* and the stramenopiles. However, the placement of *Telonema* within the stramenopiles is rejected in all inferred single-gene protein trees, where *Telonema* are placed closer to the haptophytes and cryptophytes than to the stramenopiles. This is interesting, since bipartite tubular flagella hair similar to the tripartite hairs found in stramenopiles are also found in the cryptophytes (Andersen 2004), suggesting that this type of tubular hairs may have been inherited from the common ancestor of *Telonema*, cryptophytes and stramenopiles.

The alveoli found just beneath the cell membrane in *Telonema antarcticum* is another feature connecting *Telonema* to the chromalveolates (Baldauf et al. 2000), however, this trait suggests a relationship to either alveolates or glaucophytes (plantae) . Based on phylogenetic analyses and the presence of tubulocristate mitochondria, it is not likely that *Telonema* is closely related to the Glaucophytes. Instead, the phylogenetic and morphological features (tubulocristate mitochondria, tripartite hairs, a complex cytoskeleton and alveoli) suggest that *Telonema* is a distinct, deep branching lineage related to both chromists and alveolates. The tripartite hairs found in both chromists and *Telonema* could possibly be an inheritance from a common ancestor of stramenopiles and the *Telonema*-lineage. Given that the chromist lineage is monophyletic, as several papers have suggested (Cavalier-Smith 2003b; Keeling 2004a; Yoon et al. 2002b), the tripartite hairs could have derived from a common ancestor of all chromists and the *Telonema*-lineage. This feature would then have been lost in the lineages leading to the haptophytes and possibly changed in the cryptophytes, resulting in bipartite hairs in these genera. However, at the current stage it is difficult to rule out the possibility that both the tripartite hairs and the cortical alveoli are structures that have been developed independently or converges from different flagellar hair types. The *Telonema* lineages express a alveolate-like discrete cytoskeleton that has not been found in other chromist lineages, hence, the lineage most likely separated from the chromist-lineage prior to the reduction of the cytoskeleton seen in extant chromist groups, suggesting that the *Telonema* group is a deep branching chromist lineage. As the cryptophytes currently is regarded the earliest diverging lineage among the three known chromist groups, a deep-

branching lineage comprising tubular mitochondrial cristae challenge the view that the flattened mitochondrial cristae found in cryptophytes constitute the ancestral state for chromists (Yoon et al. 2002b), however, the indications confirming *Telonema* as a basal chromist also imply that the tubular cristae is the ancestral state in chromists, while the flattened cristae is a derived state. Another intriguing possibility is that the *Telonema* lineage may have separated from chromist lineage even earlier, preceding the separation of chromists and alveolates. This would make *Telonema* a deep branching chromalveolate group, actually constituting one of the earliest diverging chromalveolates known. This scenario is supported by the fact the alveolates, like *Telonema*, stramenopiles and haptophytes, also hold tubular cristae, suggesting that this could be the ancestral state for all chromalveolates.

Telonema is on basis of these phylogenetic and morphological results now suggested to constitute a new phylum called Telonemia (Shalchian-Tabrizi et al. 2005).

4.3.5 Chromalveolate monophyly is not supported in the phylogenetic analyses including the *Telonema* lineage

The chromalveolate hypothesis has been supported by numerous data, including a number of morphological and biochemical characters such as plastid membrane topology, storage carbohydrates, flagellar structure and accessory pigments shared by all or some of the chromalveolates (Keeling et al. 2004), as well as by the replacement of the plastid-targeted nuclear genes glyceraldehyde-3-phosphatase (GAPDH) and fructose-1,6-bisphosphate aldolase (FBA) uniquely shared by the chromalveolates (Fast et al. 2001; Harper and Keeling 2003; Patron et al. 2004). However, despite this indirect evidence of common ancestry, this supergroup assembly has so far never been shown to cluster as a monophyletic group in phylogenetic trees from nuclear encoded gene sequences (Keeling 2004b; Keeling et al. 2004). Consistent with this, our analyses using SSU and three protein-encoding genes (HSP90, alpha- and beta-tubulin) also show the chromalveolates (including *Telonema*) as a polyphyletic group. In these analyses, the chromists are split into two lineages, and are incompatible with both the chromalveolate hypothesis as well as the assumption of the chromists as a monophyletic group (Yoon et al. 2002b). In the SSU phylogeny, the placement of *Thaumatomonas* (Cercozoa), branching off within a

clade comprising the alveolates, stramenopiles and *Telonema*, is probably misleading as no morphological features suggest a near relationship between Cercozoa and chromalveolates, and the suggested relationship is hence probably due to the lack of sequences from other close-related Rhizaria-members or reflect the deep and rapid divergence of these species

4.3.6 Plastid evolution and the putative monophyly of chromalveolates

The assumed chromalveolate monophyly manifested in the chromalveolate hypothesis is deduced from a particular model of plastid evolution, stating that the chromalveolate plastid originated from a single secondary endosymbiotic event where a red plastid was acquired in the common ancestor of all chromalveolates (Cavalier-Smith 1999). This model of plastid evolution is controversial as the number of secondary endosymbiotic events remains under debate. However, several findings are consistent with the chromalveolate hypothesis, and support that the plastid found in extant chromalveolates originated in only one secondary endosymbiotic event. Among the evidence supporting this model of plastid evolution are the unique gene-replacements of plastid-targeted genes GAPDH and FBA mentioned earlier, shared by apicomplexans, cryptophytes, dinoflagellates, haptophytes and heterokonts, which implies a common origin for these plastids (Fast et al. 2001; Harper and Keeling 2003; Patron et al. 2004). Additionally, a common origin of the chromist plastids rather than several independent secondary acquirements in cryptophytes, haptophytes and heterokonts is indicated in analyses of concatenated plastid genes (Yoon et al. 2002b). Despite the lack of monophyletic clustering of the chromalveolate groups in phylogenetic trees, analyses have indirectly supported the chromalveolate hypothesis by grouping different chromalveolate members, indicating the alveolates as sister group to the heterokonts and clustering haptophytes and cryptophytes (Baldauf et al. 2000; Ben Ali et al. 2001; Harper et al. 2005; Van de Peer and De Wachter 1997). In our protein and SSU analyses, these relationships are also established, including the *Telonema* as an early branching lineage the heterokont-alveolate clade in the SSU phylogeny, while affiliating with the haptophytes and the cryptophytes in the protein phylogeny. The phylogenetic placement in the protein-gene phylogenies is hence consistent with the previous SSU analyses and the classification

based on morphological investigation in affiliating the *Telonema* lineage to the chromalveolates, indicating that *Telonema* is a deeply diverging chromist or chromalveolate.

As a consequence of the phylogenetic placement of *Telonema* one should, according to the chromalveolate hypothesis, expect that the members of this lineage once harbored a red-algal derived plastid originating from the first secondary uptake in the common ancestor of chromalveolates, from which remnants may be traced as a vestigial plastid (as found in e.g. apicomplexa (McFadden et al. 1997) or as plastid-derived genes in the nuclear genome transferred by horizontal gene transfer, as reported in Trypanosomes (excavates(Hannaert et al. 2003) However a chloroplast or a vestigial plastid was not seen when investigating *Telonema*.

The absence of plastids in the basal chromalveolate branches is a challenge to the plastid-evolution model implicated in the chromalveolate hypothesis. Among the chromalveolate lineages devoid of plastids are ciliates, oomycetes and other deep-branching stramenopiles, *Cryptosporidium parvum* (apicomplexa), the deep-branching protalveolates *Oxyrrhis marina*, *Perkinsus marinus* and *Parvilucifera* and the putatively early branching dinoflagellate group syndinians (Taylor 2004). For this distribution of heterotrophy to be coherent with the chromalveolate hypothesis, independent plastid loss in all this lineages is required. This requirement is one of the major arguments opposing the chromalveolate hypothesis, as multiple plastid losses by some are considered unparsimonious and implausible (Grzebyk et al. 2004; Taylor 2004). These opponents of the chromalveolate theory recognize a more parsimonious and likely model of plastid evolution to be separate acquisitions of red algal derived plastids in haptophytes, cryptophytes, heterokonts, dinoflagellates and apicomplexa (Falkowski et al. 2004; Grzebyk et al. 2004; Grzebyk et al. 2003; Taylor 2004), and in consistence with this, there has been postulated a theory rejecting a common origin of chromalveolate plastids, providing a different explanation of the high distribution of secondary red plastids present in modern phytoplankton. This model is called “The portable plastid hypothesis” (Falkowski et al. 2004; Grzebyk et al. 2003), and is a theory based on the assumption of separate endosymbiotic uptakes of the red plastid, claiming that the wide distribution of

secondary, red plastids among phytoplankton is due to this plastid being more portable than the green plastid. The difference in portability is claimed to be caused by the amount of critically important genes retained in the red plastid, increasing this plastid's ability to integrate into a new host by secondary endosymbiosis compared to the green plastid which have less retained genes (Falkowski et al. 2004; Grzebyk et al. 2003). However, this theory is also under criticism, as it rests on assumptions that is not well supported or even contradicted. This hypothesis assumes that the red algal plastids retain more genes than do green, which is criticized as only a small number of red algal plastids hitherto has been investigated (Keeling et al. 2004). It also assumes that secondary endosymbiosis involving red plastids have happened more often than endosymbiosis involving green plastids, however, this is contradictory to the chromalveolate hypothesis (Keeling et al. 2004). Additionally, the hypothesis rests on an assumption that gene transfer from the endosymbiont nucleus to the host nucleus occurs rarely, but there are evidence that a large amount of genes are transferred from the endosymbiont to the nucleus after incorporation of a plastid (Keeling et al. 2004; Stegemann et al. 2003). There are also disagreements regarding whether five independent secondary uptakes of a red-algal plastid are a more parsimonious evolutionary event compared to the repeated plastid loss implicit in the chromalveolate hypothesis. The establishment of secondary plastids is a evolutionary complex event, where a novel organelle-specific protein-targeting machinery and the acquisition by over a thousand genes of appropriate targeting signals are required (Cavalier-Smith 2000; Cavalier-Smith 2002). Plastid losses, however, have happened repeatedly among dinoflagellates, heterokonts, cryptophytes and euglenoids, indicating that this is a relatively common feature in eukaryote algae (Cavalier-Smith 2002; Hoef-Emden et al. 2002; Preisfeld et al. 2001; Saldarriaga et al. 2001).

Thus, in the current debate regarding the origin of the red algal plastids, we have on one hand the opponents of the chromalveolate hypothesis stating that the plastid loss implicit in this theory is unlikely and un-parsimonious (Taylor 2004), while on the other hand, we have the supporters of the chromalveolate hypothesis stating that the scenario where five protist lineages independently engulf and incorporate a secondary red plastid is even

more unlikely and un-parsimonious, and that the portable-plastid hypothesis "does not hold up to scrutiny"(Keeling et al. 2004).

So, how does *Telonema* contribute to the debate concerning the putative monophyly of chromalveolates? As discussed earlier, several of the indications of the *Telonema* investigations contradicts the chromalveolate hypothesis, including the lack of a plastid in this lineage and the phylogenetic inference showing the chromalveolates as a polyphyletic group. However, the *Telonem*a lineage also expresses morphological features found in both chromists and alveolate lineages, in support of the chromalveolate hypothesis. Among the major arguments opposing the chromalveolate hypothesis is the assumption of multiple plastid loss in all heterotrophic chromalveolate lineages. However, as demonstrated in this study and other reports (Hackett et al. 2004b; Yoon et al. 2005), a dynamic and complex evolutionary history have formed the diverse distribution of plastids and heterotrophy among dinoflagellates, probably due to the extensive distribution of mixotrophy (i.e. the ability to utilize both phagotrophy and phototrophy) expressed in this group. This feature is also reported to be present in all photosynthetic chromalveolate lineages (Andersen 2004; Hackett et al. 2004a; Hoef-Emden et al. 2002), indicating that this mixotrophic ability is one of the underlying causes of the dynamic evolution of plastids seen in chromalveolates. The chromalveolate hypothesis, as postulated by Tom Cavalier-Smith (Cavalier-Smith 1999), rests on the assumption of a single uptake of a red-algal plastid in the common ancestor of chromalveolates. However, the variety of nutritional strategies and the plastid diversity seen in extant chromalveolate lineages could imply a more complex scenario of plastid evolution than described in Cavalier-Smith's hypothesis. In a recent paper, the possibility of a serial transfer of the red-algal derived plastid among the chromalveolates is suggested, implying a tertiary or even quaternary origin of some of the red-algal derived plastids (Bachvaroff et al. 2005). An intriguing scenario is presented in this paper (depicted in figure 4.1), as the first acquisition of the red-algal plastid is suggested to have occurred in a cryptophyte, which subsequently was engulfed by a heterokont, haptophyte and/or a dinoflagellate.

FIGURE 4.1

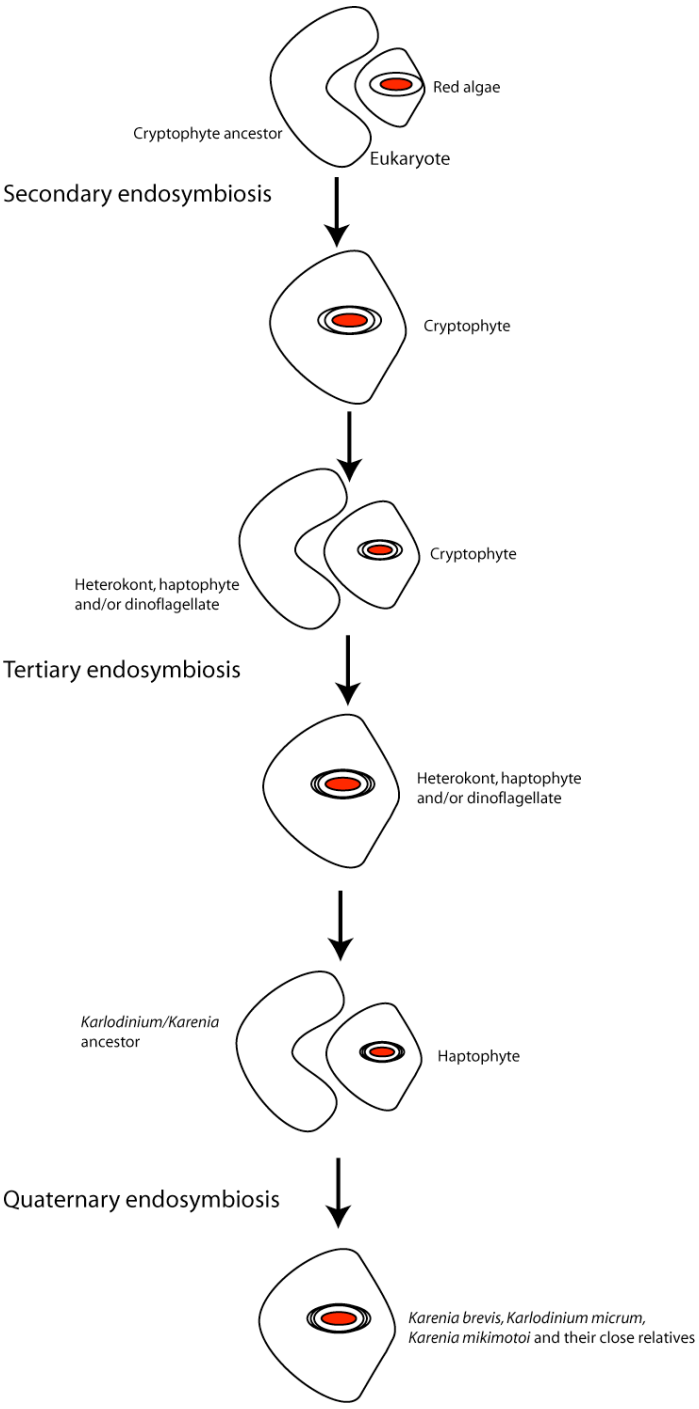

Figure 4.1: Depicting a possible scenario of the evolution of the chromalveolate plastid as presented in Bachvaroff et al. 2005, where a cryptophyte engulfs a red-algae, and later are engulfed by a heterokont, haptophyte and/dinoflagellate. The haptophyte-derived plastid in the Karlodinium/Karenia clade will in this scenario be of quaternary origin.

This scenario may seem speculative, but it is not contradicted by available data. The incongruent host-gene trees and plastid-gene trees may be consistent with this suggestion, and the shared chromalveolate GAPDH replacement can be explained by a transfer of this feature from the cryptophyte endosymbiont to the chromalveolate host lineages (Bachvaroff et al. 2005). Additionally, this scenario explains the occurrence of the basal heterotrophic heterokont, haptophyte and dinoflagellate lineages, as these may have diverged prior to the plastid uptake.

In this study, chloroplast replacements have been shown to be a relatively common event among dinoflagellates. The closest relatives to the dinoflagellates, the apicomplexans, have lost their photosynthetic ability, but still retain a vestigial plastid (McFadden, Waller et al. 1997). Even though this plastid often is presumed to be of red-algal origin, there are controversy about the origin of this plastid, as it is highly diverged and difficult to place in phylogenetic trees (Funes et al. 2004). There are however indications of both a green-algal and red-algal origin of the vestigial plastid in the apicomplexan (Funes et al. 2002; Funes et al. 2004; McFadden et al. 1997; Waller et al. 2003), indicating a chloroplast replacement event in this lineage. This might indicate that the ability of substituting plastids have been established in these lineages before the splitting of the apicomplexan and dinoflagellate lineages, which makes it tempting to speculate whether the peridinin-plastid also could have replaced another chloroplast.

These indications and speculations imply a more complex evolutionary history of the red-algal derived plastid among the chromalveolates than described in the chromalveolate hypothesis.

4.4 CONCLUDING REMARKS AND FUTURE WORK

The number of research projects applying molecular approaches for investigating microbiological eukaryotic diversity, phylogeny and evolution has increased substantially the last few years. However, extensive research is needed to extend the current knowledge about unicellular protist genomes, biological diversity and to reveal the internal relationship between the eukaryotic supergroups. The eukaryotic biological and genomic diversity can be investigated using different approaches, four of which have

been addressed in this study, namely environmental sampling, cDNA library construction, targeted PCR-amplifications and phylogenetic inference.

Further studies on the members of the *Telonema* lineage is necessary for robustly establish this group as a deep-branching chromalveolate. This can be carried out by extending the group by environmental sampling and by investigating the genomic diversity by constructing a cDNA library. Currently, specific *Telonema* PCR-primers are utilized for isolation of *Telonema* sequences from environmental samples of eukaryotic communities in freshwater lakes in order to investigate the distribution and abundance of this lineage. The pipeline for cDNA-library construction of photosynthetic eukaryotes that has been developed in this study includes culturing, harvesting, sequencing, analyses and annotation. Similar protocols could also be used to generate cDNA information from *Telonema,* but this has to be done in a slightly modified version because of the contaminating prey organism necessary for laboratory culturing of *Telonema*. Replacement of the current prey organism with a complete genome sequenced green alga would make it easier to distinguish genes obtained from *Telonema* and the prey.

The putative intron found in the *hsp90* sequence of *Alexandrium tamarense* could be of phylogenetic and functional importance. The features of the intron give indications of the properties of the dinoflagellate spliceosomal apparatus, and could also provide phylogenetic information, as it may be a specific insertion for the *Alexandrium* or gonyaulacalean species. Hence, amplification and sequencing of additional *hsp90* genes from this group are needed.

Further investigations of dinoflagellate phylogeny and genomic features have to be carried out for resolution of the internal relationship between the orders of this group, but the phylogenetic inference based on the HSP90 protein sequences suggests that this gene sequence could be a valuable contribution to this work. Extending the range of available dinoflagellate sequences and use of concatenated analyses will hopefully provide enough information to resolve phylogenetic trees, and thereby provide further information about the complex plastid evolution that has occurred in this group. Extended knowledge about the processes that have formed the plastid diversity in dinoflagellates may give important insight about general processes involved in establishment and loss of plastids. This may be the key to the understanding of the evolutionary relationships of the chromalveolates

and the other deeply related eukaryotic supergroups (unikonts, rhizaria, plantae, chromalveolates and excavates, see figure 1.1).

REFERENCES

Andersen, R. A. 2004. Biology and systematics of heterokont and haptophyte algae. American Journal of Botany 91:1508-1522.

Archibald, J. M., and P. J. Keeling. 2002. Recycled plastids: a 'green movement' in eukaryotic evolution. Trends in Genetics 18:577-584.

Archibald, J. M., D. Longet, J. Pawlowski, and P. J. Keeling. 2003. A novel polyubiquitin structure in Cercozoa and Foraminifera: Evidence for a new eukaryotic supergroup. Molecular Biology and Evolution 20:62-66.

Bachvaroff, T. R., G. T. Concepcion, C. R. Rogers, E. M. Herman, and C. F. Delwiche. 2004. Dinoflagellate expressed sequence tag data indicate massive transfer of chloroplast genes to the nuclear genome. Protist 155:65-78.

Bachvaroff, T. R., M. V. Sanchez Puerta, and C. F. Delwiche. 2005. Chlorophyll c containing plastid relationships based on analyses of a multi-gene dataset with all four chromalveolate lineages. Molecular Biology and Evolution Epub ahead of print.

Baldauf, S. L. 1999. A search for the origins of animals and fungi: Comparing and combining molecular data. American Naturalist 154:S178-S188.

Baldauf, S. L., A. J. Roger, I. Wenk-Siefert, and W. F. Doolittle. 2000. A kingdom-level phylogeny of eukaryotes based on combined protein data. Science 290:972-977.

Bapteste, E., H. Brinkmann, J. A. Lee, D. V. Moore, C. W. Sensen, P. Gordon, L. Durufle et al. 2002. The analysis of 100 genes supports the grouping of three highly divergent amoebae: Dictyostelium, Entamoeba, and Mastigamoeba. Proceedings of the National Academy of Sciences of the United States of America 99:1414-1419.

Ben Ali, A., R. De Baere, G. Van der Auwera, R. De Wachter, and Y. Van de Peer. 2001. Phylogenetic relationships among algae based on complete large-subunit rRNA sequences. International Journal of Systematic and Evolutionary Microbiology 51:737-749.

Berney, C., J. Fahrni, and J. Pawlowski. 2004. How many novel eukaryotic 'kingdoms'? Pitfalls and limitations of environmental DNA surveys. BMC Biology 4;2(1).

Bhattacharya, D., H. S. Yoon, and J. D. Hackett. 2004. Photosynthetic eukaryotes unite: endosymbiosis connects the dots. Bioessays 26:50-60.

Cavalier-Smith, T. 1998. A revised six-kingdom system of life. Biological Reviews 73:203-266.

Cavalier-Smith, T. 1999. Principles of protein and lipid targeting in secondary symbiogenesis: Euglenoid, dinoflagellate, and sporozoan plastid origins and the eukaryote family tree. Journal of Eukaryotic Microbiology 46:347-366.

Cavalier-Smith, T. 2000. Membrane heredity and early chloroplast evolution. Trends in Plant Science 5:174-182.

Cavalier-Smith, T. 2002. Chloroplast evolution: Secondary symbiogenesis and multiple losses. Current Biology 12:R62-R64.

Cavalier-Smith, T. 2003a. Genomic reduction and evolution of novel genetic membranes and protein-targeting machinery in eukaryote-eukaryote chimaeras (meta-algae). Philosophical Transactions of the Royal Society of London Series B-Biological Sciences 358:109-133.

Cavalier-Smith, T. 2003b. Protist phylogeny and the high-level classification of Protozoa. European Journal of Protistology 39:338-348.
Cavalier-Smith, T. 2004a. Chromalveolate diversity and cell megaevolution: interplay of membranes, genomes and cytoskeleton, Pages 71-103 *in* H. R. a. H. D, ed. Organelles, Genomes and Eukaryotic Evolution. London, Taylor and Francis.
Cavalier-Smith, T. 2004b. Only six kingdoms of life. Proceedings of the Royal Society of London Series B-Biological Sciences 271:1251-1262.
Cavalier-Smith, T., and E. E. Y. Chao. 2003. Phylogeny and classification of phylum Cercozoa (Protozoa). Protist 154:341-358.
Chesnick, J. M., W. Kooistra, U. Wellbrock, and L. K. Medlin. 1997. Ribosomal RNA analysis indicates a benthic pennate diatom ancestry for the endosymbionts of the dinoflagellates Peridinium foliaceum and Peridinium balticum (Pyrrhophyta). Journal of Eukaryotic Microbiology 44:314-320.
Chesnick, J. M., C. W. Morden, and A. M. Schmieg. 1996. Identity of the endosymbiont of Peridinium foliaceum (Pyrrophyta): Analysis of the rbcLS operon. Journal of Phycology 32:850-857.
Dacks, J. B., and W. F. Doolittle. 2001. Reconstructing/deconstructing the earliest eukaryotes: How comparative genomics can help. Cell 107:419-425.
Dawson, S. C., and N. R. Pace. 2002. Novel kingdom-level eukaryotic diversity in anoxic environments. Proceedings of the National Academy of Sciences of the United States of America 99:8324-8329.
de Salas, M. F., C. J. S. Bolch, L. Botes, G. Nash, S. W. Wright, and G. M. Hallegraeff. 2003. Takayama gen. nov (Gymnodiniales, Dinophyceae), a new genus of unarmored dinoflagellates with sigmoid apical grooves, including the description of two new species. Journal of Phycology 39:1233-1246.
Delwiche, C. F. 1999. Tracing the thread of plastid diversity through the tapestry of life. American Naturalist 154:S164-S177.
Edgcomb, V. P., A. J. Roger, A. G. B. Simpson, D. T. Kysela, and M. L. Sogin. 2001. Evolutionary relationships among "jakobid" flagellates as indicated by alpha- and beta-tubulin phylogenies. Molecular Biology and Evolution 18:514-522.
Edvardsen, B., K. Shalchian-Tabrizi, K. S. Jakobsen, L. K. Medlin, E. Dahl, S. Brubak, and E. Paasche. 2003. Genetic variability and molecular phylogeny of Dinophysis species (Dinophyceae) from Norwegian waters inferred from single cell analyses of rDNA. Journal of Phycology 39:395-408.
Elbrächter, M., and E. Schnepf. 1996. *Gymnodinium chlorophorum,* a new, green, bloom-forming dinoflagellate (Gymnodiniales, Dinophyceae) with a vestigial prasinophyte endosymbiont. Phycologia 35:381-393.
Eppley, R. W., R. W. Holmes, and J. D. H. Strickland. 1967. Sinking rates of marine phytoplankton measured with a fluorometer. Journal of Experimental Marine Biologi and Ecology 1:191-208.
Falkowski, P. G., M. E. Katz, A. H. Knoll, A. Quigg, J. A. Raven, O. Schofield, and F. J. R. Taylor. 2004. The evolution of modern eukaryotic phytoplankton. Science 305:354-360.
Fast, N. M., J. C. Kissinger, D. S. Roos, and P. J. Keeling. 2001. Nuclear-encoded, plastid-targeted genes suggest a single common origin for apicomplexan and dinoflagellate plastids. Molecular Biology and Evolution 18:418-426.

Fast, N. M., L. R. Xue, S. Bingham, and P. J. Keeling. 2002. Re-examining alveolate evolution using multiple protein molecular phylogenies. Journal of Eukaryotic Microbiology 49:30-37.

Felsenstein, J. 2003, Inferring Phylogenies, Sinauer.

Føyn, B. 1934. Lebenszyklus, cytologie und sexualität der Chlorophycee Cladophora suhriana Kützing. Archiv fuer Protistenkunde 83:1-56.

Funes, S., E. Davidson, A. Reyes-Prieto, S. Magallon, P. Herion, M. P. King, and D. Gonzalez-Halphen. 2002. A green algal apicoplast ancestor. Science 298:2155-2155.

Funes, S., A. Reyes-Prieto, X. Perez-Martinez, and D. Gonzalez-Halphen. 2004. On the evolutionary origins of apicoplasts: revisiting the rhodophyte vs. chlorophyte controversy. Microbes and Infection 6:305-311.

Galtier, N. 2001. Maximum-likelihood phylogenetic analysis under a covarion-like model. Molecular Biology and Evolution 18:866-873.

Grzebyk, D., M. E. Katz, A. H. Knoll, A. Quigg, J. A. Raven, O. Schofield, F. J. R. Taylor et al. 2004. Response to comment on "The evolution of modern eukaryotic phytoplankton". Science 306:2191.

Grzebyk, D., O. Schofield, C. Vetriani, and P. G. Falkowski. 2003. The mesozoic radiation of eukaryotic algae: The portable plastid hypothesis. Journal of Phycology 39:259-267.

Hackett, J. D., D. M. Anderson, D. L. Erdner, and D. Bhattacharya. 2004a. Dinoflagellates: A remarkable evolutionary experiment. American Journal of Botany 91:1523-1534.

Hackett, J. D., T. E. Sheetz, H. S. Yoon, M. B. Soares, M. F. Bonaldo, T. L. Casavant, and D. Bhattacharya. 2005. Insights into a dinoflagellate genome through a expressed sequence tag analysis. BMC Genomics 29:80.

Hackett, J. D., H. S. Yoon, M. B. Soares, M. F. Bonaldo, T. L. Casavant, T. E. Scheetz, T. Nosenko et al. 2004b. Migration of the plastid genome to the nucleus in a peridinin dinoflagellate. Current Biology 14:213-218.

Hannaert, V., E. Saavedra, F. Duffieux, J. P. Szikora, D. J. Rigden, P. A. M. Michels, and F. R. Opperdoes. 2003. Plant-like traits associated with metabolism of Trypanosoma parasites. Proceedings of the National Academy of Sciences of the United States of America 100:1067-1071.

Harper, J. T., and P. J. Keeling. 2003. Nucleus-encoded, plastid-targeted glyceraldehyde-3-phosphate dehydrogenase (GAPDH) indicates a single origin for chromalveolate plastids. Molecular Biology and Evolution 20:1730-1735.

Harper, J. T., E. Waanders, and P. J. Keeling. 2005. On the monophyly of chromalveolates using a six-protein phylogeny of eukaryotes. International Journal of Systematic and Evolutionary Microbiology 55:487-496.

Hoef-Emden, K., B. Marin, and M. Melkonian. 2002. Nuclear and nucleomorph SSU rDNA phylogeny in the cryptophyta and the evolution of cryptophyte diversity. Journal of Molecular Evolution 55:161-179.

Høiland, K. 2004. Rikenes slektskap - tre motstridende hypoteser, eller én samlende? Blyttia 6:215-222.

Howe, C. J., A. C. Barbrook, V. L. Koumandou, R. E. R. Nisbet, H. A. Symington, and T. F. Wightman. 2003. Evolution of the chloroplast genome. Philosophical

Transactions of the Royal Society of London Series B-Biological Sciences 358:99-106.
Huelsenbeck, J. P., B. Larget, R. E. Miller, and F. Ronquist. 2002. Potential applications and pitfalls of Bayesian inference of phylogeny. Systematic Biology 51:673-688.
Inagaki, Y., A. G. B. Simpson, J. B. Dacks, and A. J. Roger. 2004. Phylogenetic artifacts can be caused by leucine, serine, and arginine codon usage heterogeneity: Dinoflagellate plastid origins as a case study. Systematic Biology 53:582-593.
Ishida, K., and B. R. Green. 2002. Second- and third-hand chloroplasts in dinoflagellates: Phylogeny of oxygen-evolving enhancer 1 (PsbO) protein reveals replacement of a nuclear-encoded plastid gene by that of a haptophyte tertiary endosymbiont. Proceedings of the National Academy of Sciences of the United States of America 99:9294-9299.
Janson, S. 2004. Molecular evidence that plastids in the toxin-producing dinoflagellate genus Dinophysis originate from the free-living cryptophyte Teleaulax amphioxeia. Environmental Microbiology 6:1102-1106.
Johnson, P. J. 2002. Spliceosomal introns in a deep-branching eukaryote: The splice of life. Proceedings of the National Academy of Sciences of the United States of America 99:3359-3361.
Kass, R. E., and A. E. Raftery. 1995. Bayes Factors. Journal of the American Statistical Association 90:773-795.
Katz, L. A. 2001. Evolution of nuclear dualism in ciliates: a reanalysis in light of recent molecular data. International Journal of Systematic and Evolutionary Microbiology 51:1587-1592.
Keeling, P. 2004a. A brief history of plastids and their hosts. Protist 155:3-7.
Keeling, P. J. 2001. Foraminifera and Cercozoa are related in actin phylogeny: Two orphans find a home? Molecular Biology and Evolution 18:1551-1557.
Keeling, P. J. 2004b. Diversity and evolutionary history of plastids and their hosts. American Journal of Botany 91:1481-1493.
Keeling, P. J., J. M. Archibald, N. M. Fast, and J. D. Palmer. 2004. Comment on "The evolution of modern eukaryotic phytoplankton". Science 306:2191.
Keeling, P. J., and J. D. Palmer. 2000. Phylogeny - Parabasalian flagellates are ancient eukaryotes. Nature 405:635-637.
Klaveness, D., K. Shalchian-Tabrizi, H. A. Thomsen, W. Eikrem, and K. S. Jakobsen. 2005. *Telonema antarcticum* sp.nov., a common marine phagotrophic flagellate. International Journal of Systematic and Evolutionary Microbiology In press.
Kuo, J., M. C. Chen, C. H. Lin, and L. S. Fang. 2004. Comparative gene expression in the symbiotic and aposymbiotic Aiptasia pulchella by expressed sequence tag analysis. Biochem Biophys Res Commun 318:176-186.
Lang-Unnasch, N., M. E. Reith, J. Munholland, and J. R. Barta. 1998. Plastids are widespread and ancient in parasites of the phylum Apicomplexa. International Journal for Parasitology 28:1743-1754.
Leander, B. S., and P. J. Keeling. 2004. Early evolutionary history of dinoflagellates and apicomplexans (Alveolata) as inferred from hsp90 and actin phylogenies. Journal of Phycology 40:341-350.
Lopez, P., P. Forterre, and H. Philippe. 1999. The root of the tree of life in the light of the covarion model. Journal of Molecular Evolution 49:496-508.

Lopez-Garcia, P., F. Rodriguez-Valera, and D. Moreira. 2002. Toward the monophyly of Haeckel's Radiolaria: 18S rRNA environmental data support the sisterhood of Polycystinea and Acantharea. Molecular Biology and Evolution 19:118-121.

Lopez-Garcia, P., F. Rodriguez-Valera, C. Pedros-Alio, and D. Moreira. 2001. Unexpected diversity of small eukaryotes in deep-sea Antarctic plankton. Nature 409:603-607.

Martin, W., B. Stoebe, V. Goremykin, S. Hansmann, M. Hasegawa, and K. V. Kowallik. 1998. Gene transfer to the nucleus and the evolution of chloroplasts. Nature 393:162-165.

McEwan, M. L., and P. J. Keeling. 2004. HSP90, tubulin and actin are retained in the tertiary endosymbiont genome of Kryptoperidinium foliaceum. Journal of Eukaryotic Microbiology 51:651-659.

McFadden, G. I. 2001. Chloroplast origin and integration. Plant Physiology 125:50-53.

McFadden, G. I., R. E. Waller, M. E. Reith, and N. Lang-Unnasch. 1997. Plastids in apicomplexan parasites. Plant Systematics and Evolution:261-287.

Moon-van der Staay, S. Y., R. De Wachter, and D. Vaulot. 2001. Oceanic 18S rDNA sequences from picoplankton reveal unsuspected eukaryotic diversity. Nature 409:607-610.

Moreira, D., H. Le Guyader, and H. Philippe. 2000. The origin of red algae and the evolution of chloroplasts. Nature 405:69-72.

Newton, M. A., A. E. Raftery, A. C. Davison, M. Bacha, G. Celeux, B. P. Carlin, P. Clifford et al. 1994. Approximate Bayesian-Inference with the Weighted Likelihood Bootstrap. Journal of the Royal Statistical Society Series B-Methodological 56:3-48.

Nikolaev, S. I., C. Berney, J. F. Fahrni, I. Bolivar, S. Polet, A. P. Mylnikov, V. V. Aleshin et al. 2004. The twilight of Heliozoa and rise of Rhizaria, an emerging supergroup of amoeboid eukaryotes. Proceedings of the National Academy of Sciences of the United States of America 101:8066-8071.

Nixon, J. E. J., A. Wang, H. G. Morrison, A. G. McArthur, M. L. Sogin, B. J. Loftus, and J. Samuelson. 2002. A spliceosomal intron in Giardia lamblia. Proceedings of the National Academy of Sciences of the United States of America 99:3701-3705.

Nylander, J. A. A., F. Ronquist, J. P. Huelsenbeck, and J. L. Nieves-Aldrey. 2004. Bayesian phylogenetic analysis of combined data. Systematic Biology 53:47-67.

Okamoto, O. K., L. Y. Liu, D. L. Robertson, and J. W. Hastings. 2001. Members of a dinoflagellate luciferase gene family differ in synonymous substitution rates. Biochemistry 40:15862-15868.

Palmer, J. D. 2003. The symbiotic birth and spread of plastids: How many times and whodunit? Journal of Phycology 39:4-11.

Patron, N. J., M. B. Rogers, and P. J. Keeling. 2004. Gene replacement of fructose-1,6-bisphosphate aldolase supports the hypothesis of a single photosynthetic ancestor of chromalveolates. Eukaryot Cell 3:1169-1175.

Preisfeld, A., I. Busse, M. Klingberg, S. Talke, and H. G. Ruppel. 2001. Phylogenetic position and inter-relationships of the osmotrophic euglenids based on SSU rDNA data, with emphasis on the Rhabdomonadales (Euglenozoa). International Journal of Systematic and Evolutionary Microbiology 51:751-758.

Richards, T. A., and D. Bass. 2005. Molecular screening of free-living microbial eukaryotes: diversity and distribution using a meta-analysis. Current opinion in Microbiology In press.

Roger, A. J. 1999. Reconstructing early events in eukaryotic evolution. American Naturalist 154:S146-S163.

Roger, A. J., and J. D. Silberman. 2002. Cell evolution: Mitochondria in hiding. Nature 418:827-829.

Romari, K., and D. Vaulot. 2004. Composition and temporal variability of picoeukaryote communities at a coastal site of the English Channel from 18S rDNA sequences. Limnology and Oceanography 49:784-798.

Rudi, K., M. Kroken, O. J. Dahlberg, A. Deggerdal, K. S. Jakobsen, and F. Larsen. 1997. Rapid, universal method to isolate PCR-ready DNA using magnetic beads. Biotechniques 22:506-511.

Saldarriaga, J. F., M. L. McEwan, N. M. Fast, F. J. R. Taylor, and P. J. Keeling. 2003. Multiple protein phylogenles show that Oxyrrhis marina and Perkinsus marinus are early branches of the dinoflagellate lineage. International Journal of Systematic and Evolutionary Microbiology 53:355-365.

Saldarriaga, J. F., F. Taylor, T. Cavalier-Smith, S. Menden-Deuer, and P. J. Keeling. 2004. Molecular data and the evolutionary history of dinoflagellates. European Journal of Protistology 40:85-111.

Saldarriaga, J. F., F. J. Taylor, P. J. Keeling, and T. Cavalier-Smith. 2001. Dinoflagellate nuclear SSU rRNA phylogeny suggests multiple plastid losses and replacements. J Mol Evol 53:204-213.

Schnepf, E., and M. Elbrachter. 1988. Cryptophycean-Like Double Membrane-Bound Chloroplast in the Dinoflagellate, Dinophysis Ehrenb. - Evolutionary, Phylogenetic and Toxicological Implications. Botanica Acta 101:196-203.

Schott, E. J., J. A. F. Robledo, A. C. Wright, A. M. Silva, and G. R. Vasta. 2003. Gene organization and homology modeling of two iron superoxide dismutases of the early branching protist Perkinsus marinus. Gene 309:1-9.

Shalchian-Tabrizi, K. 2003. Studies on the evolution of chromists and alveolates. Dr.scient thesis, University of Oslo.

Shalchian-Tabrizi, K., W. Eikrem, D. Klaveness, D. Vaulot, M. A. Minge, F. Le Gall, K. Romari et al. 2005. Telonemia, a new protist phylum with ultrastructural affinities to chromalveolates. Submitted to Proceedings of the Royal Society of London Series B-Biological Sciences.

Silberman, J. D., A. G. B. Simpson, J. Kulda, I. Cepicka, V. Hampl, P. J. Johnson, and A. J. Roger. 2002. Retortamonad flagellates are closely related to diplomonads - Implications for the history of mitochondrial function in eukaryote evolution. Molecular Biology and Evolution 19:777-786.

Simpson, A. G. B. 2003. Cytoskeletal organization, phylogenetic affinities and systematics in the contentious taxon Excavata (Eukaryota). International Journal of Systematic and Evolutionary Microbiology 53:1759-1777.

Simpson, A. G. B., J. Lukes, and A. J. Roger. 2002. The evolutionary history of kinetoplastids and their kinetoplasts. Molecular Biology and Evolution 19:2071-2083.

Simpson, A. G. B., and D. J. Patterson. 2001. On core jakobids and excavate taxa: The ultrastructure of Jakoba incarcerata. Journal of Eukaryotic Microbiology 48:480-492.
Simpson, A. G. B., and A. J. Roger. 2004. The real 'kingdoms' of eukaryotes. Current Biology 14:R693-R696.
Sogin, M. L. 1991. Early evolution and the origin of eukaryotes. Current Opinion in Genetics & Development 1:457-463.
Sogin, M. L., and J. D. Silberman. 1998. Evolution of the protists and protistan parasites from the perspective of molecular systematics. International Journal for Parasitology 28:11-20.
Stechmann, A., and T. Cavalier-Smith. 2002. Rooting the eukaryote tree by using a derived gene fusion. Science 297:89-91.
Stechmann, A., and T. Cavalier-Smith. 2003. Phylogenetic analysis of eukaryotes using heat-shock protein Hsp90. Journal of Molecular Evolution 57:408-419.
Stechmann, A., and T. Cavalier-Smith. 2004. Evolutionary origins of Hsp90 chaperones and a deep paralogy in their bacterial ancestors. Journal of Eukaryotic Microbiology 51:364-373.
Stegemann, S., S. Hartmann, S. Ruf, and R. Bock. 2003. High-frequency gene transfer from the chloroplast genome to the nucleus. Proceedings of the National Academy of Sciences of the United States of America 100:8828-8833.
Stoeck, T., G. T. Taylor, and S. S. Epstein. 2003. Novel eukaryotes from the permanently anoxic Cariaco Basin (Caribbean sea). Applied and Environmental Microbiology 69:5656-5663.
Sueoka, N. 1960. Mitotic replication of deoxxyribonucleic adis in *Chlamydomonas reinhardi*. Proceedings of the National Academy of Sciences of the United States of America 46:83-91.
Takishita, K., K. Ishida, and T. Maruyama. 2003. An enigmatic GAPDH gene in the symbiotic dinoflagellate genus Symbiodinium and its related species (the order suessiales): Possible lateral gene transfer between two eukaryotic algae, dinoflagellate and euglenophyte. Protist 154:443-454.
Takishita, K., K. I. Ishida, and T. Maruyama. 2004. Phylogeny of nuclear-encoded plastid-targeted GAPDH gene supports separate origins for the peridinin- and the fucoxanthin derivative-containing plastids of dinoflagellates. Protist 155:447-458.
Takishita, K., K. Koike, T. Maruyama, and T. Ogata. 2002. Molecular evidence for plastid robbery (Kleptoplastidy) in Dinophysis, a dinoflagellate causing diarrhetic shellfish poisoning. Protist 153:293-302.
Taylor, F. J. R. 2004. Illumination or confusion? Dinoflagellate molecular phylogenetic data viewed from a primarily morphological standpoint. Phycological Research 52:308-324.
Tengs, T., O. J. Dahlberg, K. Shalchian-Tabrizi, D. Klaveness, K. Rudi, C. F. Delwiche, and K. S. Jakobsen. 2000. Phylogenetic analyses indicate that the 19 ' hexanoyloxy-fucoxanthin-containing dinoflagellates have tertiary plastids of haptophyte origin. Molecular Biology and Evolution 17:718-729.
Van de Peer, Y., and R. De Wachter. 1997. Evolutionary relationships among the eukaryotic crown taxa taking into account site-to-site rate variation in 18S rRNA. Journal of Molecular Evolution 45:619-630.

Vanacova, S., W. H. Yan, J. M. Carlton, and P. J. Johnson. 2005. Spliceosomal introns in the deep-branching eukaryote Trichomonas vaginalis. Proceedings of the National Academy of Sciences of the United States of America 102:4430-4435.

Waller, R. F., P. J. Keeling, G. G. van Dooren, and G. I. McFadden. 2003. Comment on "A green algal apicoplast ancestor". Science 301:49.

Watanabe, M. M., S. Suda, I. Inouye, T. Sawaguchi, and M. Chihara. 1990. *Lepidodinium viride* gen. et sp. nov (Gymnodiniales, Dinophyta), a green dinoflagellate with a chlorophyll A- and B-containing endosymbiont. Journal of Phycology 26:741-751.

Watanabe, M. M., Y. Takeda, T. Sasa, I. Inouye, S. Suda, T. Sawaguchi, and M. Chihara. 1987. A green dinoflagellate with chlorophylls A and B: morphology, fine strucure of the chloroplast and chlorophyll composition. Journal of Phycology 23:382-389.

Yoon, H. S., J. D. Hackett, and D. Bhattacharya. 2002a. A single origin of the peridinin- and fucoxanthin-containing plastids in dinoflagellates through tertiary endosymbiosis. Proceedings of the National Academy of Sciences of the United States of America 99:11724-11729.

Yoon, H. S., J. D. Hackett, G. Pinto, and D. Bhattacharya. 2002b. The single, ancient origin of chromist plastids. Proceedings of the National Academy of Sciences of the United States of America 99:15507-15512.

Yoon, H. S., J. D. Hackett, F. M. Van Dolah, T. Nosenko, L. Lidie, and D. Bhattacharya. 2005. Tertiary endosymbiosis driven genome evolution in dinoflagellate algae. Molecular Biology and Evolution 22:1299-1308.

Zhang, H., D. Bhattacharya, and S. Lin. 2005. Phylogeny of dinoflagellates based on mitochondrial cytochrome b and nuclear small subunit rDNA sequence comparisons. Journal of Phycology 41:411-420.

Zhang, Z. D., T. Cavalier-Smith, and B. R. Green. 2002. Evolution of dinoflagellate unigenic minicircles and the partially concerted divergence of their putative replicon origins. Molecular Biology and Evolution 19:489-500.

APPENDIX 1

PHYLOGENETIC INFERENCE OF DINOFLAGELLATES

TABLE 1

HSP90, SSU AND LSU ACCESSION NUMBERS:

Datasets used for reconstructing tree depicted in figure 3.6 – 3.9.

SPECIES	HSP90	SSU	LSU
Alexandrium tamarense	XXX**	AJ415510	AB088245
Amphidinium carterae	T.B*.	AJ415512	AF260380
Crypthecodinium cohnii	AAM02974.1|	M64245	
Cryptosporidium parvum	AAR83923	AF093494.1	AF015773
Gymnodinium chlorophorum	XXX**	XXX***	AF200669
Heterocapsa triquetra	AAR27541	AJ415514.1	AF260401.1
Karenia brevis	XXX**	AJ415518	AF200677
Karenia mikimotoi	XXX**	AF022195	U92247
Karlodinium micrum	XXX**	AJ415516.1	AF200675.1
Kryptoperidinium foliaceum	AAV32830	AF274268	
Lepidodinium viride		AF022199	
Lessardia elongata	AAR27542	AF521100.1	
Oxyrrhis marina	AAR27544	AF482425.1	AY460596
Perkinsus marinus	AAR27545	L07375	
Prorocentrum micans	AAR27546	AJ415519.1	AY822609.1
Pyrocystis lunula	BQ254029	AF274274	
Tetrahymena pyriformis	AAG00567	X56171.1	X54004
Toxoplasma gondii	AAQ24837	L37415.1	AF076901.1

*: Unpublished sequence kindly provided by Tsvetan Bachvaroff

**: Unpublished sequences generated in this study

***: Unpublished sequence generated by Joachim Nedreklepp

TABLE 2

Actin accession numbers:

Dataset used for reconstructing tree depicted in figure 3.10

SPECIES and protein version	Accession number
Actinophrys sol	AAP93829.1
CCMP421d	AAO49352.1
Crypthecodinium cohnii	AAM02969.1
Cryptosporidium parvum	AAA28295.1
Gymnodinium chlorophorum	XXX*
Heterocapsa triquetra	AAO49340.1
Karenia brevis actin 2	AAO49345.1
Karenia brevis actin 3	AAO49346.1
Karenia brevis actin 4	AAO49347.1
Karlodinium micrum	XXX*
Lingulodinium polyedrum	AAQ99154.1
Oxyrrhis marina	AAO49331.1
Peridinium willei	AAO49349.1
Perkinsus marinus 1	AAR11389.1
Perkinsus marinus 2	AAR11390.1
Perkinsus marinus 3	AAR11391.1
Toxoplasma gondii	AAC13766.1
Uncultured dinflagellate	BAC44870
Unidentified dinoflagellate	BAC44867

***: Unpublished sequences generated in this study**

TABLE 3

GAPDH accession numbers:

Dataset used to reconstruct tree depicted in figure 3.11

SPECIES AND ISOFORM OF GAPDH	Accession no.
Akashiwo sanguinea GapC2	BAC87931
Amphidinium operculatum GapC1	BAC87932.1

Amphidinium operculatum GapC2	BAC87935.1
Cryptosporidium parvum	CAD98421
Gonyaulax polyedra	AAD01872
Gonyaulax polyedra isoform2	AAD01871.1
Gymnodinium simplex GapC1	BAC87927.1
Gymnodinium simplex GapC2	BAC87928
Heterocapsa triquetra GapC1	BAC87934.1
Heterocapsa triquetra GapC2	BAC87935.1
Heterosigma akashiwo	AAK20727.1
Karenia brevis GapC1	BAD72934.1
Karenia brevis GapC2	BAD72935.1
Karenia brevis GapC3	BAD72936.1
Karenia brevis GapC4	BAD72937.1
Polarella glacialis GapC2	BAC87925
Scrippsiella trochoidea GapC1	BAC87936.1
Scrippsiella trochoidea GapC2	BAC87937
Symbiodinium sp. CS-156 GapC1	BAC87921.1
Symbiodinium sp. CS-156 GapC2	BAC87922
Symbiodinium sp. JCUCS-1 GapC1	BAC87918.1
Symbiodinium sp. JCUCS-1 GapC2	BAC87919
Tetrahymena pyriformis	AAK20727.1
Toxoplasma gondii	AAK20420.1
Karlodinium micrum	XXX*

*: Unpublished sequence generated in this study

PHYLOGENETIC INFERENCE OF EUKARYOTES, INCLUDING *TELONEMA*

TABLE 4

HSP90. alpha-tubulin and beta-tubulin accession numbers:

Dataset used to reconstruct trees depicted in figure 3.12 and 3.13

SPECIES	SSU	HSP90	Alpha-tubulin	Beta-tubulin
***Achlya ambisexualis* (1)**	M32705	AAM90674		
***Achlya klebsiana* (1)**				A35885
Arabidopsis thaliana	AC006837	AC174363.1	BAB09283	AAM10035
Babesia microti				BAC66504.1

Bodo saltans		AAM93754		
Bombyx mori			CAA58465.1	
Candida tropicalis		AAF63792		
Cercomonas ATCC50316**(2)**				AAD55354
Cercomonas ATCC50319**(2)**			AAC67375	
Chlorarachnion CCMP621			AAC68504.	
Colpoda sp.			CAA64074.1	CAA64075.1
Crypthecodinium cohnii	M64245	AAM02974		AAM02970
Cryptosporidium parvum	L16997	AAR83923	BAC07246	
Danio rerio		AAH65359	NP919369	AAN33030
Drosophila melanogaster	AY037174	AAM52592	P06604	B27810
Eimeria acervulina			CAA61255.1	
Eimeria tenella				AAB41262
Euglena gracilis	M12677	AAQ24862	CAA80497	AAK37834
Euplotes focardii			AAL73386.1	
Giardia intestinalis			AAN78305.1	CAA29923.1
Goniomonas sp.* (3*)		AAP72158		
Goniomonas truncata **(3)**	U03072		AAD02566	AAD02567
Guillardia theta			AAD02569.1	AAD02571.1
Heterocapsa triquetra	AJ415514	AAR27541	AAO49341	AA049343
Hexamita inflata		AAR26695		
Homo sapiens	M10098	XP08514	NP006073	AAH24038
Imantonia rotunda **(4)**			XXX	XXX
Isochrysis sp.				XXX
Jakoba_incarcerata			AAK27844	AAK37434
Jakoba_libera			AAK27845	AAK37435
Leishmania_donovani* (5*)	X07773	X07773	A44888	
Leishmania_major **(5)**				CAA63780
Malawimonas jakobiformis			AAK27846.1	
Monosiga_brevicollis	AF100940	AAP51213	AAK27410	AAK27411
Naegleria_gruberi	M18732	AAM93756	P11237C	AA78362
Neurospora crassa			CAA55940.1	P05220
Ochromonas danica* (6*)	M32704.1			
Ochromonas_sp.**(6*)***		AAP72159		
Oomycete-like MacKay 2000				CAA91941.1
Oryza sativa	AF069218.1	BAD33406	CAA62916	BAC82429

Oxyrrhis_marina	AB033717	AAR27544	AAO49332	AAO49333
Paramecium_tetraurelia	X03772	AAG00569	CAA67847	CAE75646
Pavlova aff. salina	L34669.1	AAP72160		
Pelvetia fastigiata			AAB68032.1	
Perkinsus_marinus	AF126013	AAR27545	AAO49328	AAO49330
Phytophthora_cinnamomi				AAC05441
Pisum sativum			AAA79910	
Pisum sativum				CAA38615.1
Plasmondium_falciparum	M19172	CAA82765	NP704579	A44949
***Prymnesium_patelliferum* (4)**	AY236716	AAP72161		
Pythium_ultimum				AAF22655
Schizosaccharomyces_pombe	AY251644	NP594365	NP596774	
Spironucleus vortens			AAB81021.1	
***Spumella uniguttata* (7)**		AAR27540		
***Spumella danica* (7)**	AJ236861			
Telonema antarcticum	AJ564773.1	XXX	XXX	XXX
***Telonema subtilis* (RCC404.5)**	AJ564771.1	XXX	XXX	XXX
Tetrahymena_pyriformis	AAG00567	AAG00567	CAA31256	CAA31258
***Thaumatomonas sp.* (2)**	AAP72162	AAP72162		
Toxoplasma gondii	AAQ24837	AAQ24837	M20024	S16340
Trichomonas vaginalis			AAC13755.1	
Trypanosoma_cruzi	X53917	A26125	AAL75955	AAL75957
Zea mays	AF168884	AAB26482	CAA44862	CAA37060

1. The *Achlya_ambisexualis and A. klebsiana* sequences were concatenated, named as Achlya in Fig. 3.13.

2. The *Cercomonas* and *Thaumatomonas sp.* sequences were concatenated and denoted as *Cercozoa* in Fig 3.13.

3. The *Goniomonas sp.* and *G. truncata* were concatenated and named Goniomonas in trees in Fig. 3.13 and 3.14.

4. The *Prymnesium* and *Imantonia* sequences were concatenated and named as Prymnesium in Fig 3.13 and 3.14.

5. The *Leishmania dovani* and *L. major* were concatenated and named *Leishmania* in Fig. 3.13.

6. The *Ochromonas* danica and *Ochromonas* sp. sequences were concatenated and named *Ocromonas* in figure 3.14

7. *Spumella uniguttata* and *S.danica* sequences were concatenated and named *Spumella* in figure 3.14.

APPENDIX 2

CULTURE MEDIA

Erdschreiber medium (Føyn 1934)

1 liter filtrated seawater

5 ml soilwater supernatant

2 ml $NaNO_3$

2 ml $Na_2HPO4 \times 12H_2O$

2 ml vitamins	100 mg thiamin, 1 mg biotin, 1 mg B12 pr liter
0.5 ml NaFeEDTA	150 mg/100ml

Pasteurized at 80°C for 15 minutes.

IMR/2 medium (Eppley et al. 1967)

1 liter filtrated seawater

0.5 ml KNO_3	5g / 100 ml
0.5 ml KH_2PO_4	0.68g/ 100 ml
0.5 ml vitamins	100 mg thiamin pr 1000 ml
	1 mg biotin pr 1000 ml
	1 mg B12 pr 1000 ml
0.5 ml trace metals:	6 g Na2EDTA / 1000 ml
	1000 mg $FeCl3 \times 6H_2O$
	620 mg $MnSO4 \times H_2O$
	250 mg $ZnSO4 \times 7 H_2O$
	130 mg $Na2MoO4 \times 2 H_2O$
	4 mg $CoCl2 \times 6 H_2O$
	4 mg $CuSO4 \times 5 H_2O$

Autoclaved at 111°C for 15 minutes.

HS medium (high salt) (Sueoka 1960)

1 liter

20 ml salt stock (see below)
20 ml phosphate stock (see below)
1 ml trace elements (Hutner)

Salt stock (50X):
For 500 ml
12.50 g NH_4Cl
0.50 g $MgSO_4 \cdot 7 H_2O$
0.25 g $CaCl_2 \cdot 2 H_2O$

Phosphate stock (50X):
For 500 ml
47 g $K_2HPO_4 \cdot 3 H_2O$
18 g KH_2PO_4